



universität
wien

DIPLOMARBEIT

Titel der Diplomarbeit

The Roles of Urocanic Acid in the Response of Epidermal Cells to UVB

angestrebter akademischer Grad

Magistra der Naturwissenschaften (Mag. rer.nat.)

Verfasserin / Verfasser:	Caroline Stremnitzer
Matrikel-Nummer:	8971014
Studienrichtung (lt. Studienblatt):	A490
Betreuerin / Betreuer:	Ao. Univ.-Prof. Mag. Dr. Pavel Kovarik, Univ.-Prof. Dr. Erwin Tschachler

Wien, am 08.03.2010

Durchgeführt an der Medizinischen Universität Wien, Universitätsklinik für Dermatologie, Forschungseinheit für Biologie und Pathobiologie der Haut unter der Leitung von Univ. Prof. Dr. Erwin Tschachler.

Acknowledgement

The last year was an all-scientific and life-experimental assay and has given me great insights in being a scientist. I want to thank all people who supported and guided me through this exciting and educational time.

At first, I want to thank Dr. Erwin Tschachler for giving me the chance to work for his division, for discussions and offering his help.

I'm grateful to DDr. Leopold Eckhart for helpful discussions, for challenging me with an incredible big reservoir of ideas and for being critical.

I thank Dr. Caterina Barresi for teaching me all about mice and techniques, sharing ideas, inspiring discussions and giving me advice and help even when she was already off caring for her own private family project.

Furthermore, I'm very grateful for my colleagues of the Tschachler-Lab, who became not only colleagues but also friends to me. I sincerely thank Veronika Mlitz, Maria Buchberger, Minoo Gannadhan and Katja Posa-Markaryan, who participated in the project and also supported me with their practical knowledge. Thanks to Heidi Rossiter and Florian Gruber for giving me advice and help.

For informative discussions, help and a warm welcome I'd also like to thank Arby Abtin, Claudia Ballaun, Susanne Drexler, Heinz Fischer, Ramona Gmeiner, Petra Gross, Barbara Lengauer, Michael Mildner, Elsa Motuk, Christopher Nava, Christina Reinisch, Jennifer Scherz, Martin Stichenwirth and especially Sandra Szabo, who shared not only the journey of achieving a good diploma thesis with me but also friendship and challenges of general life.

I would also like to thank Professor Dr. Pavel Kovarik for his interest in my diploma thesis and his offer for being my supervising tutor at the university.

My thanks go to my family and friends as well, especially my parents – I would not have been able to do that all without their patience and support, and my sister Marie for being the best sister and friend I could imagine; Nicole Amberg for being a great fellow student and even a better friend. And I want to thank Jörg for listening, supporting, cheering me up and sharing the happy and the frustration.

February 2010

Abstract

UVB irradiation causes skin damage which underlies skin aging and various forms of skin cancer. DNA is one of the main photoreceptors for UVB light, and UVB-induced DNA mutations have been shown to cause malignant transformation of skin cells. Moreover, DNA mutations have been implicated in UVB-induced suppression of immune responses, which may further sensitize the skin to the development of cancer. Urocanic acid (UCA) is another endogenous UVB-photoreceptor and is proposed to prevent high levels of DNA damage. It is generated by the enzyme histidase from histidine, a protein breakdown product in the cornified layer (stratum corneum) of the epidermis. By absorption of UVB irradiation, UCA is converted from the trans- to the cis-isomer. The latter has been proposed to contribute to UVB-induced immunosuppression by altering the antigen-presenting function and the number of Langerhans cells in the epidermis. The various roles of UCA in the skin have been discussed for many years, however an evaluation in an appropriate *in vivo* model has been lacking.

Here, the photoprotective role and the immunosuppressive role of endogenous UCA were investigated in the histidinemic mouse model. Histidinemic mice carry a deleterious mutation in the gene encoding histidase and, therefore, have a strongly reduced UCA concentration in the stratum corneum. The UVB absorption capacity of aqueous extracts from the stratum corneum was significantly reduced in histidinemic mice as compared to mice carrying at least one wild-type allele of histidase. When newborn mice and the shaved back skin of adult mice were irradiated with 25 or 250 mJ/cm² UVB, histidinemic mice accumulated significantly more DNA damage in the form of cyclobutane pyrimidine dimers than wild-type mice. Furthermore, UVB irradiation induced significantly higher levels of apoptosis in the epidermis of histidinemic mice. These results provide strong evidence for an important contribution of endogenous UCA to the protection of the epidermis against the damaging effects of UVB light.

To evaluate the influence of UVB-induced cis-UCA on immune responses, the UVB-induced alteration in the number of Langerhans cells was determined in normal mice and in histidinemic mice. UVB irradiation induced high levels of cis-UCA in wild-type mice whereas cis-UCA concentrations were low in irradiated mutant mice. In line with the proposed role of cis-UCA in immunomodulation, UVB induced a stronger reduction of Langerhans cell densities in wild-type mice than in mutant mice.

Taken together, the results of this study establish UCA as an important endogenous UVB protection factor and as a critical modulator of immunosuppression by UVB light.

Zusammenfassung

UVB Strahlung kann erhebliche Schäden in der Haut bewirken und zur Entstehung von Krebs führen. DNS ist einer der wichtigsten Photorezeptoren von UVB Strahlung und UVB-induzierte Mutationen in der DNS sind Hauptfaktoren bei der Entstehung von Hautkrebs. Eine Rolle von DNS-Mutationen wird auch in der UVB-induzierten Immunsuppression vermutet, die durch ein Versagen des Immunsystems beim Erkennen und Bekämpfen von malignen Hautzellen die Tumorentstehung verhindert. Endogene Urocaninsäure, die von dem Enzym Histidase aus Histidin generiert wird, akkumuliert in der äußersten Schicht der Haut und absorbiert sehr effizient UVB-Strahlung. Dementsprechend wurde Urocaninsäure als körpereigener Schutzfaktor gegen UV-verursachte DNS-Schädigung vorgeschlagen. Durch Absorption von UVB Strahlung wird das trans-Isomer von UCA, das in der Histidase-Reaktion entsteht, partiell in das cis-Isomer umgewandelt. Es wird vermutet, dass cis-UCA an der UVB-induzierten Immunsuppression beteiligt ist, indem es sowohl die Auswanderung von Langerhans Zellen aus der Epidermis als auch Beeinträchtigungen der Langerhanszell-Funktionen, insbesondere der Antigen-Präsentation bewirkt.

In dieser Arbeit wird die photoprotektive und die immunsuppressive Rolle von endogener Urocaninsäure in einem *in vivo* Model, der Histidinämie Maus, untersucht. Histidinämie Mäuse tragen eine Mutation in dem Gen, das das Enzym Histidase kodiert. Diese führt zu stark reduzierten UCA Konzentrationen im Stratum Corneum (der obersten Schicht der Epidermis), wodurch die UVB Absorptionskapazität des Stratum Corneums von mutierten Tieren im Vergleich zu Wildtyp- oder Histidase-heterozygoten Mäusen stark wird.

Die Haut von neugeborenen Mäusen und die rasierte Rückenhaut von adulten Mäusen wurde mit 2 UVB-Dosen bestrahlt. Die Quantifizierung von Cyclobutandimeren zeigte, dass in histidinämischen Mäusen signifikant mehr DNS Schaden induziert wurde als in Wildtypmäusen. Auch die Zahl apoptotischer Zellen war in der Epidermis von mutanten Mäusen signifikant höher als in Kontrollmäusen.

Diese Ergebnisse implizieren, dass endogene Urocaninsäure als ein wichtiger Schutzfaktor der Epidermis gegen die schädigenden Effekte von UVB Strahlung fungiert.

Um den Einfluss von UVB-induzierter cis-Urocaninsäure auf das Immunsystem in der Haut zu untersuchen, wurde die UVB-induzierte Veränderung der Zahl der epidermalen Langerhanszellen in histidinämischen und Wildtyp-Mäusen bestimmt. UVB Strahlung

bewirkte einen hohen Anstieg der cis-UCA Konzentration in Wildtyp-Mäusen, während nur sehr geringe cis-UCA Konzentrationen im Stratum Corneum von mutierten Mäusen nachgewiesen werden konnten. Übereinstimmend mit der erörterten Rolle von cis-UCA bei der Modulation des Immunsystems, bewirkte UVB Bestrahlung eine stärkere Reduktion der Zahl der Langerhanszellen in der Epidermis von Wildtyp-Mäusen als in Histidinämie-Mäusen.

Die Ergebnisse dieser Studie liefern experimentelle Bestätigungen für die früher postulierten Rollen von Urocaninsäure als wichtiger endogener UV-Schutzfaktor und Signalstoff in der UVB-induzierten Immunsuppression.

TABLE OF CONTENT

1. INTRODUCTION.....	11
1.1. Epidermis.....	11
1.2 Ultraviolet Light.....	12
1.3 L-Histidine Ammonia Lyase (or Histidase).....	15
1.3.1 Mouse model: mutation of histidase.....	15
1.4 The photoprotective role of UCA.....	16
1.4.1 DNA damage (Thymine dimer formation).....	16
1.4.2 Effects of UVB light on tissue integrity and photoaging of the skin.....	17
1.5 Effects of UVB-induced cis-urocanic acid on Langerhans cells.....	18
1.5.1 Skin – immunology.....	18
1.5.2 Innate immune system.....	19
1.5.3 Adaptive immune system.....	19
1.5.4 UV radiation influences the immune system of the skin and alters LC function and morphology.....	21
1.5.5 Urocanic acid acts as UVB photoreceptor.....	22
1.5.6 UCA as signaling molecule for LC migration.....	23
2. AIM OF THESIS.....	25
3. RESULTS.....	27
3.1. The photoprotective role of endogenous UCA.....	27
3.1.1 The mutation of HAL destabilizes the histidase protein.....	27
3.1.2 Mutant mice have a reduced UCA content in the stratum corneum and show suppression of UVB absorption capacity of the stratum corneum.....	29
3.1.3 UV absorption by the stratum corneum is reduced in mutant mice.....	30
3.1.4 Effect of UVB radiation on DNA damage and thymine-dimer-formation.....	31
3.1.5 Effect of UVB radiation on apoptosis.....	34
3.1.6 Effect of UVB radiation on skin morphology.....	36
3.1.6.1. High doses of UVB irradiation can cause burns, wrinkles and open wounds.....	36
3.1.6.2 Lack of wild-type histidase causes enhanced apoptosis in the epidermis.....	38
3.1.6.3 There is no visible change in HAL-expression due to UVB irradiation.....	42
3.1.6.4 Histology of high-dose UVB irradiated skin.....	43
3.1.6.5 Thymine dimers are repaired in both WT and histidinemic mice.....	46
3.1.6.6 Topical application of UCA rescued the UVB-photosensitive phenotype of histidinemic mice and increased UVB-photoprotection of wild-type mice.....	47
3.1.7 Effect of lack of HAL on histidine- and histamine levels.....	49

3.2. Effect of UVB-induced cis-urocanic acid on the number Langerhans cells in mouse epidermis.....	50
3.2.1. Single-high-dose protocol.....	51
3.2.2. Repeated-low-dose protocol.....	52
3.2.3 UVB irradiation alters morphology of Langerhans cells.....	54
4. DISCUSSION.....	57
4.1 Lack of UCA in the epidermis leads to increased DNA damage.....	57
4.2 Influence of UVB-induced cis-urocanic acid on Langerhans cell migration.....	60
4.2.1 Limitations.....	60
4.2.2 Lack of UVB-induced cis-urocanic acid alters, but does not completely inhibit UVB-induced decrease of epidermal Langerhans cells.....	60
4.4 Conclusion and future aims.....	62
5. MATERIALS.....	64
5.1 Buffers.....	64
5.2 Kits.....	64
5.3 Reagents and solutions.....	65
5.4 Antibodies.....	66
5.5 Primer.....	66
5.6 Mice.....	67
5.7 Equipment.....	67
5.8 Programs.....	68
6. METHODS.....	68
6.1 Animal handling and tissue preparation.....	68
6.1.1 Tail DNA preparation.....	68
6.1.2 Epidermis-dermis separation.....	68
6.1.3 Isolation of genomic DNA from murine epidermis.....	69
6.1.4 Anesthesia.....	69
6.1.5 Tape-stripping of adult mice.....	69
6.1.6 Tape-stripping of newborns.....	70
6.1.7 Topical UCA application.....	70
6.2 Irradiation protocols.....	70
6.2.1 UVB irradiation for studying the effects of UVB on Langerhans cells.....	70
6.2.1.1 Single high-dose protocol.....	71
6.2.1.2 Repeated low-dose protocol.....	71
6.2.2 UVB irradiation to study the long-term effects of UVB-light on the skin.....	71
6.2.3 UVB irradiation for studying the photoprotective role of UCA – newborn mice.....	72

6.2.4 UVB irradiation for studying the photoprotective role of UCA – adult mice.....	72
6.2.5 Calculation mode for irradiation time (UVB irradiation of mouse skin).....	72
6.2.6 UV-lamp-spectra-comparison.....	73
6.3 Molecular biology.....	73
6.3.1 RNA-isolation using RNeasy 96 protocol for isolation of total RNA from animal cells.....	73
6.3.2 RNA-isolation using Trizol.....	74
6.3.3 cDNA-synthesis.....	74
6.3.4 Quantitative real time PCR (qPCR).....	74
6.3.5 Genotyping of mice.....	75
6.3.6 Protein-isolation.....	75
6.4 Biochemistry.....	76
6.4.1 Western blot analysis.....	76
6.4.2 Determination of urocanic acid concentrations in the stratum corneum.....	76
6.4.3 Determination of UV absorption of stratum corneum extracts.....	76
6.4.4 Vacuum-Dot-Blot (South-Western Blot for thymine dimers).....	77
6.4.5 ELISA for thymine dimers (determination of DNA damage).....	77
6.4.6 Histamine-Elisa (IBL International GmbH).....	78
6.5 Microscopy.....	78
6.5.1 Immunohistochemistry: paraffin (HRP) – staining (TUNEL, thymine-timers and active Caspase 3).....	78
6.5.2 Haematoxylin and Eosin (H&E) staining.....	79
6.5.3 Preparation/staining of ears for evaluation of LC-density.....	80
6.5.4 Preparation/double-staining of ears for active Caspase-3-positive cells.....	80
6.6 Statistical Analysis.....	81
7. REFERENCES.....	82
8. APPENDIX.....	92
8.1. List of Figures.....	92
8.2. List of Tables.....	94
8.3 List of Abbreviations.....	94
8.4 Curriculum Vitae.....	96

1. INTRODUCTION

1.1 Epidermis

The epidermis is the outermost layer of the skin. It is a continually renewing, stratified, squamous epithelium that keratinizes and gives rise to derivative structures (nails, sweat glands) tissue and composed of 4 layers: stratum corneum, stratum granulosum, stratum spinosum and stratum basale. It consists of four different cell types: keratinocytes, melanocytes, Langerhans cells and Merkel cells.

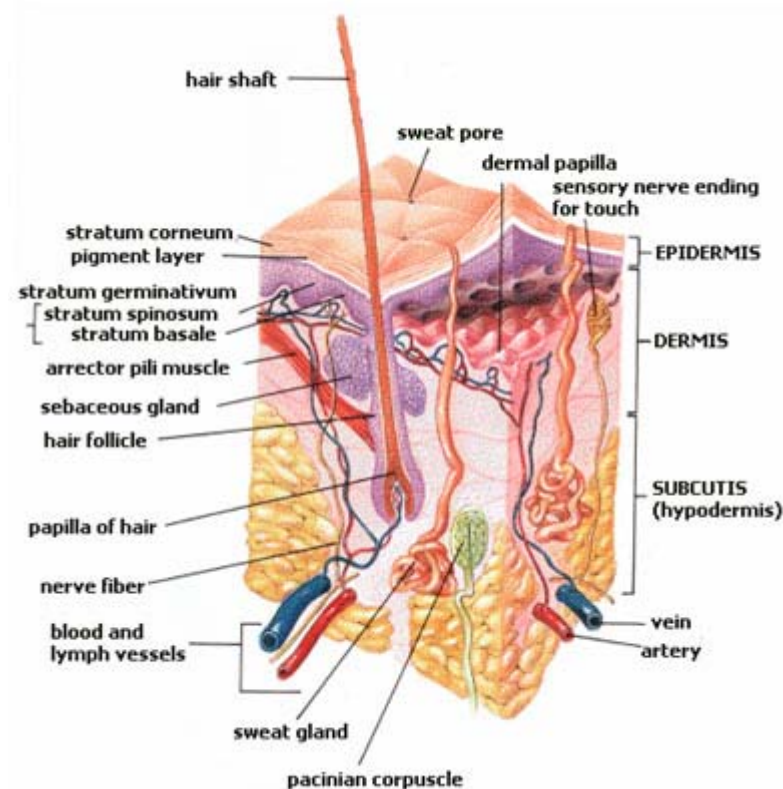


Figure 1: Morphology of the skin [<http://upload.wikimedia.org/wikipedia/commons/3/34/Skin.jpg>]

The epidermis is avascular and nourished by diffusion from the dermis. It can increase in thickness and contains antioxidative enzymes, which quench reactive oxygen species.

Melanocytes are specialised dendritic cells of neural crest origin and produce melanin, which determines the skin colour and its most important function is photoprotection of the skin. Melanin production is constitutive and inducible and represents a mixture of different polymerized pigments. Production of melanin in a process called melanogenesis occurs in specialized organelles called melanosomes and can be triggered due to different stimuli, particularly by UV irradiation [Fritsch, 2003; Park et al. 2009]. Exposure of the skin to UV light and furthermore generation of DNA damage and thymidine dinucleotide fragments from

damaged DNA trigger melanocytes to produce melanosomes, which are then transferred by dendrites to the basal keratinocytes. [Eller et al., 1997]. UV-induced activation of dormant melanocytes leads to an upregulation of the tyrosinase, which starts the synthesis of melanin. Keratinocytes produce mitogenic (bFGF, TGF- α) and inhibitory (IL1, IL6, TGF- β) factors for melanocytes. In addition, the proliferation of melanocytes, melanogenesis and the transfer of pigment also rely on hormonal controls (α MSH, sex hormones), agouti signal protein and inflammatory mediators in skin [Chu et al., 2003; Agar et al., 2005]. Downregulation to normal activity of melanocytes occurs slowly (over weeks) after termination of UVR exposure [Fritsch; 2003].

In mice, melanocytes are located primarily within the hair follicles determining the fur colour, but not within the epidermis thus they do not contribute to photoprotection of epidermal keratinocytes.

1.2 Ultraviolet Light

The UV-spectrum is subdivided into UVA (400 – 320 nm), UVB (320 – 290 nm) and UVC (290 – 200 nm). UVC and much of the UVB, are absorbed by the oxygen and ozone in the earth's atmosphere. Remaining UV radiation can still be absorbed by biologic molecules (DNA, proteins, lipids), and it can damage and kill unprotected cells. Protective mechanisms to prevent or reduce the damage of the skin include the formation of a superficial layer of dead keratinocyte remnants, i.e. the stratum corneum, which reflects and absorbs significant portion of the UV irradiation, the production of melanin, i.e. a polymer with high UV absorption capacity, by epidermal melanocytes and enzymatic as well as non-enzymatic antioxidative defenses. UV damage also induces repair processes, and the removal of irreversibly damaged cells by apoptosis. The remaining UV-induced damage is a major cause of skin aging and formation of tumors. The latter is likely to involve both malignant transformation of cells by inducing mutations in the genomic DNA and suppression of immune responses that might otherwise remove malignant cells. Regarding the skin, the longer the wavelength of UV light, the deeper it penetrates into the tissue. UVA reaches the dermis, including the deeper portions whereas most of the UVB is absorbed in the epidermis, and only a small proportion reaches the upper dermis.

Effects of UV light on the skin depend on wavelength and doses.

There are acute, short-term effects and chronic, long-term effects.

These effects include DNA damage (wave-length dependent), including formation of pyrimidine dimers and oxidative guanine base modifications on the molecular level; and the affection of the skin's immune system, exerting pro- as well as anti-inflammatory responses.

Studies on effects of exposure of skin to UV light are also important regarding therapeutic applications. Phototherapy for inflammatory skin diseases is always a matter of risk versus the benefit and alternatives or improvement are desired. A down-regulation of the overshooting immune-response via UV-radiation can improve the patient's condition and ease the severity of symptoms of diseases like psoriasis but are also accompanied with negative side-effects, e.g. DNA damage, accelerated skin aging and a higher risk for skin-cancer [El-Ghorr et al., 1997; Honigsmann, 1990].

Absorption of UV light by light-absorbing biomolecules (= chromophores) elicit photochemical and photobiological responses. The chromophore is elevated to an excited state. The chromophore is changed directly due to photochemical reaction or a molecule other than the chromophore can be indirectly changed through energy transfer in a so-called photosensitized reaction. The effects of UV radiation can even be seen in layers that are not reached by the UV light itself – for example, through secretion of proinflammatory mediators.

Short-term effects include alteration and redistribution of existing melanin, increased number of melanocytes, increased melanin synthesis, increased aborization of melanocytes and transfer of melanosomes to keratinocytes, inflammatory filtrates within the skin, vasodilation, formation of sunburn cells (i.e. apoptotic keratinocytes and depletion of Langerhans cells from the epidermis. Pathological consequences are sunburns (solar erythema, blister formation, desquamation); physiologically, UV irradiation leads to pigmentation and thickening of the epidermis with acanthosis and hyperkeratosis. Cells exposed to UV light respond in a variety of ways. Transcription and translation of stress proteins is induced, cell-specific repair processes are started (nucleotide excision repair, base excision repair, translesional DNA synthesis, recombination repair) and several cytokines are produced. If doses are higher so that UV-damage cannot be repaired, cells can either undergo apoptosis or at least cease proliferation, sometimes followed by hyperproliferation of less damaged cells (visible as epidermal thickening).

UV light can have proinflammatory effects and therefore challenge the cutaneous immune system, visible by phototoxic or photoallergic reactions or its effects may be immunosuppressive. UV-mediated immunosuppression may result in negative health effects such as reactivation of herpes labialis after sun exposure, an increased risk of skin cancer but may have also therapeutic effects used for treatment of certain inflammatory skin disorders.

For inducing immune suppression it is not necessary to irradiate the entire body surface since UV irradiation can have a systemic effect and also areas not directly exposed develop tolerance to antigens applied to the skin after irradiation [Toews et al., 1980; Fisher et al., 1977].

Local effects of UV-irradiation include depletion of Langerhans cells from the epidermis or modulation of their functions (ability to present antigens) and/or alteration of their morphology and activation of a variety of signaling cascades in skin cells (release of cytokines, neuropeptides, neuroendocrine hormones). This systemic immunosuppression and tolerance is mediated by regulatory T-cells [Schwarz et al., 2005].

Cellular photoreceptors for UV light are DNA, membrane lipids and proteins and, within the stratum corneum, urocanic acid (UCA).

Urocanic acid is produced in the skin by an enzymatic deamination of the amino acid histidine by the enzyme histidase (histidine ammonia lyase) and accumulates in the stratum corneum.

In vivo experiments have shown, that after UVR exposure LC density decreases – as determined by Ia antigen expression and ATPase staining. Whether LC emigrate, lose various markers, or die remains unknown. The ability to induce CHS (contact hypersensitivity) in mice appears to have a relationship to the density of ATPase-positive cells in the epidermis [references cf 1.5].

Ultraviolet Radiation Effects on Immune Cells in Vitro

- Alters ability of antigen-presenting cells (including Langerhans cells) to present antigen
- Alters the ability of lymphocytes to respond to mitogens or antigens
- Alters cytokine production
- Induces the release of immunosuppressive factors

Ultraviolet Radiation Effects in Vivo

- Induces skin cancer formation
- Alters Langerhans cell morphology and function
- Suppresses the induction of contact hypersensitivity
- Suppresses the induction of delayed-type hypersensitivity
- Alters cell trafficking
- Increases circulating levels of cytokines (IL-1, IL-6)
- Alters proportions of lymphocyte subtypes in peripheral blood

Table 1: Effects of UV-radiation in-vitro and in-vivo [Fitzpatrick's Dermatology in General Medicine, 6th edition, Volume 1; Table 39-1]

1.3 L-Histidine Ammonia Lyase (or Histidase)

The enzyme L-histidine ammonia lyase (EC 4.3.1.3), also referred to as histidase is the producer of endogenous UCA of the stratum corneum. The histidase-encoding gene (HAL) is not only expressed in the epidermis, but also in the liver [Taylor et al., 1990; Eckhart et al., 2008]. Proliferating keratinocytes show very weak to negative expression patterns of histidase, but histidase expression is upregulated during differentiation of human epidermal keratinocytes *in vitro* [Eckhart et al., 2008]. Mutations in the HAL gene cause histidinemia, which is characterized by decreased concentrations of UCA in the blood, urine, and also in the epidermis [Baden, 1969]. UV sensitivity has not been systematically investigated in these patients. In an anecdotal report, two siblings affected by histidinemia showed either normal or increased photosensitivity (Baden et al., 1969).

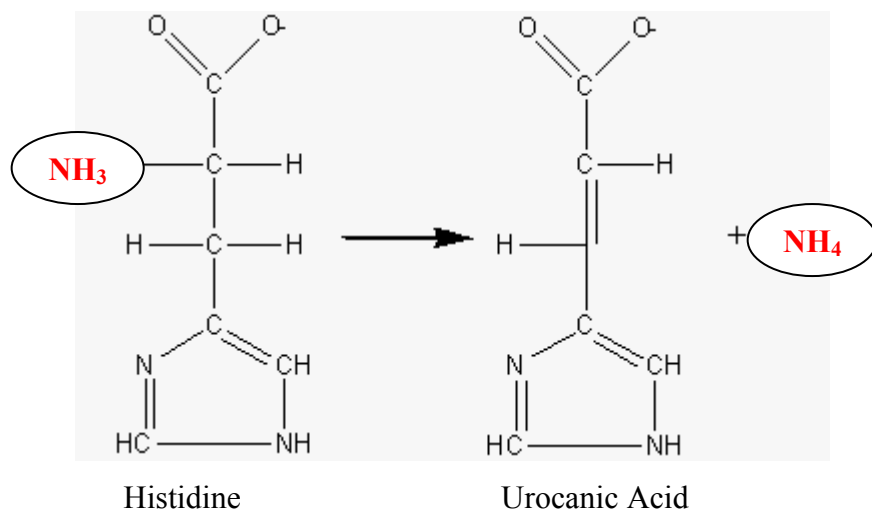


**Figure 2: Conversion of Histidine into Urocanic Acid by deamination.
Responsible enzyme is the L-Histidine Ammonia Lyase.**

1.3.1 Mouse model: mutation of histidase

Peruvian mice, a strain of the house mouse, carrying a spontaneous functional deletion – a mutation of HAL (R322Q) (Fig. 3) – has been described [Kacser et al., 1972; Selden et al., 1995]. Mice were backcrossed into the C57BL/6 background for more than 20 generations [Mellor et al., 2004].

C57BL/6 is the most widely used inbred strain and the first to have its genome sequenced. It is commonly used as a general purpose strain and background strain for the generation of congenics carrying both spontaneous and induced mutations. Although this strain is refractory

to many tumors, it is a permissive background for maximal expression of most mutations. Overall, C57BL/6 mice breed well, are long-lived, and have a low susceptibility to tumors. The C57BL/6J inbred strain was created by Dr. CC Little from the mating of female 57 with male 52 from Miss Abbie Lathrop's stock [JAX Mice Database – 000664 C57BL/6].

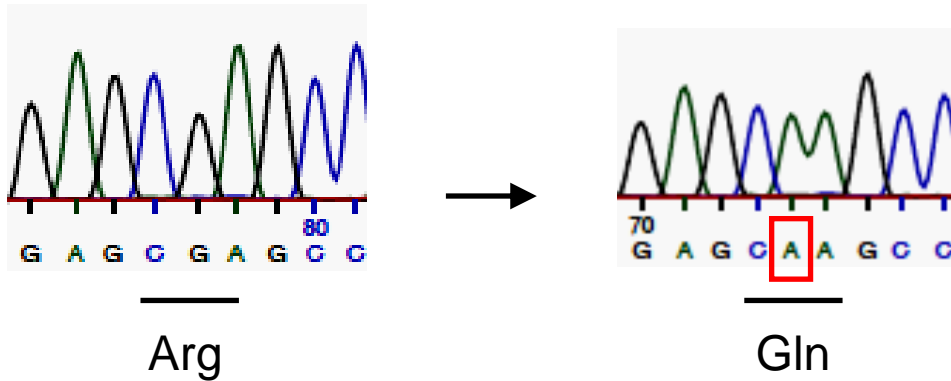


Figure 3: A spontaneous mutation of HAL gene (R322Q) results into Glutamine instead of Arginine at position 322. This leads to lack of Urocanic Acid within the epidermis of his-mutant mice. Phenotype of mice is supposed to be comparable to those of humans suffering from histidinemia.

1.4 The photoprotective role of UCA

1.4.1 DNA damage (thymine-dimer-formation)

The three major steps in photocarcinogenesis are:

- DNA damage
- mutation of the nucleotide sequence
- malignant transformation of cells

UVB-induced immunosuppression is thought to prevent effective elimination of transformed cells.

The two major types of pyrimidine dimers are cyclobutane dimers (CPDs – thymine-thymine dimers, cytosine-thymine dimers, rarely cytosine-cytosine dimers) and 6,4 photoproducts. The damage responses include cell cycle arrest, apoptosis (in other cells than melanocytes), induction of DNA excision repair pathways, change in expression of cell surface proteins, secretion of cytokines, etc., which explains acute effects like erythema and immunosuppression.

The absorption maximum of DNA is at 260 nm. UVC would be most effective to trigger pyrimidine dimer formation in naked DNA. However, UVC under natural conditions does only reach the earth surface in marginal amounts. Within the natural spectrum of solar irradiation, UVB with a wavelength of 300 nm is most effective for inducing DNA photoproducts. While UVA light causes DNA damage indirectly through photoactivation of endogenous and

exogenous photosensitizers [Fu et al., 2002], UVB light possessing higher energy than UVA light, is capable of causing DNA damage directly. UVB-induced DNA damage can result in cytotoxicity, mutagenicity, initiation of tumorigenicity, and formation of skin cancer in humans [Fu et al., 2002; Sarasin et al., 1999; Ahmad et al., 2004]. Indirect damage by UVA, but also by UVB [Xia et al., 2006] occurs after absorption of photons by other chromophores, followed by energy transfer either to DNA or to molecular oxygen, with reactive oxygen species (singlet oxygen, hydrogen peroxide and the superoxide radical) in turn being able to damage DNA [Bologna, Jorizzo, Rapini et al., *Dermatology*; Fitzpatrick's *Dermatology In General Medicine*, 6th edition].

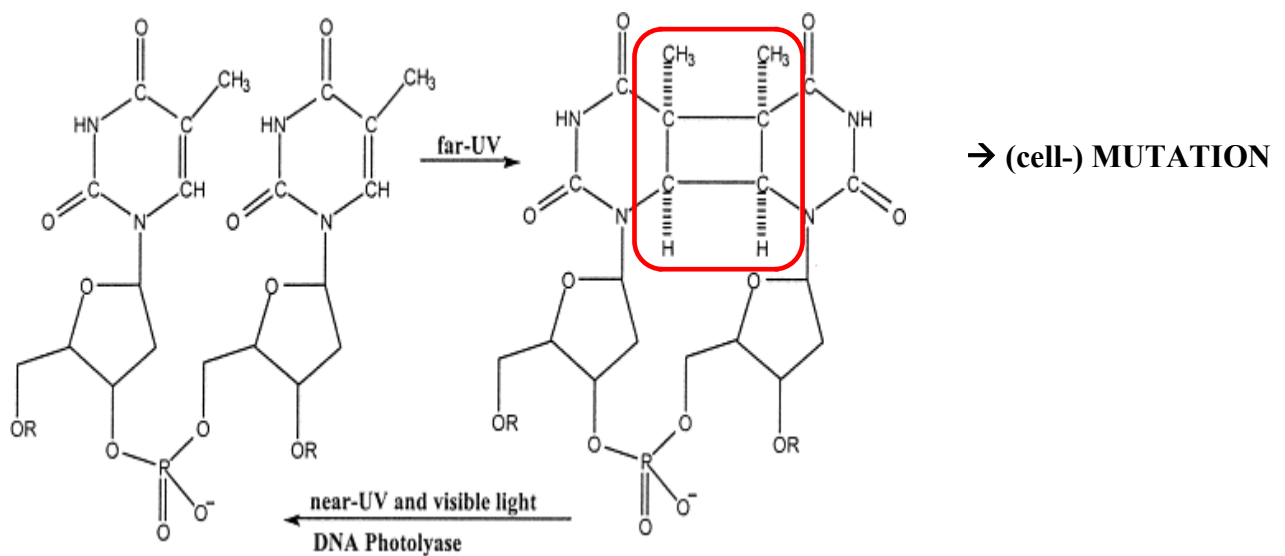


Figure 4: UV light induced thymine dimer formation (*cis-syn* stereoisomer) between two adjacent thymine bases in the same strand of a DNA molecule, possibly generating a mutated cell later on. The photoreactivation process is catalyzed by DNA photolyase, which uses near-UV and visible light [Durbeej B. and Eriksson L., 2002].

1.4.2 Effects of UVB light on tissue integrity and photoaging of the skin

Besides DNA damage, UV light has several other deleterious effects. Exposure to sun has acute short-term effects as well as chronic long-term effects. These effects include sunburns, photoaging, sun-induced carcinogenesis and immune-modulation within the skin. Cellular changes as well as qualitative and quantitative alterations of dermal extracellular matrix proteins are involved, resulting in loss of recoil capacity and tensile strength with wrinkle formation, increased fragility and impaired wound healing [Wlaschek et al., 2001]. The generation of oxidative stress in skin cells via interaction with intracellular chromophores and photosensitizers results in transient and permanent genetic damage. Oxidative stress due to UV

light can also activate cytoplasmic signal transduction pathways that are related to growth, differentiation, replicative senescence and connective tissue degradation [Wlaschek et al., 2001]. ROS (reactive oxygen species), generated by UV light are not only known to play an essential role in collagen oxidation and degradation but also interfere directly with signal transduction pathways involved in the expression of collagen-metabolism involved genes. Low levels of ROS are continuously produced in vivo and are involved in physiological processes. There is accumulating evidence for the damaging effects of higher concentrations of ROS generated in vitro and in vivo following UV (UVA and UVB) radiation of the skin [Jurkiewicz et al., 1996; Masaki et al., 1995; Yasui et al., 2000]. UCA has also been suggested to be responsible for UVR-linked photoaging and failure of tissue integrity. The excitation of trans-UCA initiates chemical processes that result in the photoaging of the skin. The excited trans-UCA subsequently reacts with oxygen, which results in the generation of ROS [Hanson et al., 1998]. Singlet oxygen (one of the cis-UCA generated ROS), can initiate lipid peroxidation of cellular membranes [Brenneisen et al., 1998] accompanied with the generation of carbonyls.

1.5 Effects of UVB-induced cis-Urocanic Acid on Langerhans cells

1.5.1 Skin – immunology

The skin represents one of the major barriers against environmental injuries and protects from microbial, chemical and physical insults.

The capacity of the skin to generate an immune response resides in the so called skin-associated lymphoid tissues (SALT). It consists of antigen-presenting cells (e.g. Langerhans cells) capable of communicating with T- and probably non T-lymphocytes, cytokine-producing keratinocytes (depending on their state of activation) and the regional draining lymph nodes [Bolognia, Jorizzo, Rapini et. al., Dermatology]. Two major immune response mechanisms have been identified. The classical pathway is called the “adaptive immune response” and is characterized by the immunologic memory. The more primitive pathway which is more rapid but less specific and requires no memory is referred to as innate immunity. Both of them can be initiated in the skin. Under certain conditions immune responses can overshoot and cause harmful allergic and autoimmune reactions and results in skin diseases (dermatoses), which might require treatment with immunosuppressive therapies [Bolognia, Jorizzo, Rapini et. al., Dermatology].

1.5.2 Innate immune system

Essential components of the innate immunity are neutrophils, eosinophils, natural killer cells, mast cells, cytokines, complement, and antimicrobial peptides.

Toll-like receptors are a family of pattern recognition receptors that mediate responses to pathogen-associated molecular patterns (PAMPs) that are conserved among microorganisms.

Human epithelia, including the epidermis, secrete antimicrobial peptides and exert innate chemical defence (e.g. psoriasin).

Cytokines are secreted messenger molecules which may modulate immune responses. They are secreted by a wide variety of cell types and can act in an autocrine, paracrine or endocrine manner. Differences in composition of cytokines during an immune response are able to affect the final biological response [Kuby et.al., Immunology]

Macrophages are phagocytic cells differentiated from blood-borne monocytes, which can engulf microorganisms as well as process and present antigens to T- and B-cells. Neutrophils circulate in the bloodstream or roll along the vascular endothelium and are recruited by chemoattractants and chemokines to sites of infection/inflammation.

Eosinophils are weakly phagocytotic cells and protect the host from infections by parasites by release of toxic products after activation via IgE to kill the parasite.

Basophils (found in the blood) and Mast Cells (found in the tissues) play an important role in immediate anaphylactic allergic reactions and hypersensitivity reactions as they release a variety of immune response mediators (e.g. histamine, serotonin...) after crosslinking of surface-bound IgE molecules.

Natural Killer Cells eliminate infected or malignant cells (due to viral infection and other intracellular infections, tumour cells...) [Bolognia, Jorizzo, Rapini et. al., Dermatology].

1.5.3 Adaptive immune system

The adaptive immune response is – in contrast to the innate immunity – antigen-specific and has the ability to augment with each successive encounter with the same antigen. Therefore, antigen presentation is a critical event.

Dendritic cells are the most effective antigen-presenting-cells (APCs). They are located in the T cell areas of the spleen and lymph nodes. Within the epidermis, **Langerhans cells (LCs)** are the relevant APCs and are specialized to induce and regulate T cell immunity and tolerance [Banchereau and Steinman, 1998; Steinman and Nussenzweig, 2002]. Langerhans cells are dendritic cells, which form a contiguous network within the epidermis and are able to take up invading pathogens or antigens [Romani et al., 2003]. LC are Ia-bearing and they are derived

from bone marrow. After antigen contact LC can leave the epidermis and can be found in dermal lymphatics and in the draining lymph nodes where they are supposed to present antigens to T cells [Romani et al., 2003].

Langerhans cells contain rod-shaped organelles termed Birbeck granules. Fate and functions of Birbeck granules are still not fully identified and understood. Langerin, a Ca²⁺-dependent lectin with mannose-binding specificity was found to be associated with Birbeck granules and even to induce formation of Birbeck granules. If Langerin captures antigens, induction of Birbeck granules appears to be a consequence, allowing routing of antigen into these organelles.

Another class of APC within the skin are dermal DC (dermal dendritic cells), which are located in the dermis, underlying the epidermis. They are phenotypically and probably also functionally distinct from LC. However, a subset of dermal DC expresses langerin [Nagao et al., 2009]. This recent discovery calls for a careful reinvestigation of the proposed roles of LC, previously presumed to represent the entire langerin-positive cell population in the skin and the until then believed pivotal role of LC in the initiation and control of skin (auto-)immunity and allergy [Schuler and Steinman, 1987; Cumberbatch et al., 2003; Romani et al., 2003] and also by findings that LC do not initiate essential T-cell responses to viral antigens [Allan et al., 2003; Allan et al., 2006] or initiate contact hypersensitivity reactions in murine models [Bennett et al., 2007; Bennet et al., 2005; Kissenpfennig et al., 2005].

Visualization of LCs can be achieved by staining for adenosine triphosphatase (ATPase) and a variety of antigenic determinants such as panhematopoietic marker CD45, MHC class II antigens (HLA-DR), CD1a, S100 protein, vimentin and langerin. Murine LCs are stained for MHC class II antigens in most studies.

CD34⁺ precursor cells can develop into Langerhans cells or a monocyte/macrophage phenotype which ultimately differentiates into non-Langerhans dendritic cells.

Presence of particular cytokines decides about differentiation pathway. If TNF- α and GM-CSF are present, dermal dendritic cells develop. IL-3, stem cell factor (SCF) and Flt3-ligand can amplify the effects of GM-CSF and TNF- α . TGF- β shifts differentiation into LC development. The mechanisms of homing LCs into the epidermis and maturational stage in which LCs enter the epidermis remain to be determined. Recent evidence shows that under steady-state conditions, LCs are maintained locally and only or mostly inflammatory changes in the skin result in their replacement by blood-borne progenitors [Bolognia, Jorizzo, Rapini et. al., *Dermatology*; Fitzpatrick et. al. *Dermatology In General Medicine*, 4th edition].

1.5.4 UV radiation influences the immune system of the skin and alters LC function and morphology

Ultraviolet light is known to influence the immune system of the skin and to affect Langerhans cells as the major APC within the epidermis. LCs are important targets in the induction of UVB-induced immunosuppression: (1) UVB irradiation of skin leads to their dose-dependent reduction and injury [Toews et al, 1980]; (2) the injection of purified UVB-irradiated LCs into naïve mice not only fails to sensitize, but even tolerizes these animals [Cruz et al, 1989]; and (3) UVB irradiation of single LCs leads to a dose-dependent inhibition of their immunostimulatory properties [Stingl et al, 1981; Fitzpatrick et al, 4th edition], cell-mediated immunity is downregulated and morphology, surface markers and number of Langerhans cells are altered and clearly differ from normal homeostatic conditions.

This altering effect of UVB radiation on both morphology and phenotype of LC is clearly dose- and wave-length dependent [Aberer et al., 1981; Aberer et al., 1986; De Fabo et al., 1979; Noonan et al., 1981].

The impact of UVB radiation on the immune system of the skin and density as well as function of Langerhans cells has been matter of many projects and publications with partly contradictory outcomes [Aberer et al., 1981; Aberer et al., 1986; Toews et al., 1980; Bergstresser et al., 1980].

Some publications proposed that the density of LCs within the epidermis determines immune-responses and its outcome towards an antigen introduced via the skin [Toews et al., 1980; Elmetts et al., 1983]; others differ from those proposed mechanisms as they haven't found any visible changes in number, phenotype or structure of Ia-positive/ADPase-positive ECs after high-dose UVB treatment but only a significant reduction or depletion of surface markers [Aberer et al., 1986].

UVB-induced LC decrease in the epidermis can be explained by two mechanisms [Kolgen et al., 2002]: one explanation is demonstrated migration of structurally altered and functionally impaired LC from the epidermis to the regional draining lymph nodes [Vink et al., 1996; Dandie et al., 1998]. Application of FITC (fluorescein isothiocyanate) to UVB-exposed skin showed a migratory effect, as number of FITC+ and Ia+ cells with pyrimidine dimers increased in the draining lymph nodes. Second explanation is that the induction of apoptosis in remaining epidermal LC might be responsible for depletion of cell markers and immunosuppression [Schwarz et al., 1998; Nakagawa et al., 1999]. Another proposed mechanism of UVB-induced immunosuppression is UVB-induced DNA damage to epidermal LC as initiating event for migration [Vink et al., 1997].

In man, high doses of UVB cause heavy damage to Langerhans cells, leading to cell death as shown by electron microscopy [Mommas et al., 1993] and Langerhans cells undergo apoptosis in situ after UVR treatment [Obata et al., 1985].

Reports of impaired LC migration capacity and their accumulation in the dermis [Kolgen et al., 2002] are contradictory to reports that migration of LCs is increased after UVB irradiation and that LC migration into the draining lymph nodes is altered due to UVB irradiation [Schwarz et al., 2005; Vink et al., 1996; Bennett et al., 2005; Duthie et al., 2000]. Secretion of tumour necrosis factors (TNF- α) and interleukins are also reported to be altered and to interact with immunocompetent cells and modulate their behaviour [Kock et al., 1990; Yoshikawa and Streilein, 1990; Beissert et al., 2001; Timares et al., 2008].

1.5.5 Urocanic acid acts as UVB photoreceptor

Molecules that directly absorb the energy of UV radiation and undergo a conformational or structural change due to UVR-absorption are biologic receptors of UV damage. DNA is one identified photoreceptors within the skin. By undergoing a structural change (cf 1.4.1) UVR-induced damage acts as an alarm signal and several cellular photodamage response mechanisms become activated. Urocanic acid (UCA), by undergoing a trans- to cis-isomerisation on to exposure to UV, has been proposed to act as another major UVB photoreceptor [Zenisek et al., 1955; Tabachnik, 1957]. In a dose-dependent response, this photoisomerisation from trans- to cis-UCA takes place until the photostationary state is reached, with approximately equal quantities of the two isomers. The elevation of epidermal cis-UCA levels lasts for at least one week following UV irradiation [Norval et al., 2002].

UCA has a high extinction coefficient in the wavelength range from 260 to 310 nm [Zenisek et al., 1955; Tabachnik, 1957], its maximum efficiency of photoisomerisation occurs at about 300-310 nm in vivo in mouse and human skin [Gibbs et al., 1993], although wavelengths in the UVA range (315 – 400 nm) can also induce cis-UCA formation [Kammeyer et al., 1995].

The ability of UCA to absorb UVB under conditions present in the outermost layer of the skin was confirmed by topical application of UCA onto human skin which led to an increase in photoprotection [Baden and Pathak, 1967]. For several years UCA was used as a component of commercial sunscreens until reports about the immunosuppressive properties of cis-UCA, the conversion product of trans-UCA upon UV absorption, prompted the withdrawal of UCA-containing sunscreens from the market [Andersen, 1995]. The immunosuppressive effects of UVB were mimicked by topically applied cis-UCA on the skin or intraepidermal injected cis-UCA [Hemelaar et al., 1996; Norval et al., 1995; Noonan et al., 1988; Jaksic et al., 1995].

Furthermore, UCA has been suggested to account for the action spectrum of photoaging [Hanson et al., 1998]. Cis-UCA reacts subsequently with oxygen, resulting in the generation of ROS including superoxide anion radical (O⁻²) and singlet oxygen. Singlet oxygen and hydroxyl radicals (which can be generated from anion radicals) can initiate lipid peroxidation of cellular membranes [Brenneisen et al., 1998] with the generation of carbonyls.

The immunomodulative effect could be the conversion of trans-urocanic acid into cis-urocanic acid by providing or acting as a signaling molecule. Topically applied UCA does not photobind to DNA of keratinocytes, indicating that UCA does not transmit the immunosuppressive signal via UCA-DNA photoadducts [Ijland et al., 1998]. Recently the serotonin (5-hydroxytryptamine (5-HT) 2a) receptor was shown to bind cis-UCA and mediate suppression. UV- and cis-UCA-induced immunosuppression was blocked by antiserotonin antibodies or with 5-HT_{2a} receptor antagonists [Walterscheid et al., 2006; Idzko et al., 2004; Gordon et al., 2007; Slominski et al., 2003]. This serotonin receptor or its gene has been shown to be expressed by human dendritic cells (DC), monocytes, mast cells, activated murine T-cells and keratinocytes.

1.5.6 UCA as signaling molecule for LC migration

Cis-UCA is thought to promote systemic suppressive effects that occur with high doses of UV-irradiation [Moodycliffe et al., 1992; El-Ghorr et al., 1997]. In mice, given a histidine-rich diet, the total UCA concentration increased significantly compared with the concentration in mice fed a normal diet. Following UVB exposure, the suppression of contact hypersensitivity was significantly higher in the former group [Reilly et al., 1991].

The direct effect of UVB and cis-UCA on Langerhans cells and effects on local tolerance mechanisms have not been shown or fully proven yet. Both arguments for [De Fabo et al., 1983; Kurimoto and Streilein, 1992] and against [Moodycliffe et al., 1992; El-Ghorr et al., 1997] such effects have been put forward in the past. Trans-UCA can be seen as protective factor in the development of UV-induced skin cancer as it prevents DNA damage by absorbing radiation. Otherwise, its UV-induced conversion product cis-UCA downregulates the immune system, which enables survival of UV-damaged cells and development of malignant tumor cells.

Immunosuppressive effects of cis-UCA have been demonstrated, including the cis-UCA-induced decrease of epidermal LC numbers and reduction in antigen-presenting function [El Ghorr et al., 1995], suppression of contact hypersensitivity in mice after intradermal injection

[Kurimoto et al., 1992] and suppression of delayed-type hypersensitivity to herpes simplex virus in mice after subcutaneous or epicutaneous administration [Gilmour et al., 1992].

A single epicutaneous application of cis-UCA on murine ears is sufficient to reduce the number of Langerhans cells by 62% whereas the control application of trans-UCA leads to a reduction of Langerhans cells by only 13% [Norval et al., 1990]. In addition a change in morphology from dendritic to round has been observed. Interestingly, chronic intradermal administration of cis-UCA did not lead to a reduction in Langerhans cell numbers when measured after the end of the treatment, suggesting that mechanisms exist which allow for repopulating the Langerhans cells if the animal is chronically exposed cis-UCA [El Ghorri et al., 1997].

Many hypotheses around the mechanism underlying this change in immunocompetent skin cells have been suggested, but none have resulted in a satisfying conclusion. The most likely explanation appears to be a multicomponent pathway consisting of interaction between several pathways and signaling molecules.

In the present study, the impact of endogenously produced UCA on the number of Langerhans cells in the skin after UVB irradiation, the change of number in Langerhans cells in the epidermis after UVB irradiation was investigated in a mouse model – comparing wild type C57 BL/6 mice and C57 BL/6 histidase-mutant-mice.

2. AIM OF THESIS

The aims of the study were

- (1) to determine the UV-induced DNA damage in histidase-mutant and in control mice, measured in enhanced apoptosis and thymine-dimer formation
- (2) to determine the impact of UVB irradiation on the number of Langerhans cells in the skin of histidase-mutant and in control mice.

Comparison of the UV sensitivity of histidase-mutant mice and wild-type mice should allow testing both the protective role of UCA against UV-induced DNA damage and the immunosuppressive role after UV-induced isomerisation. Another aim was to determine whether lack of the immunosuppressive response after UVB-irradiation in histidase-deficient mice depends upon less absorption of UVB by UCA (leading to penetration of more UVB light into the skin) or directly upon suppression of UCA-isomerization. This part of my diploma thesis analyses which role urocanic acid in the skin plays in the UVB-triggered decrease of Langerhans cell in the epidermis. Experimental procedures were set to find the UVB dose yielding the maximum difference in DNA damage, number of Langerhans cells in the epidermis and morphology of LCs.

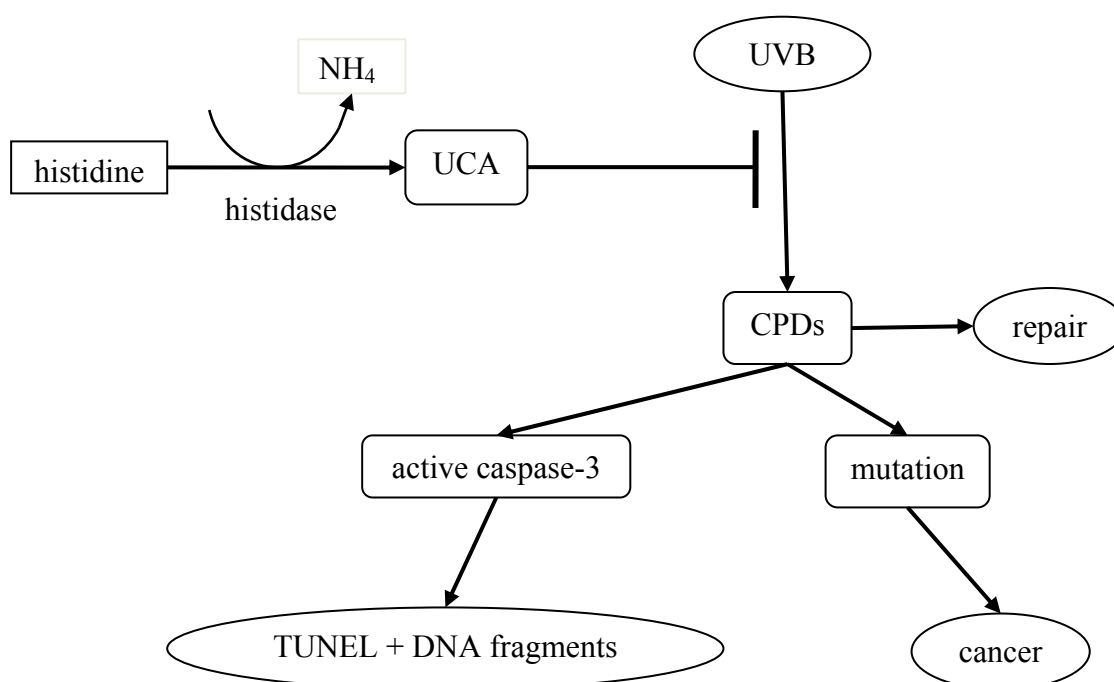


Figure 5: Short scheme of thesis showing the effects of UCA on UVB-induced DNA damage. Lack of UCA in the epidermis leads to enhanced formation of CPDs. If repair is insufficient, apoptosis is induced or mutations within the DNA can lead to malignant cells and cancer.

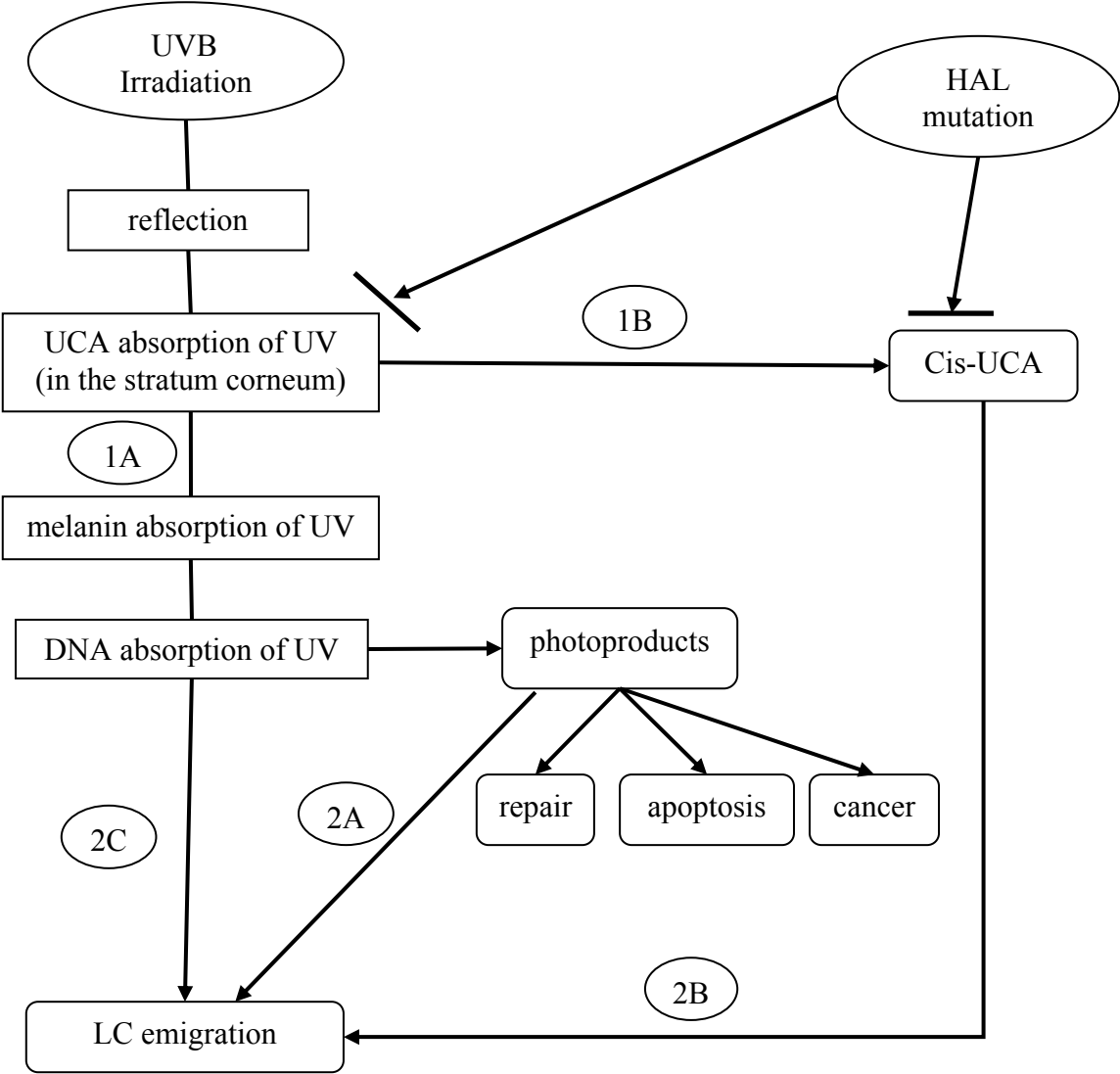


Figure 6: Scheme of thesis showing the effects of UVB irradiation on the skin and possible mechanism-failure resulting from the mutation in HAL gene and lack of histidase. UCA is acting photoreceptor for UVB radiation – less UVB radiation can reach deeper layers of the skin (1A) and is simultaneously UVB-induced converted into its cis-form (1B). Three proposed mechanisms cause LC emigration and following immunosuppression: the generation of photoproduct due to DNA absorption of UV light (2A); UV(B)-generated cis-UCA as a signaling molecule for emigration (2B) or DNA damage itself as initiating signal for LC alteration (2C).

3. RESULTS

3.1 The photoprotective role of endogenous UCA

Urocanic acid is generated from the amino acid histidine by the enzyme histidase, also known as L-Histidine Ammonia Lyase (HAL). It is constitutively present in normal stratum corneum of mice and humans. Previous studies have proven that exogenous supplied UCA protects against UVB damage. The photoprotective effect of endogenous UCA has not been tested yet. Furthermore, it has been suggested, that the cis-isomer of UCA may be involved in immunosuppression [Walterscheid et. al., 2006; Eckhart et al., 2008].

3.1.1 The mutation of HAL destabilizes the histidase protein

At first, we aimed to determine which step of the expression of histidase is deficient in histidinemic mice. Amounts of histidase mRNA were compared between wild-type and mutant mice was investigated by quantitative Real-Time-PCR using house-keeping genes ALAS (aminolevulinic acid synthase) and β 2M (β -2-microglobulin) as reference-genes and normalization factors. Results showed no significant difference in the levels of histidase mRNA. Both wild-type C57BL/6 and histidase-mutant C57BL/6 express the HAL-gene at equally levels within the skin (Fig. 7).

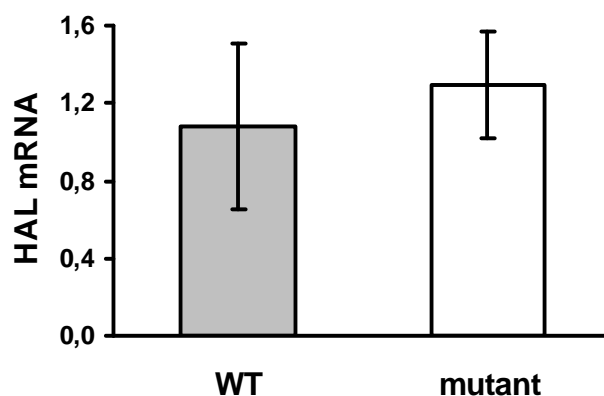


Figure 7: Histidase mRNA in the skin, measured by qRT-PCR; standardized upon the expression of house-keeping-genes β 2M. Bars indicate mean +/- SD. The difference between WT and mutant mice is not significant.

Protein expression patterns were analysed by Western blotting, using an antibody against the conserved C-terminus of histidase. In lysates of wild-type epidermis a protein band at the

predicted size of histidase was detected whereas this band was absent in homozygous mutant mice (Fig. 8A). Liver lysates of mutant mice showed some formation of full length histidase-protein but clearly less than in wild-type liver (Fig. 8B).



Figure 8A: Histidase-protein expression in the epidermis of wild-type (left band) and his-mutants (right band). A protein band at predicted size of 72 kDa is completely absent in his-mutant epidermis lysates.

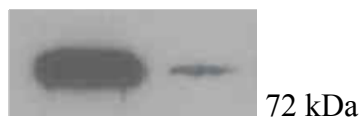


Figure 8B: Histidase-protein expression in the liver of wild-type (left band) and his-mutants (right band). Small amounts of full length his-protein are also detectable in liver lysates of mutant-mice.

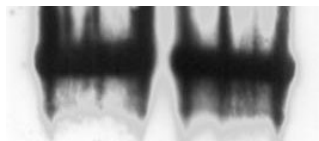


Figure 8C: Western Blot keratin-control. Amounts of expressed keratins are equal in both Wild-type (right band) and histidase-mutants (left band).

This gene expression analysis suggests that the point mutation in the Hal gene affects a posttranscriptional step and does not inhibit proper mRNA-transcription or stability. Inhibition or retardation of histidase-protein expression or protein destabilization/accelerated breakdown leads to a strong decrease in the abundance of the protein at its natural sites of expression.

Immunofluorescence labelling of loricrin demonstrated that keratinocyte terminal differentiation is normal in both, WT and mutant mice [Barresi et al., 2009; unpublished data].

Additional immunohistochemical staining of murine liver showed high histidase expression in the areas surrounding the portal tracts of wild-type liver whereas no histidase expression was visible in his-mutant mice and an immunohistochemical screening of murine tissues revealed that histidase was not expressed in the oral epithelium, esophagus, stomach, hair follicle, nail matrix and thymus [data not shown].

3.1.2 Mutant mice have a reduced UCA content in the stratum corneum and show suppression of UVB absorption capacity of the stratum corneum

Urocanic acid is the product of L-histidine ammonia lyase. Considered consequence of the absent UCA-generating enzyme histidase would be a diminished concentration if not deficiency of UCA in the epidermis of his-mutant mice. We evaluated the concentration of UCA in the stratum corneum of untreated and UVB-irradiated wild-type, heterozygous and homozygous mice. Mice were shaved on their backs and back skin or irradiated back skin was tape-stripped. By HPLC concentrations of all tape-strips were determined. Stratum corneum of untreated wild-type and heterozygous mice contained roughly 10 times more UCA than that of homozygous mutant mice (Fig. 9A). Concentrations of cis-UCA within the stratum corneum after UVB irradiation (250 mJ/cm²) were significantly higher in wild-type mice than in mutant mice (Fig. 9B).

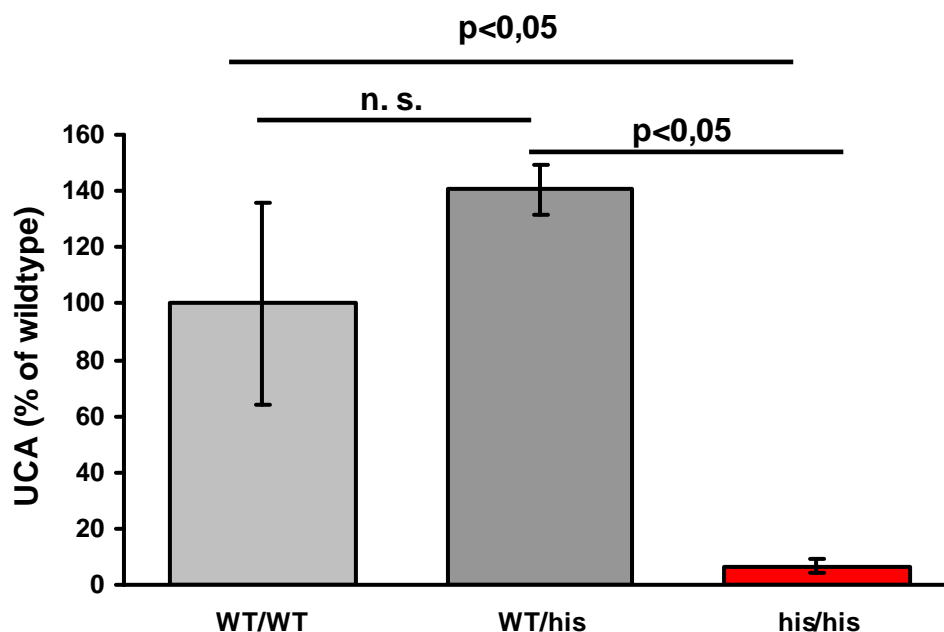


Figure 9 (A): Determination of concentration of urocanic acid in the epidermis of wildtype, his-heterozygous and his-homozygous-mutant mice. Concentrations relative to the mean value of WT mice (100%) are shown. Tape-strips were taken from shaved back skin; UCA determination was proceeded by HPLC. UCA concentration is highly decreased in homozygous-mutant mice compared to wildtype mice and mice heterozygous for the HAL-mutation. Mice per group: n = 3; bars indicate mean +/- SD. Statistical analysis was determined using student's t-test.

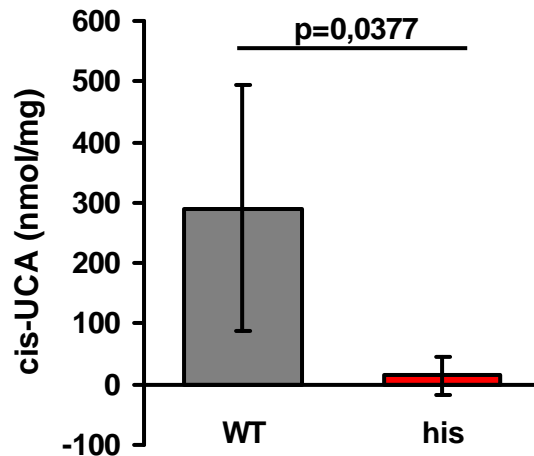


Figure 9 (B): concentration of cis-UCA in the epidermis of wildtype and his-mutant mice after UVB irradiation proceeded by HPLC. Mice per group: n = 5; bars indicate mean +/- SD. Statistical analysis was determined using student's t-test.

3.1.3 UV absorption by stratum corneum extracts is reduced in mutant mice

In an additional experiment we wanted to determine the absorbance of stratum corneum extracts in the UV range. We tape-stripped shaved backs of wild-type, heterozygous and homozygous mice and extracted this tape strips with an aqueous buffer. At a wavelength of 220 nm (an absorbance that corresponds to the absorption by peptide bonds of soluble proteins) there was no significant difference between wild-type, heterozygous and homozygous mutant mice (Fig. 10 and data not shown). Shape of absorption curves of wild-type stratum corneum (Fig. 10) and heterozygous stratum corneum strongly resembled that of UCA [Hanson and Simon, 1998]. Absorption maximum by both UCA-isomers occurs mainly in the region of 270 nm (at approximately 277 nm) under physiological conditions, with the absorption varying characteristically with pH and the cis-isomer showing a minimal lower overall molar absorptivity [Brookman et al., 2002].

In our assay, homozygous mutant mice showed a decreased absorbance at the wavelength of 280 nm. Compared to heterozygous or wild-type mice, absorption was decreased by 94% in his-mutant mice (Fig. 11 and data not shown). The absorption capacity of stratum corneum extracts from homozygous mice was clearly reduced at all wavelengths of the UVB range (Fig. 10 and data not shown).

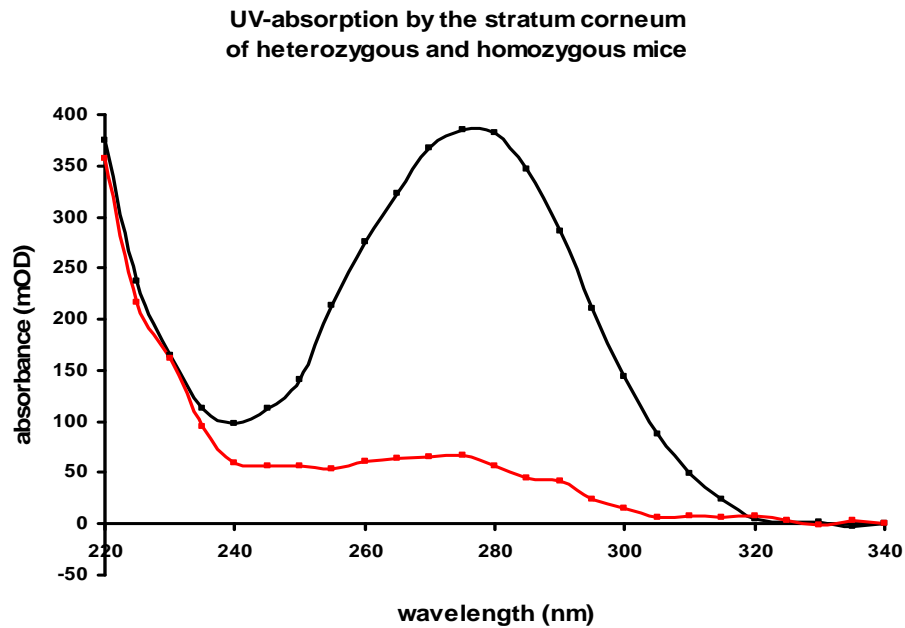


Figure 10: Tape-strips from shaved back skin. Extraction with PBST. Photometric analysis of skin-extracts. Absorbance at a wavelength of 280 nm is highly decreased in homozygous mutant-mice (red) compared to heterozygous mice (black).

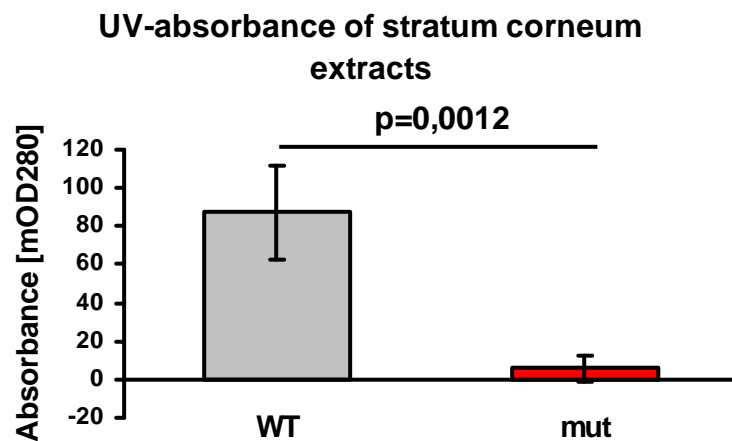


Figure 11: Comparison of UV-absorbance of stratum corneum extracts WT vs. mutant mice at a wavelength of 280 nm. Mice per group: n=5; bars indicate mean +/- SD. Difference between WT and mutants: -94%. Statistics were performed with t-test with p=0.001.

3.1.4 Effect of UVB radiation on DNA damage and thymine-dimer-formation

As most of the UVB is absorbed in the epidermis, formation of cyclobutane pyrimidine dimers by UVB irradiation is mostly caused in the cells of the epidermis with only some CPDs detectable also in dermal cells (Fig. 12).

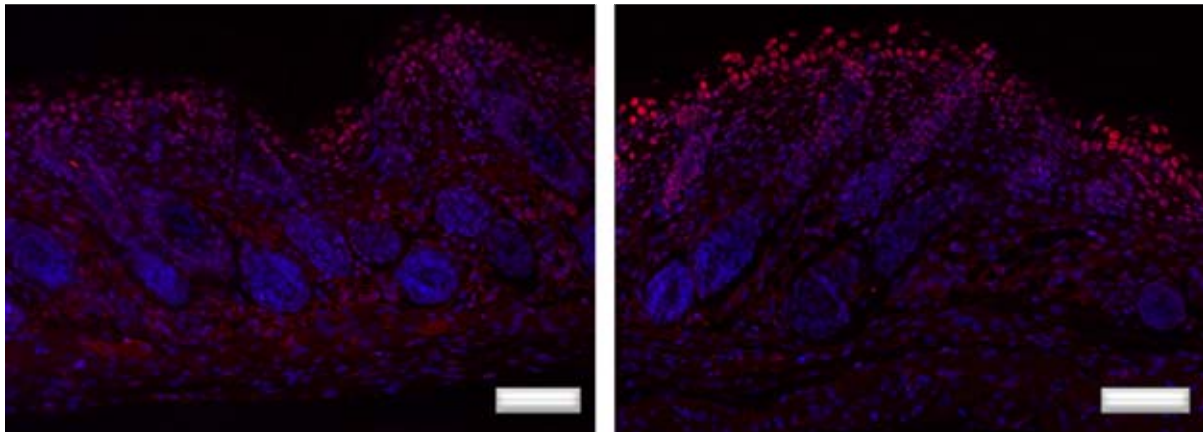


Figure 12: anti-CPD + Hoechst staining of prepared skin of heterozygous (WT/mut) mice (left) and homozygous (mut/mut) mice (right) 24 hours after irradiation. The nuclei of skin homozygous mutant mice were consistently more anti-CPD-positive than the nuclei in the skin of their heterozygous littermates. bar: 40 μ m.

As a control to the data obtained by the immunofluorescence studies, an ELISA-assay was used to compare the levels of UVB-induced DNA damage in mice carrying at least one wild-type allele of HAL and homozygous mutant mice. Newborns and shaved back skin of adult mice were irradiated with a lamp that emits light in the UVB range with a peak emission at 313 nm. DNA of irradiated epidermis was extracted and DNA damage was analyzed and quantified with an ELISA specific for CPDs. Increase of DNA damage 1 hour after a high-dose of 250 mJ/cm² of UVB light in newborn homozygous mutant mice was about 80% more compared to DNA damage in the epidermis of their heterozygous littermates (Fig. 13A). In adult mice increase of DNA damage 24 hours after irradiation was still 40% stronger in homozygous mice than in age-matched WT-mice (Fig.13B). UCA-deficient mice are significantly more sensitive to UVB-induced CPD formation.

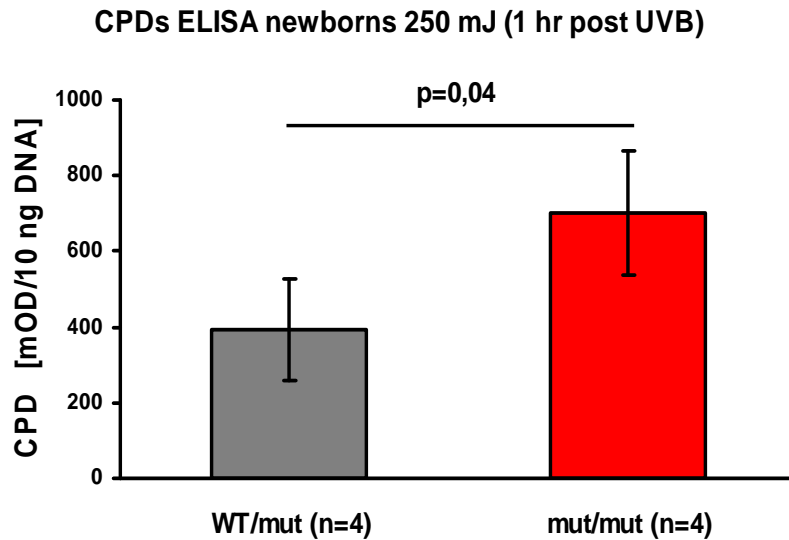


Figure 13A: Quantification of DNA damage in heterozygous and homozygous newborns 1 hour after UVB irradiation with a dose of 250 mJ/cm². Mean OD in WT/mut: 0,391 (standard deviation: 0,134) and in mut/mut: 0,702 (standard deviation: 0,166). Increase in mutants: 79,8 %. Bars indicate mean +/- SD.

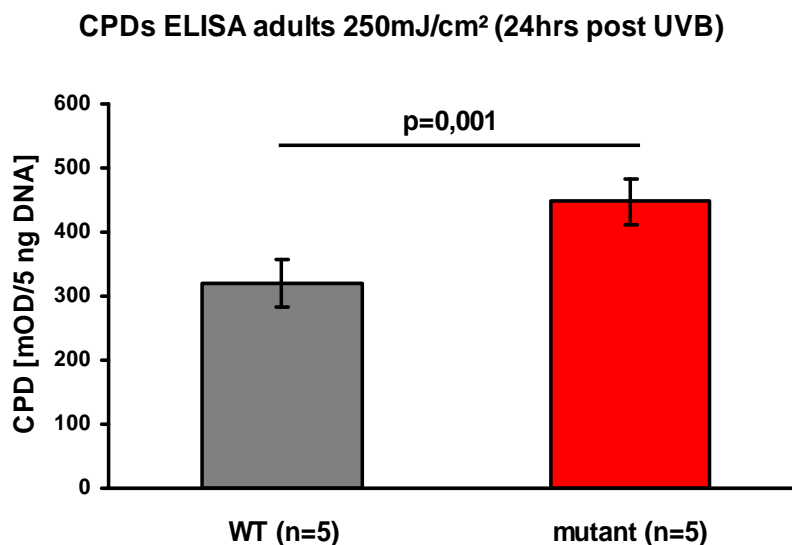


Figure 13B: Quantification of DNA damage in wild-type and homozygous adults 24 hour after UVB irradiation with a dose of 250 mJ/cm². Mean OD in WT/WT: 0,320 (standard deviation: 0,038) and in mut/mut: 0,448 (standard deviation: 0,036). Increase in mutants: 40,1 %. Bars indicate mean +/- SD.

Lower doses of UVB (i.e. 25 mJ/ cm²) resulted in a significant increase in CPD formation in mutant mice compared to their wild-type conspecifics or compared to their littermates with at least one wild-type allele of the histidase gene (Fig. 14A, B).

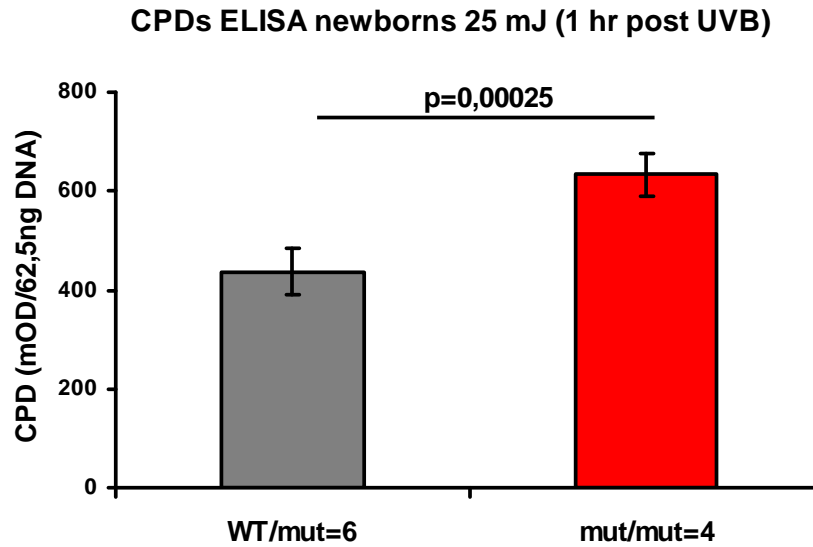


Figure 14A: DNA damage in the epidermis of heterozygous and homozygous littermates 1 hour after UVB irradiation with 25 mJ/cm². Mean OD in WT/mut: 0,437 (standard deviation: 0,048) and in mut/mut: 0,634 (standard deviation: 0,043). Increase: 44,9%. Bars indicate mean +/- SD.

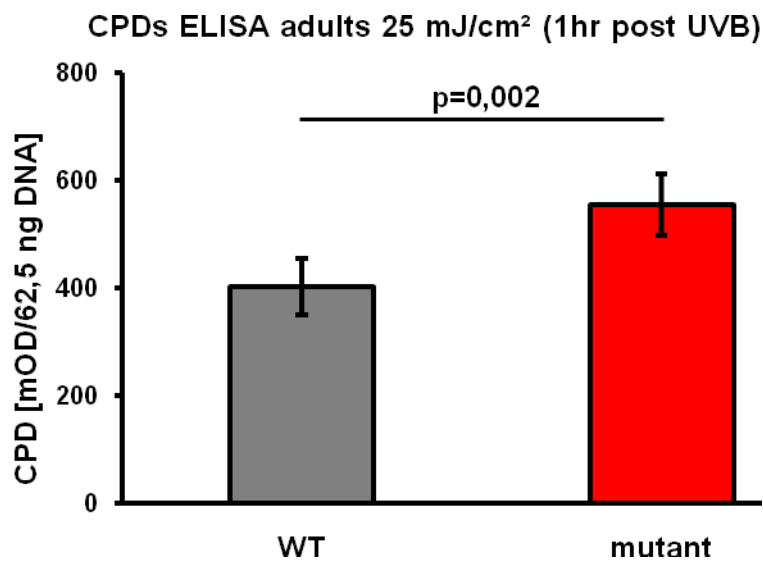


Figure 14B: DNA damage in the epidermis of age-matched wild-type and homozygous mutant mice 1 hour after UVB irradiation with 25 mJ/cm². Mean OD in WT: 0,402 (standard deviation: 0,052) and in mutants: 0,554 (standard deviation: 0,057). Increase: 37,8%. Bars indicate mean +/- SD.

3.1.5 Effect of UVB radiation on apoptosis

As our previous results have shown that the UVB-dependent formation of CPDs is highly increased in histidinemic mice we investigated whether this increase would lead to a similar increase in DNA damage-induced apoptosis. Cell apoptosis, also known as programmed cell death, is a well-characterized response to DNA damage. This cellular suicide program utilizes

specific proteases of the caspase family, in particular the executioner caspase, caspase-3 to cleave a broad range of survival proteins as well as an inhibitor of an exonuclease in order to trigger cleavage of nuclear DNA [Enari et al., 1998]. The TUNEL-assay is another indicator for programmed cell death as it marks nuclei containing DNA fragments with free 3'-OH ends, which occurs during and after breakdown of nuclear DNA. We determined the average number of apoptotic cells by counting cells for activation of caspase-3 (with an antibody against the active form of caspase-3) and nuclei positive for DNA-breakdown in the epidermis after UVB irradiation. The number of apoptotic cells was increased in both wild-type and histidase-mutant mice as a result of DNA damage. However, increase of cell apoptosis within the epidermis of homozygous mice was significantly higher compared to wild-type mice 24 hours after UVB irradiation with 250 mJ/cm² (Fig. 15A, B).

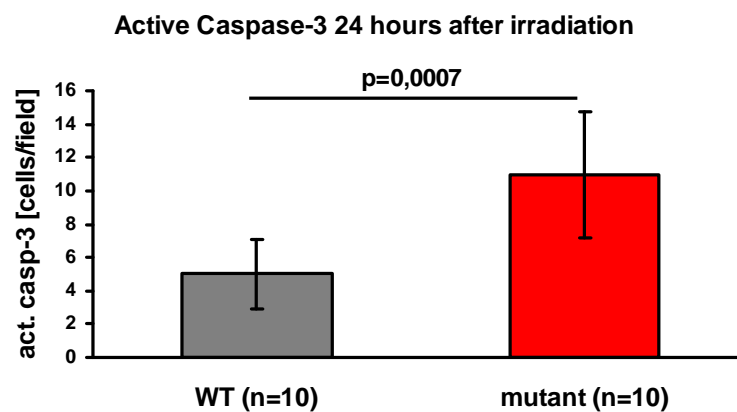


Figure 15A: Active Caspase-3-positive cells (cells/field of view) 24 hours after UVB irradiation (250 mJ/cm²). Mutant mice have more than twice as much apoptotic cells than wild-type mice (increase of 119%); p= 0,00069. Bars indicate mean +/- SD.

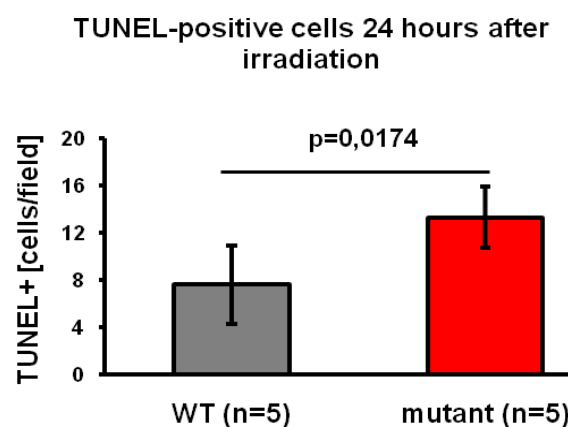


Figure 15B: TUNEL-positive cells (cells/field of view) 24 hours after UVB irradiation (250 mJ/cm²). 3 different cross sections/per mouse were stained and counted. Mutant mice have significantly more TUNEL-positive cells than wild-type mice (increase of 75,07 %); p= 0,0174. Bars indicate mean +/- SD.

3.1.6 Effects of UVB radiation on skin-morphology

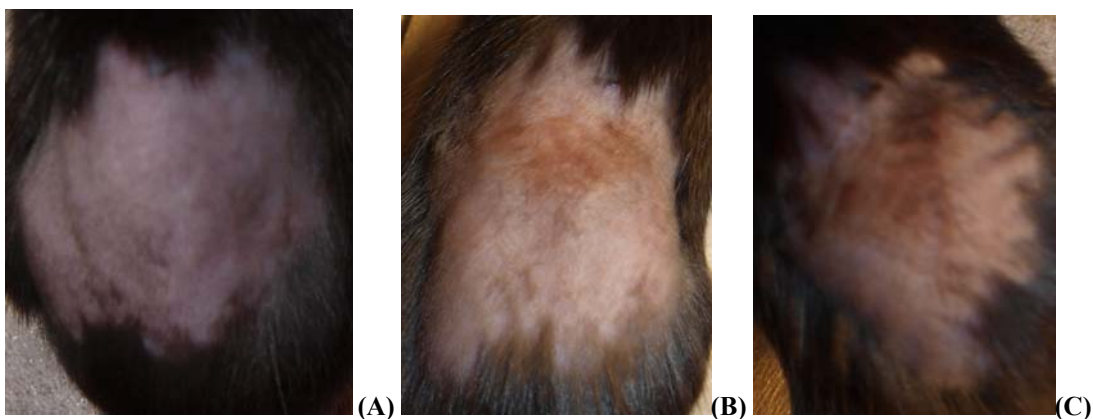
Age-matched mice of both groups (WT and His-mutants) were shaved on their backs and both backs and ears were irradiated with an UVB dose of 250 mJ/cm² (single-high-dose protocol). After chosen timeframes, an adjusted number of mice for each group were sacrificed and skin samples of back skin and ears were analyzed microscopically for skin morphology, apoptotic cells, thymine-dimer formation and repair, expression of the enzyme histidine ammonia lyase and Langerhans cell-migration. The macroscopical phenotype was documented by photography.

3.1.6.1 High doses of UVB irradiation can cause burns, wrinkles and open wounds

Acute high-doses of UV-light can also cause burns of variable severity. Depending on dose and individual skin sensitivity to UV-irradiation deep injuries even involving subcutaneous tissues can appear.

In this experiment, we investigated whether the effects of the previously shown enhanced DNA damage affect skin morphology and can be documented in phenotype and other markers concerning cell- and tissue integrity and/or damage.

A high-UVB-dose of 250 mJ/cm² caused macroscopic skin damage in both groups of mice, wild-type and mutant mice. 24 hours after irradiation skin of most mice developed wrinkles which differed in intensity and deepness from mouse to mouse (Fig. 16A, 17A). After 48 hours burns became visible, the skin started crusting and/or thickening and showed coloration that indicated corrosion of cell integrity within the skin and development of wounds (Fig. 16B, 17B). Development of wounds became visible more clearly after 72 hours (Fig. 16C, 17C). 96 and 120 hours post irradiation, wounds were all crusted, some were even chapped and open, and necrotic tissue was visibly coming off irradiated sites (Fig. 16D, 17D; Fig. 16E, 17E).



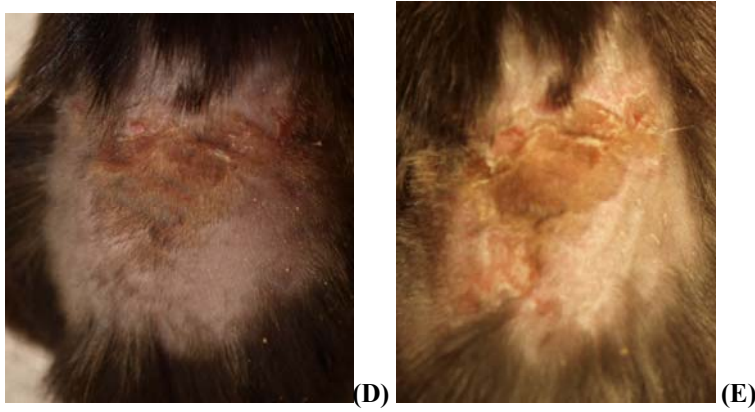


Figure 16 (A-E): Changes in skin appearance of a homozygous his-mutant mouse after high-dose UVB irradiation. (A) 24 hours, (B) 48 hours, (C) 72 hours (D) 96 hours (E) 120 hours after irradiation

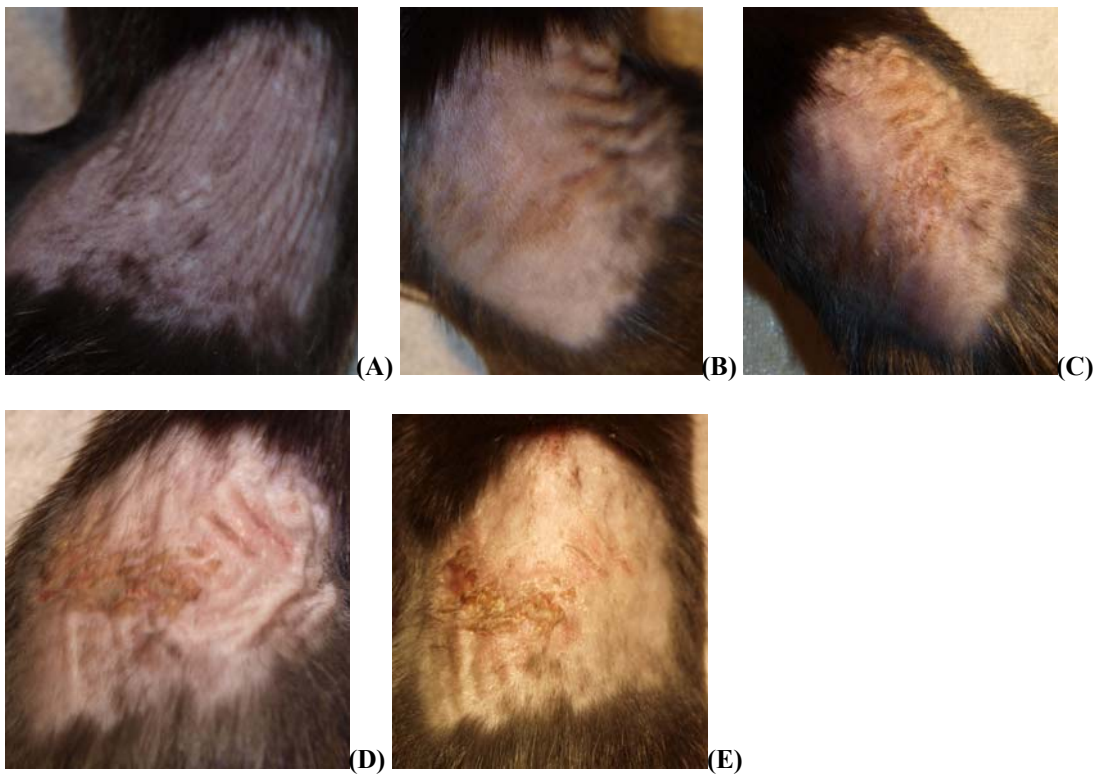


Figure 17 (A-E): Changes in skin appearance of a wild-type mouse after high-dose UVB irradiation. (A) 24 hours (B) 48 hours (C) 72 hours (D) 96 hours (E) 120 hours after irradiation

Two researchers with experience in mouse histopathology evaluated the photos in a blinded manner and analysed probable tendencies of stronger or weaker injuries or other differences in morphologically visible effects between wild-type and mutant mice. Pictures of all mice (at least 3 wild-type and 3 mutants/timeframe) were put together and presented as well as rated in a blindfold manner. At early time points, skin appearance is highly comparable in injury grade and occurrence, as deep wrinkles and also burns appear within the skin of both genotypes.

A tendency for more and deeper grade injury became visible in later time points. At the 96 hours-after-irradiation time point WT-mice sustain an overall of grade 1.55 injury on a scale

between 0 – 4 (0 = normal, unwounded skin, 4 = high-grade injury with deep (open) wounds and crusts), while mutant mice showed an overall of grade 2,58 injury (Fig. 18). Number of evaluated mice at time point 96 was 6 WT and 6 histidase-mutant mice. 120 hours after irradiation, WT-mice suffered an overall of grade 2,67 injury (n =3) and mutant mice grade 3,67 injury (nWT = 3, nMut = 3; p = 0,1).

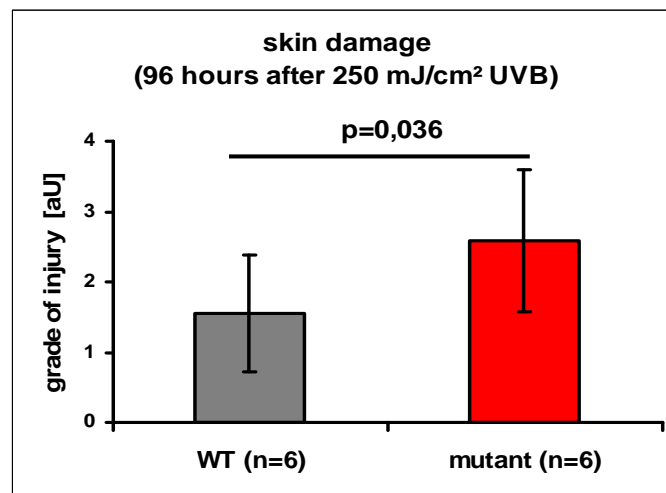


Figure 18: Evaluation of injury grade 96 hours after UVB irradiation with high-dose UVB (250 mJ/cm²). Bars indicate mean +/- SD.

3.1.6.2 Lack of wild-type histidase causes enhanced apoptosis in the epidermis

We have already evaluated the number of apoptotic cells in wild-type and histidase-mutant mice as a result of DNA damage 24 hours after irradiation with a high-dose of 250 mJ/cm² UVB light. Increase of cell apoptosis within the epidermis of homozygous mice was significantly higher compared to wild-type mice after 24 hours (Fig. 15A, B). In addition to the macroscopical analysis, we monitored the time course of disturbed cell integrity and increased DNA damage. Apoptotic markers (active Caspase-3 and TUNEL) were also analyzed 48, 72, 96 and 120 hours after UVB-high-dose-irradiation. Active-Caspase-3-positive cells and TUNEL-positive cells were counted in the epidermis of irradiated ears from age-matched WT and mutant mice. Number of TUNEL-positive cells increases later on even more as TUNEL is a late-point marker for apoptosis (Fig. 19B-22B), number of active-Caspase-3-positive cells is aligning between wild-type and histidase-mutant mice, both decreasing in later time-points (Fig. 19A-22A).

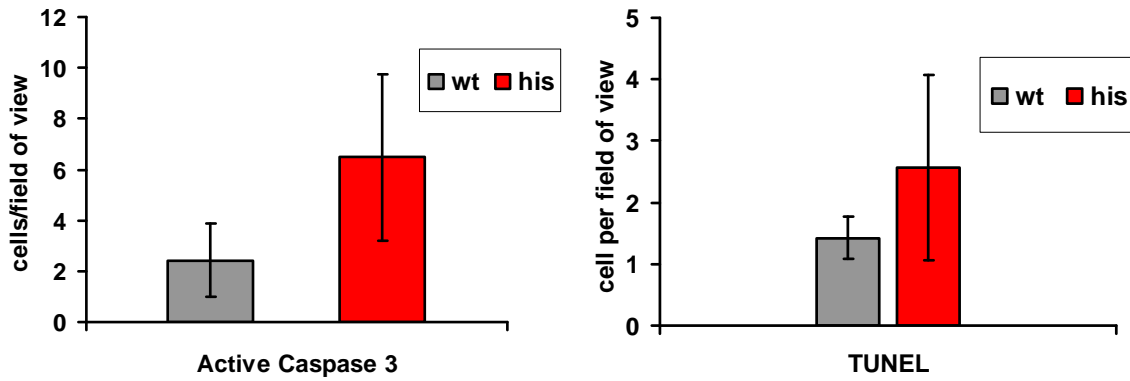


Figure 19 (A-B): Number of Active Caspase-3-positive cells and TUNEL-positive cells in the epidermis of irradiated ears from WT (n=3) and mutant mice (n=3) 48 hours after irradiation. Bars indicate mean +/- SD. p=0,15 (A), p=0,317 (B).

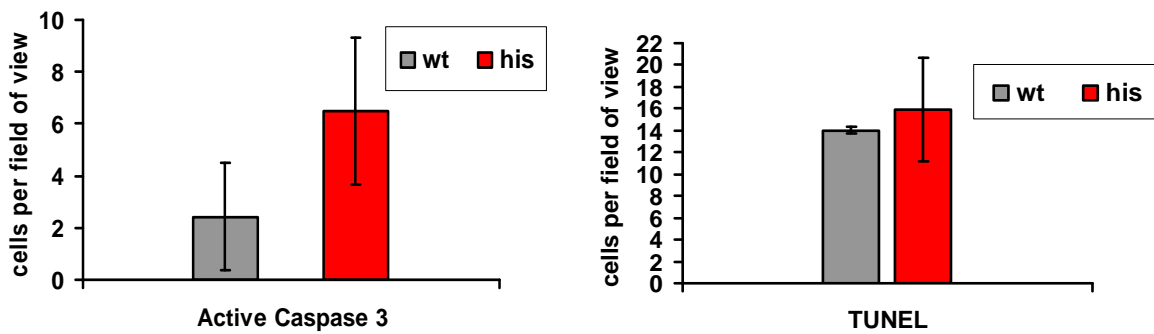


Figure 20 (A-B): Number of Active Caspase-3-positive cells and TUNEL-positive cells in the epidermis of irradiated ears from WT (n=2) and mutant mice (n=2) 72 hours after irradiation. Bars indicate mean +/- SD. p=0,97 (A), p=0,67 (B).

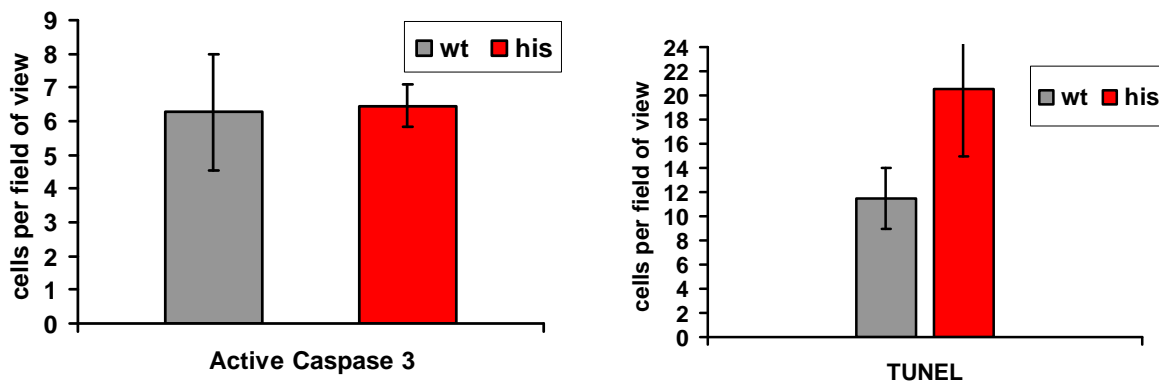


Figure 21 (A-B): Number of Active Caspase-3-positive cells and TUNEL-positive cells in the epidermis of irradiated ears from WT (n=3) and mutant mice (n=3) 96 hours after irradiation. Bars indicate mean +/- SD. p=0,87 (A), p=0,09 (B).

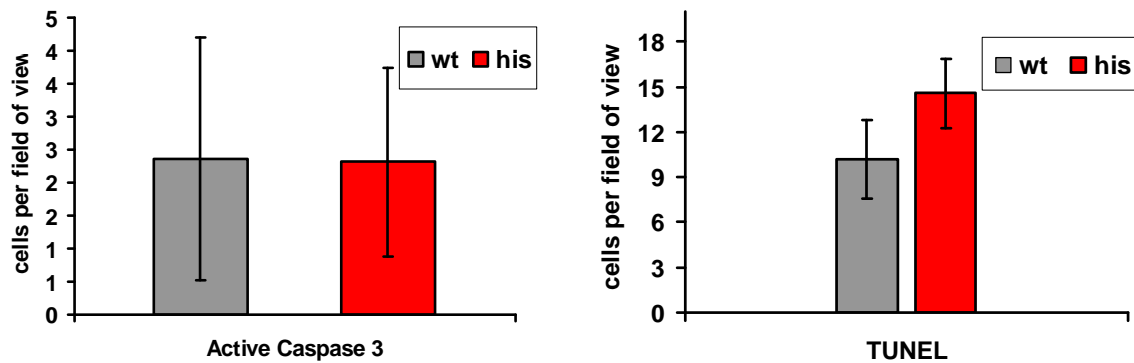


Figure 22 (A-B): Number of Active Caspase-3-positive cells and TUNEL-positive cells in the epidermis of irradiated ears from WT (n=3) and mutant mice (n=3) 120 hours after irradiation. Bars indicate mean +/- SD. p=0,97 (A), p=0,09 (B).

Preparation of ear sheets and double staining with a MHC-II-FITC conjugated antibody and an active Caspase-3 antibody (texas red-labelled) provided information about the 2-dimensional distribution of apoptotic cells and specifically on the role of apoptosis in LCs after high-dose irradiation. Epidermal ear sheets of irradiated ears were prepared 48, 72, 96 and 120 hours after irradiation (Fig. 23A, B; Fig. 24A, B and data not shown). 48 hours after irradiation, increase of active Caspase-3 positive cells was immense in wild-type and homozygous mice.

Individual apoptotic cells were hardly distinguishable from each other. Blinded evaluation of individual ear sheets indicated a higher increase of cell apoptosis in mutant mice compared to wild-type mice.

120 hours after irradiation, epidermal ear tissues were still highly apoptotic, although a tendency towards weak decrease could be seen (Fig. 24A, B and data not shown).

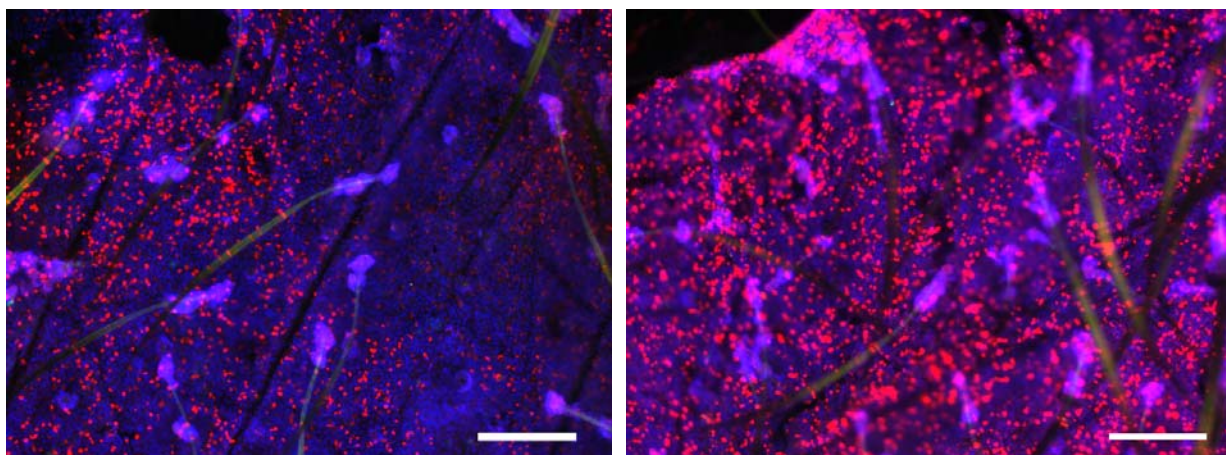


Figure 23 (A-B): MHC II/Active Casp-3/Hoechst stained epidermal ear sheet, 48 hours after high-dose UVB irradiation. Both show high increase in cell apoptosis. Active Caspase-3 positive cells are even more increased in homozygous sheet (right) than in WT sheet (left). Magnification: x100; bar: 200µm

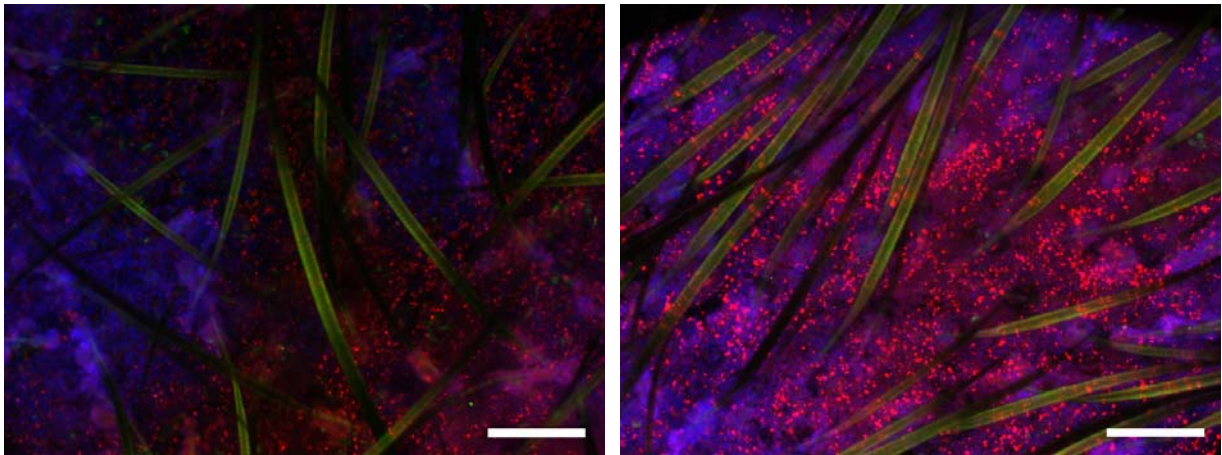


Figure 24 (A-B): MHC II/Active Casp-3/Hoechst stained epidermal ear sheet, 120 hours post irradiation. Both show high increase in cell apoptosis. Active Caspase-3 positive cells are still even more increased in homozygous sheet (right) than in WT sheet (left). At sites with high numbers of Active-Caspase-3 positive cells, MHC II positive cells are mostly lacking (cp Fig. 25-27). Bar: 200µm

Double-staining assay with a MHC II and an active Caspase-3 antibody was meant to provide a method to distinguish between LC-apoptosis and LC-migration after UVB treatment.

This assay gave no evidence of direct correlation between apoptosis and decrease in number of Langerhans cells. Sites with highly increased cell apoptosis have lost almost all LC-surface markers and sites in which LCs were detectable, apoptotic markers were almost absent (Fig. 25B and 26A & 27A). Epidermal tissue of homozygotes showed more damage and loss of tissue-integrity. In some areas, there are still LC-surface markers visible although the tissue around shows increased apoptosis (Fig. 26B, 27B).

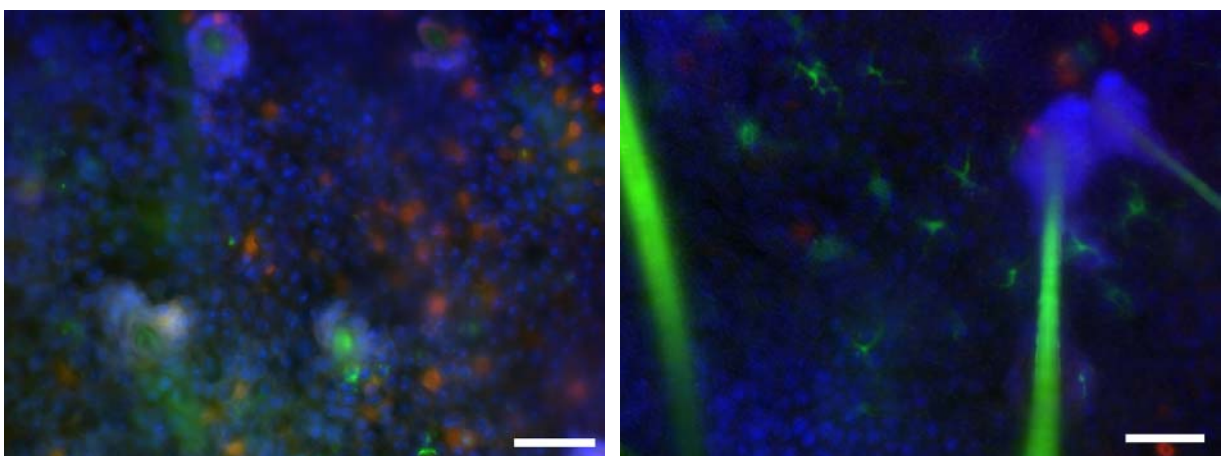


Figure 25 (A-B): MHC II/Active Casp-3/Hoechst stained epidermal wild-type ear-sheets, 48 hours post irradiation. Magnification: x400; bar: 40 µm

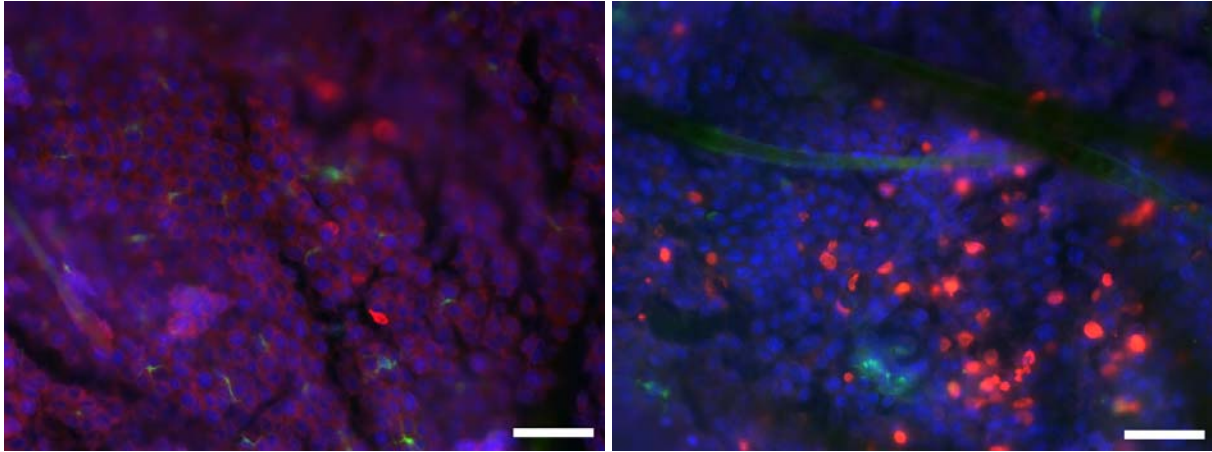


Figure 26 (A-B): MHC II/Active Casp-3/Hoechst stained epidermal mutant ear-sheets, 48 hours post irradiation. Magnification: x400; bar: 40 μ m

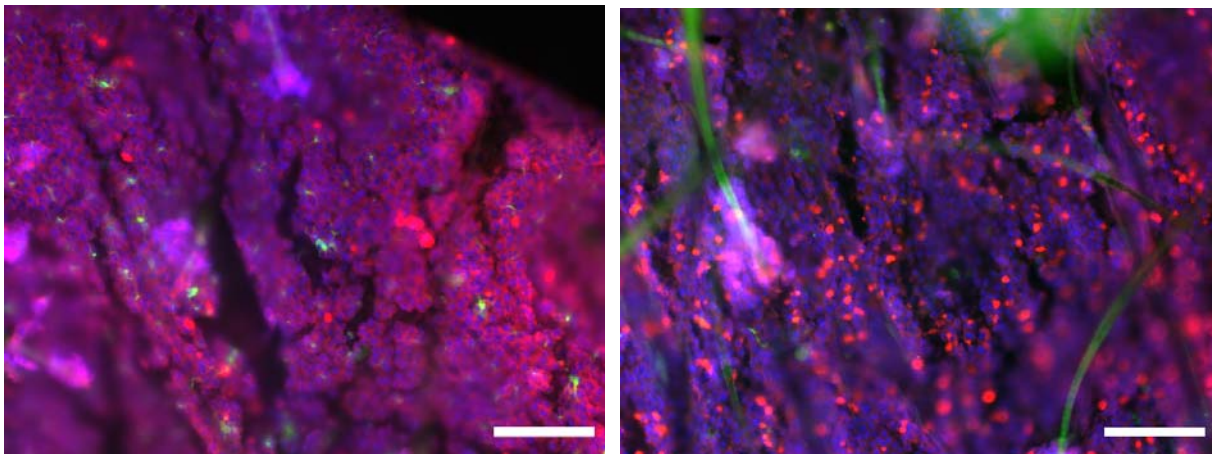


Figure 27 (A-B): MHC II/Active Casp-3/Hoechst stained epidermal mutant ear-sheets, 48 hours post irradiation. Magnification: x200; bar: 100 μ m

3.1.6.3 There is no visible change in HAL-expression due to UVB irradiation

Expression of HAL is impaired in homozygous mutant mice and HAL is not detectable with immunofluorescence staining with an antibody against the enzyme histidase (Fig. 10A-F). 24 hours after irradiation expression of HAL appears normal in wild type mice and absent in mutant mice (data not shown). 48 hours after irradiation expression of HAL is neither up- nor downregulated in wild-type mice (Fig. 28B) and is yet not to be detected in homozygous mice (Fig. 28A).

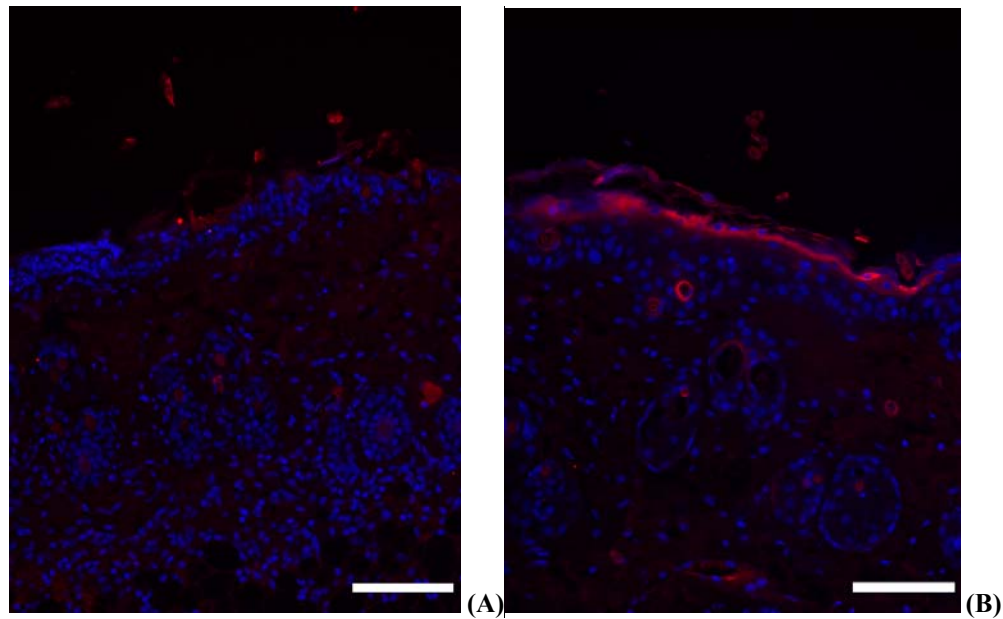


Figure 28 (A-B): HAL expression doesn't change due to UVB irradiation. There is consistent HAL expression in the stratum granulosum of wild-type epidermis 48 hours after high-dose irradiation (B). Homozygous HAL expression remains deficient (A). bar: 100 μ m

3.1.6.4 Histology of high-dose UVB irradiated skin

The epidermis is composed of keratinized stratified squamous epithelium, the dermis is composed of a dense connective tissue. The subcutaneous connective tissue, called the hypodermis, is a looser connective tissue than the dermis. It contains variable amounts of adipose tissues. Epidermal derivatives of the skin include the following organ structures and integumentary products: Hair follicles and hair, sweat (sudoriferous) glands, sebaceous glands, nails and mammary glands. UVB irradiation leads to cellular changes within the skin of irradiated areas. Alterations and damage in cells and tissue-structures result wrinkle formation, increased fragility and impaired wound healing. UVB-induced oxidative stress in skin cells via interaction with intracellular chromophores and photosensitizers results in transient and permanent genetic damage. Effects of UVB irradiation are: altered growth and differentiation, degradation of connective tissue, replicative senescence, vasodilation, inflammation [Wlaschek et al. 2001]. After UVB irradiation with a single high-dose of 250 mJ/cm², skin samples of WT and mutant mice were taken 24, 48, 72, 96 and 120 hours after irradiation.

24 hours after irradiation, inflammation factors are upregulated, skin starts wrinkling, stratum corneum and epidermis appear irregular in many areas and enhanced vasodilation can be observed as a result of UVB radiation (Fig. 29 and data not shown). Breakdown of adipose tissue, thickening of epidermis, development of wounds and crusts within the epidermis and increasing infiltration can be documented after 48 hours. Tissue integration is highly damaged

and altered in WT and mutant mice. A tendency for more crusting can be seen in most of the histidinemic mice (Fig. 30 and data not shown).

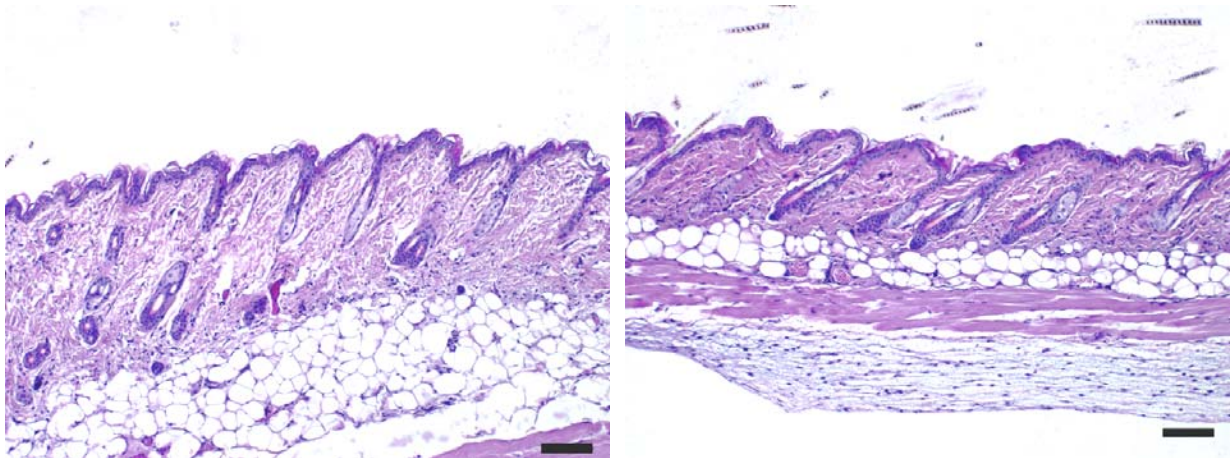


Figure 29(A-B): back skin of a WT (left) and a mutant (right) mouse 24 hours after 250 mJ/cm² UVB irradiation.

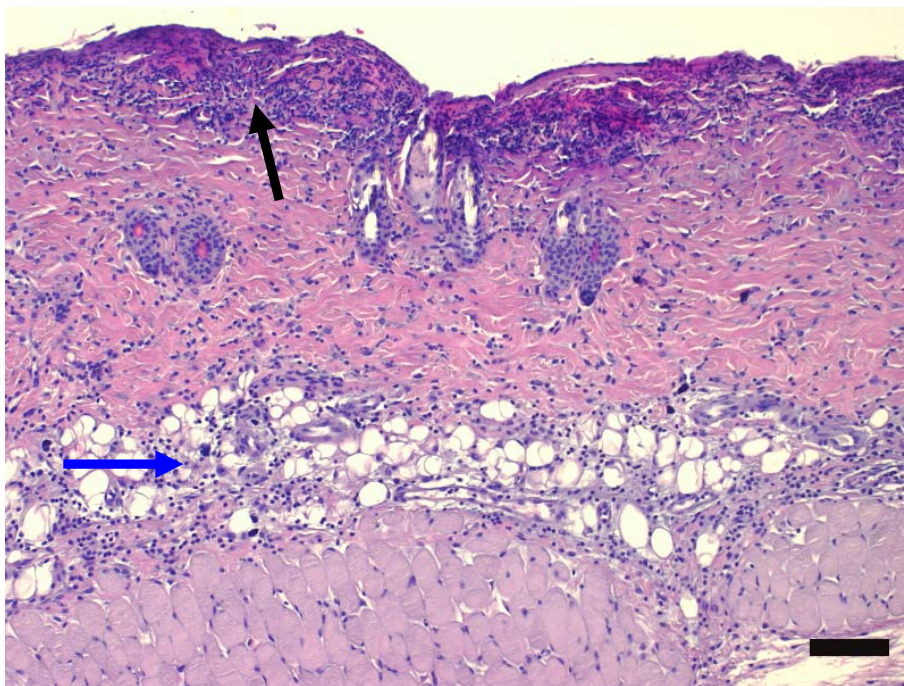


Figure 30: back skin cross section of a mutant mouse, 48 hours after high-dose UVB irradiation; blue arrow: break down of fat-tissue can be observed, as well as infiltration with inflammatory cells. Black arrow: Epidermis consists of crusts on many sites. bar 100µm

72, 96 and 120 hours after irradiation, vasodilation and invasion of granulocytes as a result of inflammation within the tissue are an indicator for activated signal pathways concerning tissue breakdown, differentiation, growth and immune responses. Epidermal structures are still highly

abnormal and the tissue appears necrotic. In some areas, the epidermis is thickened and hyperkeratotic (Fig. 31-33 and data not shown). Infiltrate is distributed within the muscle tissue beyond the skin, within the adipose tissue and within dermis and epidermis (Fig. 30-33 and data not shown).

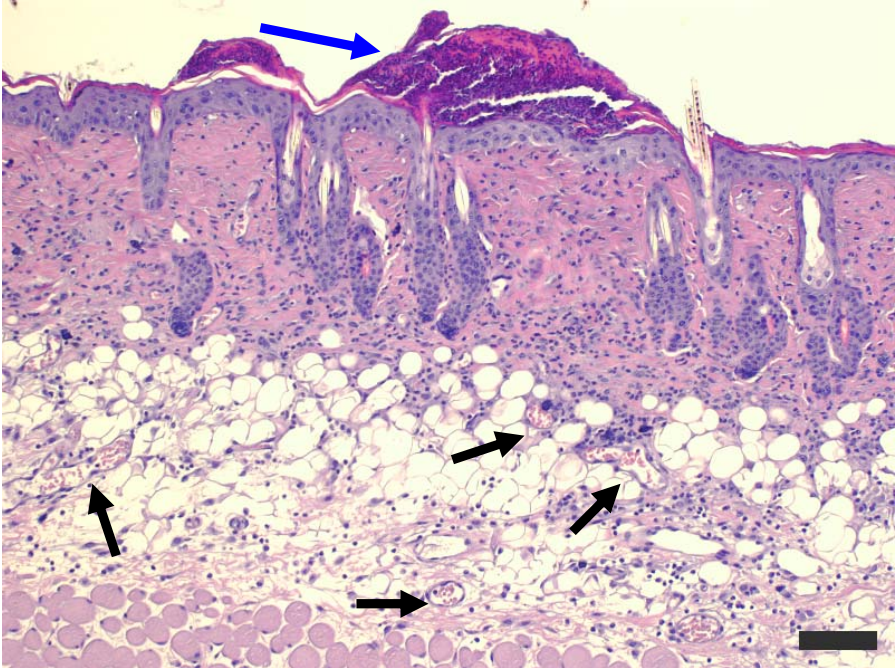


Figure 31: Cross section of irradiated back skin of a WT mouse 72 hours after high-dose UVB irradiation. Blue arrow marks crusts on the epidermis, black arrows mark blood vessels, built up within the epidermis as a reaction to inflammation (vasodilation); bar: 100µm

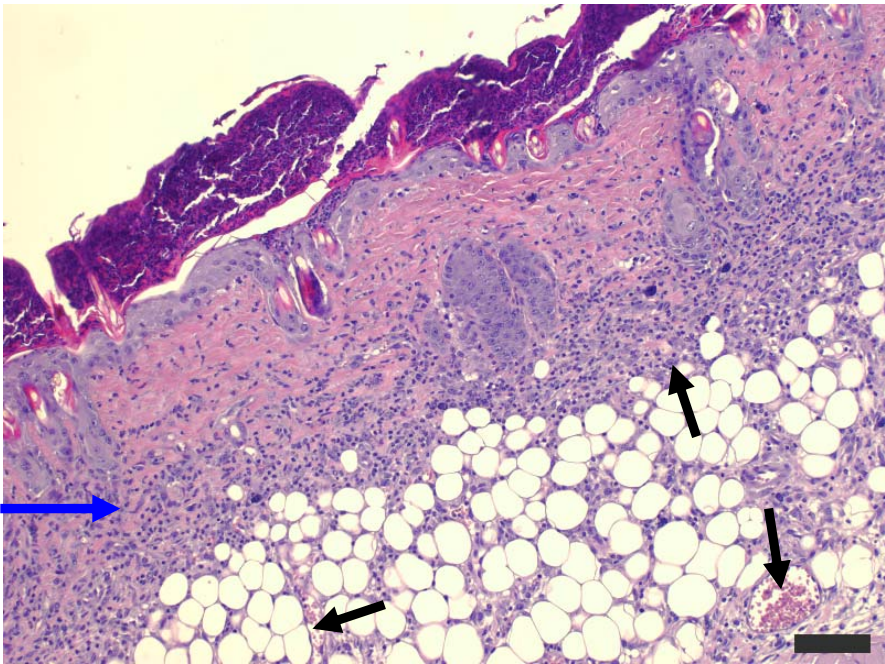


Figure 32: Irradiated back skin of a mutant mouse 96 hours after high-dose irradiation with UVB. Blue arrow marks part of the area where high infiltration of inflammatory markers can be seen. Black arrows mark several blood vessels. bar: 100µm

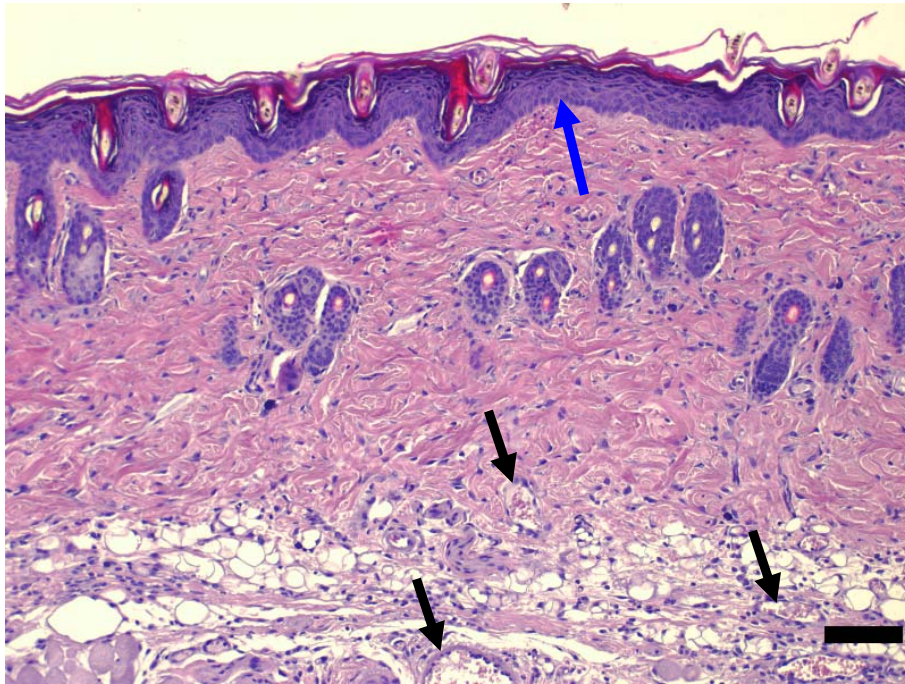


Figure 33: wild type mouse 120 hours after UVB irradiation, Blue arrow: epidermis of irradiated back skinn is thicker than normal epidermis and shows hyperkeratosis. Black arrows: Blood vessels. bar: 100µm

3.1.6.5 Thymine dimers are repaired in both WT and histidinemic mice

Results of thymine-dimer ELISA assays showed high abundance of thymine dimers 24 hours after UVB irradiation, depending on dose of UVB light. This increase of thymine dimers was significantly higher in histidase-mutant mice than in wild-type mice. To get first insights into long-term effects on DNA damage and DNA repair, cross sections of irradiated ears were stained with an immunofluorescent antibody against thymine-dimers 48, 72, 96 and 120 hours after irradiation. At all time points, intensity of the staining was stronger in histidinemic mouse cells compared to wild-type epidermal cells. 120 hours after high-dose irradiation the signal for TD-staining has almost vanished in wild-type mice and was highly decreased in mutant mice. However, the difference between histidinemic and wild-type mice remains visible as thymine dimers are yet more in histidinemic mice (Fig 34-35 and data not shown). A quantitative evaluation of the rates of repair in WT and his mice was not feasible using this approach. However, a strong difference between roles in WT and his-mutant mice was not suggested by these preliminary results.

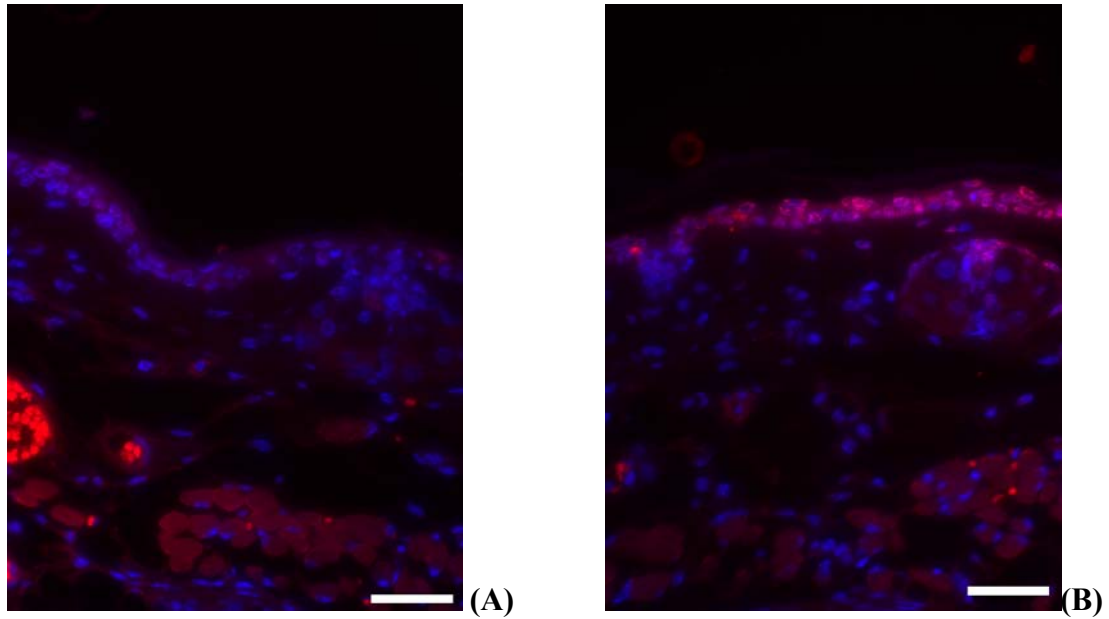


Figure 34 (A-B): cross section of an irradiated ear of a WT mouse (A) and of a histidinemic mouse (B) 48 h after UVB irradiation, stained for detection of CPD formation. In WT mice, CPD formation signal is lower than in mutant mice. bar: 40 μm .

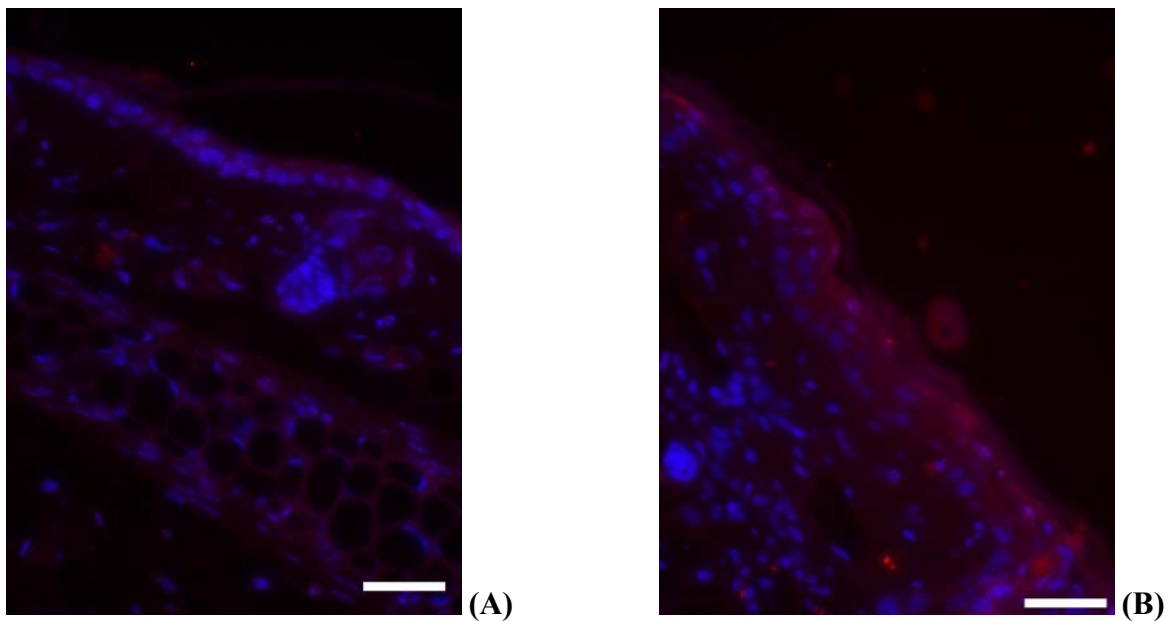


Figure 35 (A-B): cross section of an irradiated ear of a WT mouse (A) and a histidinemic-mouse (B) 120 h after UVB irradiation. Thymine-dimer formation is still visible on some sites of the epidermis. bar: 40 μm

3.1.6.6 Topical application of UCA rescued the UVB-photosensitive phenotype of histidinemic mice and increased UVB-photoprotection of wild-type mice

To investigate whether exogenous UCA would rescue the UVB-photosensitive phenotype of histidinemic mice and also increase UVB-photoprotection of wild-type mice, we applied UCA

topically on the backs of newborn mice. 1 litter was homozygous for his-mutation, the other litter was of WT-origin.

One half of each litter was skin-painted with UCA in a concentration of 50 µg UCA per mouse supplied in a DMSO/ethanol absolute vehicle, the other half of each litter was skin-painted with the vehicle only and served as control. Mice were then irradiated with an UVB-dose of 25 mJ/cm². CPD-formation was evaluated 1 hour after irradiation. DNA of irradiated epidermis was extracted and DNA damage was analyzed and quantified with an ELISA specific for CPDs. Increase of DNA damage 1 hour after a high-dose of 250 mJ/cm² of UVB light in newborn homozygous mutant mice was about 80% more compared to DNA damage in the epidermis of their heterozygous littermates (Fig. 13A). In adult mice increase of DNA damage 24 hours after irradiation was still 40% stronger in homozygous mice than in age-matched WT-mice (Fig.13B). UCA-deficient mice are significantly more sensitive to UVB-induced CPD formation.

Either in WT as well as in mutant mice, topically applied UCA decreased DNA damage significantly. In homozygotes, the difference of between treated and control mice is outstanding by a reduction of CPD-formation of almost 50%, showing almost equal low levels of dimer formation as treated wild-type mice (Fig. 36)

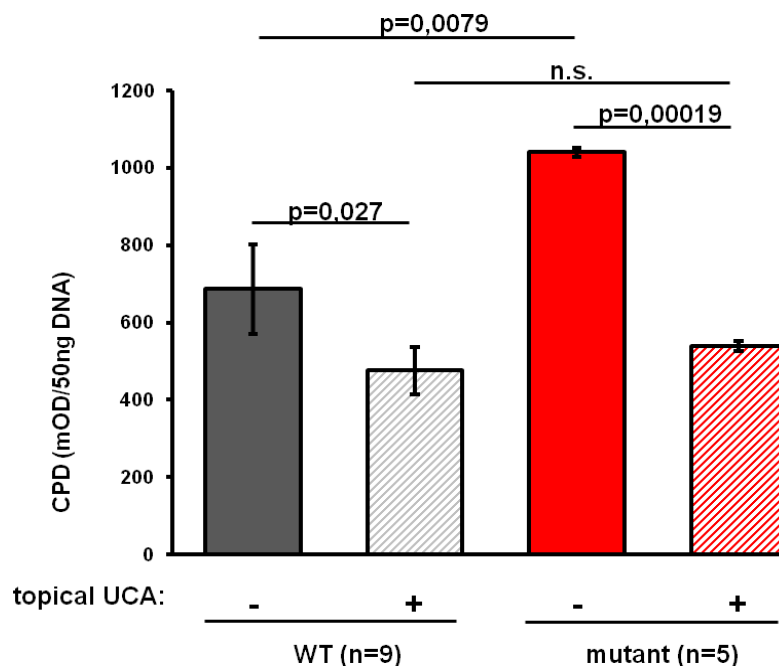


Figure 36: Quantification of DNA damage in WT and histidase mutant mice after topical application of UCA. Exogenous UCA leads to significantly less CPD formation in both, WT (+UCA: n=5; -UCA: n=4) and histidase mutant mice (+UCA: n=3; -UCA: n=2).

3.1.7 Effect of lack of HAL on histidine- and histamine-levels

The amino acid histidine is not only metabolized in the histidase-dependent pathway but also converted into histamine, by decarboxylation of histidine. The reaction is catalyzed by the enzyme L-histidine decarboxylase. Histamine is a hydrophilic vasoactive amine and physiological levels can be tested in the blood plasma or urine of a mammal. As the histidine converting histidase-dependent-pathway is deficient in histidase-mutant mice, we questioned if histamine-levels would be elevated as a result of a reported histidine excess in HAL-deficient mammals [Mellor et al., 2004]. Urine of untreated and unstressed mice (3 wild-type and 3 histidase-mutant mice) was collected and treated as suggested in the IBL standard protocol for Histamine-Elisa of urine samples. Results showed that histamine concentrations in urine of histidase-mutant mice are highly increased. Relative difference between wild-type and homozygotes was 218% in average (Fig. 37).

Furthermore, concentrations of histidine must be elevated in the skin. Tape-strips from non-irradiated mice were analysed for histidine content by HPLC. Histidine concentrations were increased in a significant manner in histidase mutant mice. Compared to wild-type mice, histidase mutant mice had a more than 10 times higher histidine concentration within the stratum corneum extracts (Fig. 38).

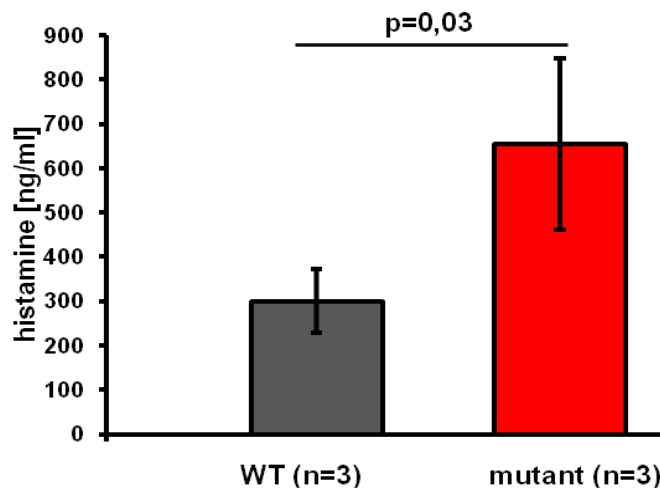


Figure 37: With a mean of histamine concentration of 300,54 ng/ml in wild-type-urine, a relative difference of 218% can be seen compared to the mean of 655,44 ng/ml histamine in histidase-mutant mice. Levels of histamine are highly increased, if histidase is impaired.

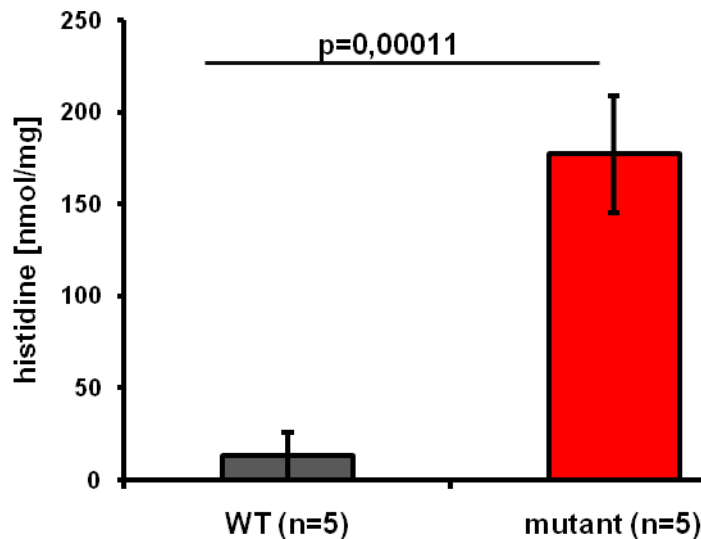


Figure 38: histidine concentration in stratum corneum extracts of unirradiated adult mice. Histidase mutant mice show a high increase of histidine in stratum corneum extracts, compared to wild-type mice the increase is more than 10 times higher.

3.2 Effect of UVB-induced cis-urocanic acid on the number Langerhans cells in mouse epidermis

Comparison of histidase-mutant (His) and wildtype (WT) mice

To get a preliminary impression of the effect of UVB on LC numbers in WT and histidase mutant mice, tissues from previously shown experiments (e.g. 3.1.4) were analyzed. Since these experiments were designed to yield information on short term effects of UVB on Keratinocytes (CPD formation, apoptosis) but not on LCs, the results provided only a starting point for optimization of the protocol and reference (dose, irradiation regimen) for the actual tests of the hypothesis. LCs were counted already 24 hours after single-dose irradiation, which is protocolled to be early for following UV-induced LC migration [Aberer et al., 1981; Bennett et al., 2005], after single low-dose (25 mJ/cm²), middle-dose (100 mJ/cm²) and high-dose (250 mJ/cm²) and gave first impressions about differences between WT and histidase mutant mice in LC density after UVB irradiation.

Established protocols in literature suggested a repeated-low-dose-protocol with an accumulative dose of 400 mJ/cm² and a single-high-dose protocol with a dose of 250 mJ/cm² [Schwarz et al., 2005; Aberer et al., 1986; Bacci et al., 2001] as a decrease in Langerhans cells becomes more obvious with high doses and is considered to be proven in wild-type mice [Aberer et al., 1986]. The following experimental settings aimed to characterize impact of

UVB irradiation on the number of Langerhans cells in the skin of histidase-mutant and in control mice.

Mice (wild-type (HIS/HIS) and histidase mutant mice (*his/his*) at the age of 7-10 weeks) were anesthetized and irradiated with an UVB dose of 250 mJ/cm² (single-high-dose protocol) and an accumulative dose of 400 mJ/cm² (repeated low-dose protocol). Respectively 24 hours after irradiation respectively 24 hours after last irradiation of the 4x100 mJ/cm² repeated-low-dose protocol, density of LC was determined in the skin of an irradiated and a non-irradiated ear. Epidermal sheets were prepared and density and morphology of LC was assessed by immunohistochemical detection using an appropriate monoclonal antibody. Field of view using a magnification of x400 equals an area of 70 964 μm² (Fig. 41, 43, 44).

3.2.1 Single-high-dose protocol

Wild-type (HIS/HIS) and histidase mutant mice (*his/his*) at the age of 7-10 weeks were irradiated with 250 mJ/cm² UVB. In the single-high-dose protocol, both ears were irradiated, as evaluation of number of LC in non-irradiated ears (referring to results of preliminary tests and results of repeated-low-dose protocol) gave no significant differences between WT and his mice (data not shown). 24 hours after irradiation, Langerhans cells were counted and the difference in total decrease was evaluated. 30 – 40 fields of view per ear (ear-punch of 6 mm in diameter) were counted manually in a blinded manner and the mean of both ears taken together was calculated and compared. In mutant mice an average of 28,41% more LC than in wild type mice was counted (Fig.39). Field of view using 400x magnification equals an area of 70 964 μm² or 0,071 mm².

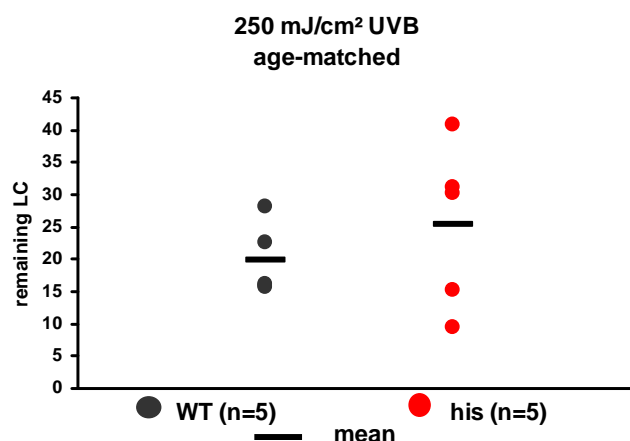


Figure 39: Number of remaining Langerhans cells in irradiated epidermis of ears from WT and mutant mice. Distribution of LCs was analyzed 24 hours after UVB irradiation with high-dose UVB of 250 mJ/cm². Results in counted Langerhans cells per area of view. Difference between wild-type and mutant mice equals 28,41%; p=0,4. Black bars mark average percentage of LC density/group.

3.2.2 Repeated-low-dose protocol

Wild-type (HIS/HIS) and histidase mutant mice (*his/his*) at the age of 7-10 weeks were exposed to 100 mJ/cm² UVB daily for four consecutive days with a cumulative dose of 400 mJ/cm². 24 hours after last irradiation mice were sacrificed and ear sheet were prepared. In two experiments a total of 18 age-matched WT and histidinemic mice (9 per genotype) were treated following the protocol. 30-40 fields/view/ear using x400 magnification were determined and decrease of number of LC was evaluated for each mouse by calculation of relative decrease of LC between unirradiated and radiated ear. Statistical analysis for evaluation of each genotype and comparison between WT and mutant mice was performed using the SPSS software. Decrease in number of LC reached an average of 72 % in WT mice and 58 % in his-mutant mice with considerable fluctuations within and between both groups (Fig. 40).

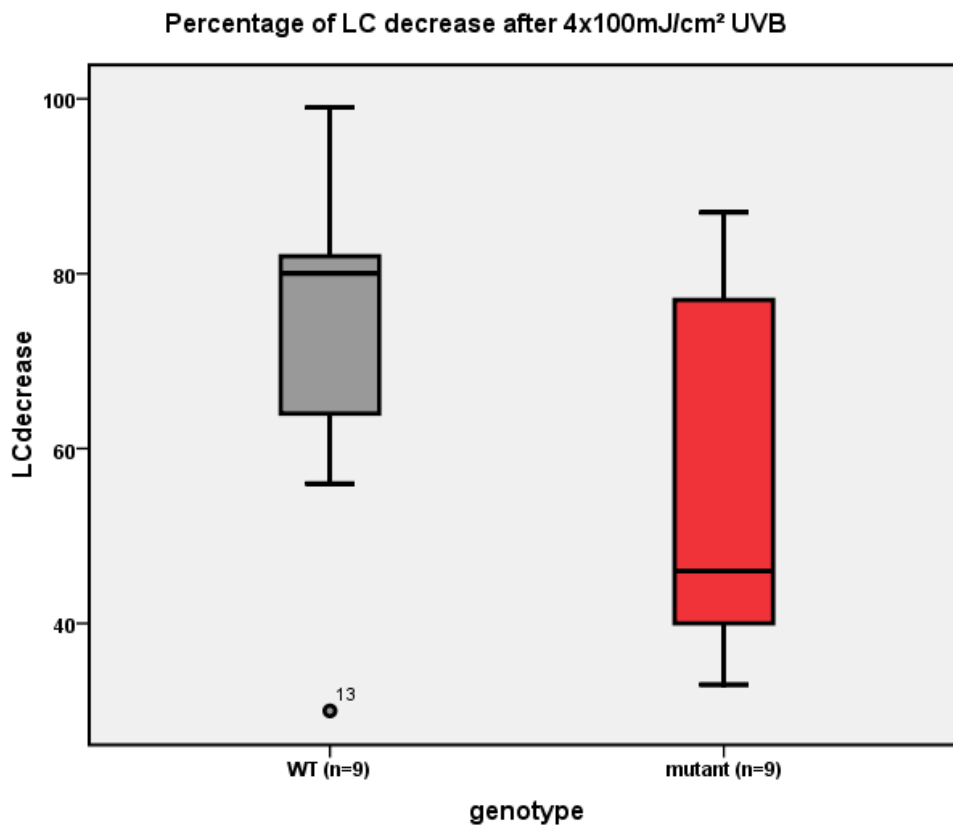


Figure 40: Boxplot showing decrease-distribution of number of LCs in age-matched WT and in mutant mice. One WT mice was marked as outlier by SPSS program. Data from 2 independent experiments are combined.

In a second approach, a whole litter of mixed genotypes was used. Littermates were HIS/HIS, HIS/his and his/his in phenotype. Assay and evaluation of assay resembled accurately the first approach with age-matched mice. As in the first approach, fluctuations were also considerable.

Decrease in number of LC was 71 % in WT, 73 % in heterozygous and 56 % in homozygous mice. As heterozygous mice do not differ in phenotypic characteristics from WT mice, but show the same difference from mutant mice as WT mice, WT and heterozygous mice were combined and evaluated as one group (non-histidinemic mice). Therefore WT/heterozygous decrease yields an average of 72 % (Fig. 41).

For better illustration of fluctuations and results, diagrams for both approaches were drawn in which the percentage of remaining Langerhans cells for each mouse is presented (Fig. 42A-C).

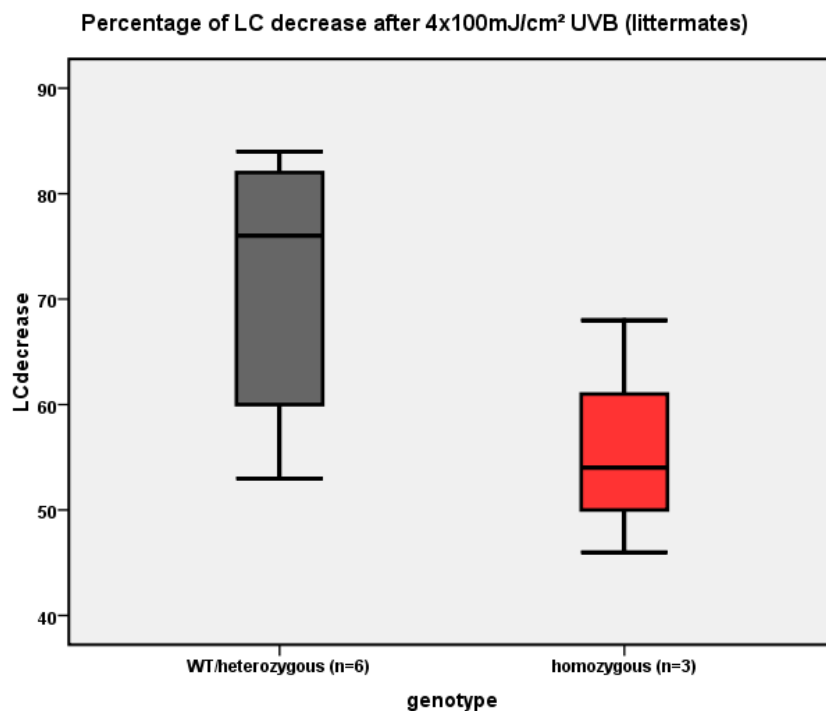


Figure 41: Boxplot showing decrease-distribution of number of LCs in a mixed litter of WT, his-heterozygous and his-homozygous mice.

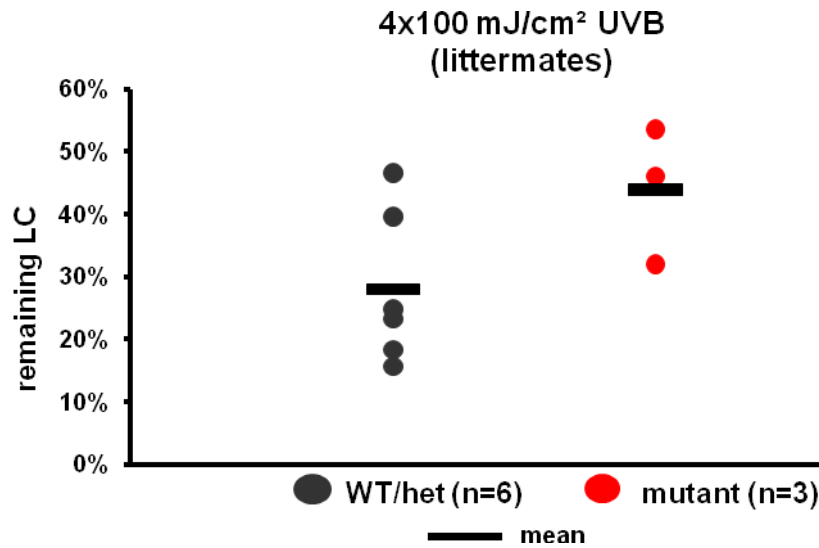


Figure 42A: percent of remaining LC in irradiated epidermis of ears in WT and his-mutant mice (of one litter) after 4x100 mJ/cm² UVB irradiation. Black bars mark average percentage of LC density/group. Difference between WT and mutant mice equals 16% of the density of the irradiated ears.

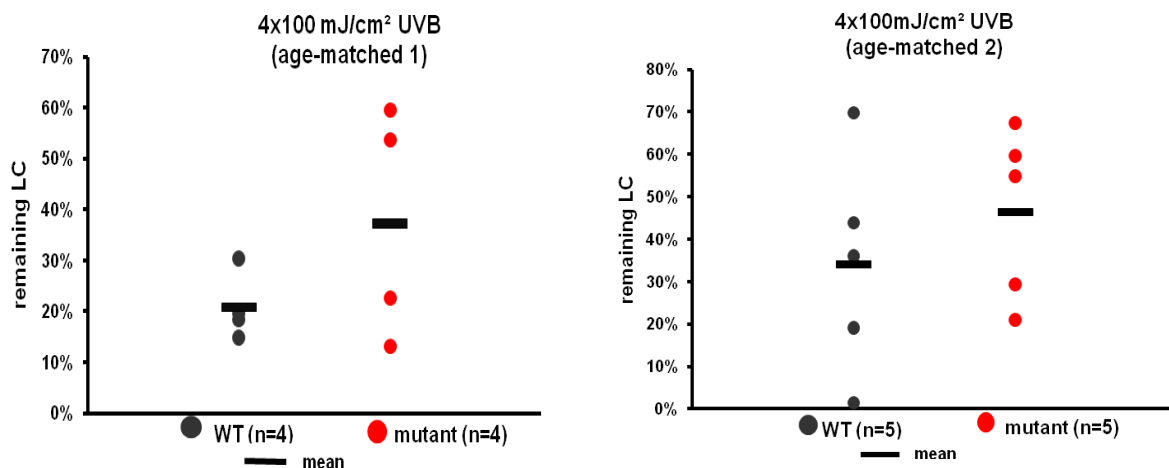


Figure 42B-C: percent of remaining LC in irradiated epidermis of ears in age-matched WT and his-mutant mice after 4x100 mJ/cm² UVB irradiation. Black bars mark average percentage of LC density/group. Difference between WT and mutant mice equals 16,46% (B: age-matched 1) and 12,38% (C: age-matched 2) of the LC density of the irradiated ears.

3.2.3 UVB irradiation alters morphology of Langerhans cells

Besides decrease in density (Fig. 43, 45, 46A-B), alteration of function and morphology of Langerhans cells induced by UVB-irradiation has been described [Aberer et al., 1981; Aberer et al., 1986; De Fabo et al., 1979; Noonan et al., 1981]. Loss of dendricity as well as abnormal dendricity is a characteristic for UVB-induced change in LC morphology. But also the body of LC is altered and becomes smaller and rounder. In contrast, few cells become larger and vapoured. These abnormalities can be seen in irradiated ears of wild type and histidase-mutant

mice (Fig. 43 & 44). A qualitative comparison of morphological differences between LC in WT and histidinemic mice was not an aim of this study. Major differences in morphology were not noted in either irradiated or non-irradiated ears of the genotypes. Changes in morphology are similar in WT and mutant mice.

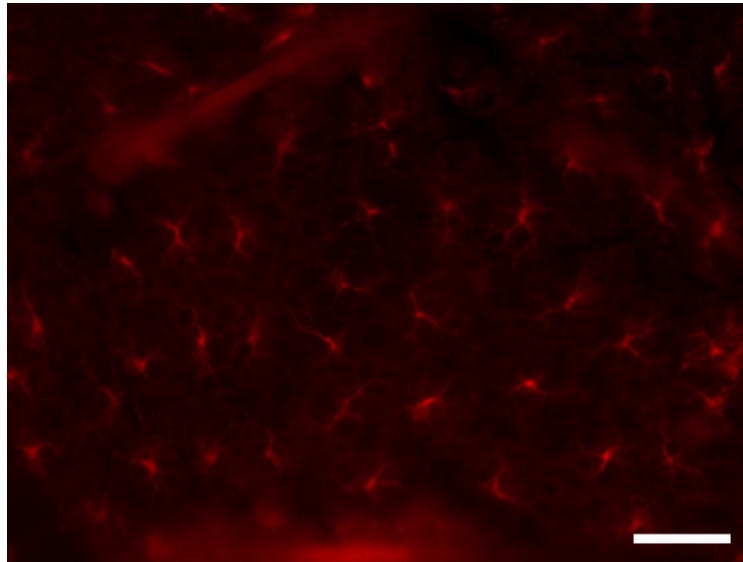


Figure 43: distribution and morphology of LC in unirradiated ear-epidermis of a mutant mouse. magnification: x400; bar: 40 μ m

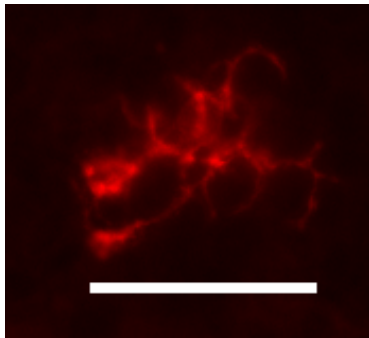


Figure 44: example for an UVB-altered LC in a WT mouse after irradiation with 4x100 mJ/cm². magnification: x400; bar: 40 μ m

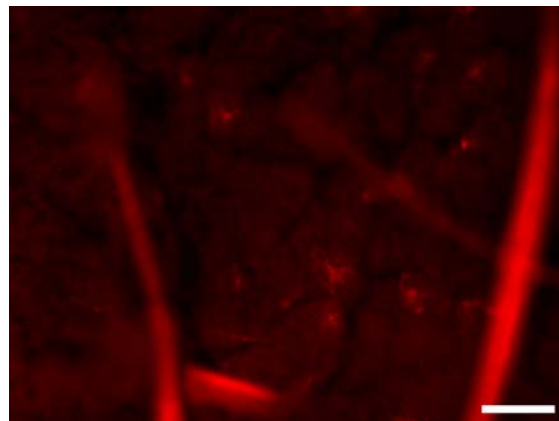


Figure 45: example for density and distribution of LC in a his-mutant mouse 24 hours after irradiation with 4x100 mJ/cm² UVB. Ear sheet was stained for Ia⁺ cells. magnification: x400; bar: 40 μ m

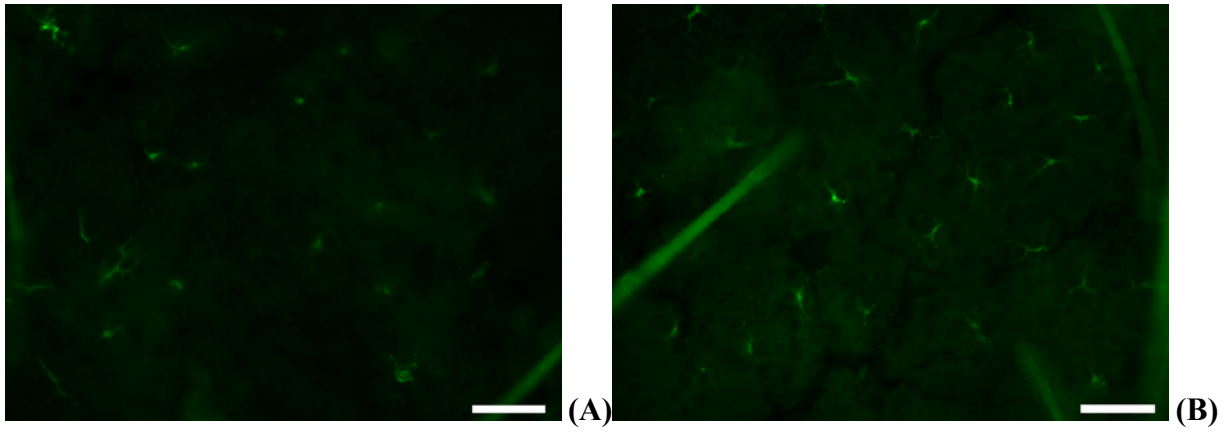


Figure 46 (A-B): epidermal sheet stained for Ia⁺ cells from WT (A) and his-mutant mice (B) 48 hours after irradiation with 250 mJ/cm² UVB. magnification: x400; bar: 40 μ m

4. DISCUSSION

4.1 Lack of UCA in the epidermis leads to increased DNA damage

Urocanic acid has been proposed to act as an important photoreceptor for UV-light, especially UVB irradiation and to be an important factor in the photoprotection of the skin [Zenisek, 1955; Tabachnik, 1957; de Fine Olivarius et al., 1996; de Fine Olivarius et al., 1998].

This study gives experimental proof of the proposed photoprotective role of UCA by using a genetically well defined model system. Mice with histidase deficiency were previously shown to have a strongly reduced enzyme activity and reduced half life of the protein in the liver [Taylor et al. 1993].

First, we have characterised expression patterns of histidase mRNA and histidase protein as well as concentration levels in WT and histidase-mutant mice.

As the mutant mice have been back-crossed into the C57BL/6 background for more than 20 generations, physiological differences identified can be attributed to the mutation in the HAL gene. Immunohistochemical analysis of murine and human skin showed that expression patterns of histidase are identical, suggesting that histidase and its product UCA are regulated similarly in mice and in humans. Further immunohistochemical analysis showed that expression of HAL was not dramatically changed after UVB irradiation.

Soluble extracts from tape-strips from human stratum corneum and wild type mouse stratum corneum gave similar results in UV-absorbance [our unpublished data]. SC soluble extracts from mice mutant in the histidase gene demonstrated that UCA directly affects absorption capacity of the stratum corneum. Relevance of photoprotection by UCA in humans remains to be tested, but contribution of UCA to UVB absorption in human skin is probably similar. Absorbance curves similar to those of WT stratum corneum extracts gave evidence for this conclusion [data not shown]. Other factors like reflection of light at the skin surface and scattering, pH (which alters the wavelength of peak absorption of UCA [Kurogochi et al. 1957]), melanin and skin hair have to be taken in account as they clearly differ between mice and humans. The role of UCA in humans remains to be tested by including tests with human stratum corneum and especially including human patients carrying mutations in the HAL genes and deficient in histidase.

In our studies, the relevance of endogenous UCA in protection of UV-induced DNA damage as a physiologically essential parameter was tested. Aim was to show overall relevance of UV-

absorption of endogenous UCA in photoprotection. UV-induced DNA damage can be measured as the formation of DNA-photoproducts. DNA is another known UVB photoreceptor in the skin and more absorption of UVB by the chromophore DNA would be the logical consequence of lack in UCA. DNA photoproducts are precursors of DNA mutations.

CPD formation was indeed statistically significantly increased in the epidermis of irradiated back skin of mice. Compared to wild-type mice, this UV-induced increase of CPDs was significantly more increased in mice homozygous for the mutation in the HAL gene and with significantly decreased UCA concentration.

Since decreased UCA concentrations result in higher DNA damage due to UVB irradiation, we also investigated whether topical application of UCA rescues the UVB-photosensitive phenotype of histidinemic mice and increases UVB-photoprotection of wild-type mice. Indeed did topical application of UCA rescue the UVB-photosensitive phenotype of histidinemic mice in a significant high manner by lowering the UVB-induced DNA damage even comparable to the increased UVB-photoprotection in UCA-treated wild-type mice.

DNA damage does not necessarily lead to disturbed cell integrity and cell death; hence we also investigated if UVB irradiation effects cell physiology and enhances activation of cell apoptosis pathways. Activation of Caspase-3, a cysteine protease with aspartic specificity and a well-characterized early activator of apoptosis or programmed cell death signalling and endonuclease-mediated fragmentation of nuclear DNA (by use of the in situ terminal deoxyribonucleotidyl transferase-mediated deoxyuridine triphosphate nick end labelling (TUNEL) assay that detects DNA strand breaks in situ in tissue sections), were quantified within time frames of 24, 48, 72, 96 and 120 hours. Results of quantification of apoptosis positive cells show a strong activation of cell death mechanisms in mice with low concentrations of UCA. Time frame of 24 hours was evaluated first and within another experimental context what would explain little variations and an eventual decrease in number of active Caspase-3-positive and Tunel-positive cells between 24 and 48 hours. For exact evaluation, this experiment might be repeated for reduction of interexperimental variations.

In accordance with the increased DNA damage upon UVB irradiation, histidinemic mice showed a more pronounced activation of the cell death machinery as compared to control mice. In time frames between 24 to 72 hours, the difference between WT and mutant mice was stronger in the activation of active Caspase-3; in later time frames Tunel-positive cells were more increased in mutant mice than in WT mice. This can be explained by active Casp-3 being an early apoptosis marker and fragmentation of DNA being a late apoptosis marker.

The number of apoptotic cells was already decreasing 120 hours after irradiation, meaning that most apoptotic cells have already been degraded properly and/or sloughed with crusts. Decrease of CPD-positive cells can be considered of being a result of DNA repair or extended DNA damage leading to apoptosis and later on degradation or loss of these cells due to enhanced cell turnover. Other skin responses to UVB irradiation like erythema, tissue damage including wrinkle formation, wounding, crusts, necrotic tissue, infiltration, break down of connective tissue and adipose tissue as well as vasodilation are hard to quantify in a standardised manner, but first results have given evidence of more damage to skin tissue and cell integrity in histidase-deficient mice than in WT mice.

Further evaluations should include the determination of concentrations of inflammation markers, more specified samples of cross sections (sites of most skin damage versus sites of less skin damage) and FACS analysis for relative quantification of apoptotic cells.

Taken together, these results strongly suggest that endogenous UCA absorbs a physiologically relevant fraction of incident UVB light and thereby partially prevents DNA damage.

Critical events and physiological parameters following the response to UVB irradiation at later time points remain to be investigated. As t-UCA significantly diminishes DNA damage, it might be an important factor to prevent malignant formation. But deficiency in t-UCA also leads to reduced formation of cis-UCA (Fig. 9B), a component that is proposed to suppress the immune system in the skin and the immune response to tumors. Does the immune system of histidase mutant mice retain a better defence against tumors than normal mice and counteracts increased rate of tumor initiation due to lack of UCA? Another factor potentially affecting the immune response is the redirection of histidine into the histamine metabolism and increased histamine levels in the blood and urine of histidinemic mammals [Taylor et al. 1991]. Histamine, like UCA, has multiple only incompletely characterised effects on various cell types, several of which affect tumorigenesis and other long term effects of UV irradiation.

A consistently low concentration of UCA in the stratum corneum has also been reported for patients with atopic dermatitis (Kezic et al., 2009). This disease is associated with deleterious mutations in the gene encoding filaggrin, the main source of the UCA precursor histidine in the epidermis (Scott et al., 1982). Easy extraction of the UCA with an aqueous buffer from stratum corneum samples suggests that UCA concentration is influenced by body hygiene. (Extensive) washing and bathing may enhance the photosensitivity of normal skin.

4.2 Influence of UVB-induced cis-urocanic acid on Langerhans cell migration

4.2.1 Limitations

Although this study provides important new insights into the photobiology of the skin, some experimental limitations concerning the evaluation of UV-induced immunosuppression have been identified. The quantification of LC by manually counting an adequate number of fields/view/ear punch is still not to be considered the most effective method, an alternative method to assure and cover previous results should be established. Natural irregularities in radiation concerning different sites due to shape and morphology of mouse-ears might influence results in one or the other direction. It is likely that these factors cause high variance in the results so that high numbers of animals are required to identify differences between genotypes at a level of statistical significance. Consequently, it is desirable to establish qRT-PCR or FACS protocols for the quantification of LCs in the epidermis.

Importantly, the quantification of Langerhans cells can only provide an incomplete evaluation of the immune status. Functional studies involving contact hypersensitivity assays and other assays are required. Preliminary investigations of the contact hypersensitivity response in normal and histidinemic mice have suggested a critical role of the UV dose. The data of the present study will provide the basis for further investigations concerning the immune status that are to be performed in the course of cooperation with the laboratory of Dr. Agatha Schwarz, University of Kiel, Germany.

4.2.2 Lack of UVB-induced cis-urocanic acid alters, but does not completely inhibit UVB-induced decrease of epidermal Langerhans cells

The immune system of the skin is known to be altered and influenced by UV radiation. Many studies have tried to explain and determine the mechanisms of the impairment of the cellular immune responses after UV(B) irradiation. The effect on Langerhans cells as the major APC within the epidermis and their disappearance after irradiation is one major mechanism. The mechanism of disappearance has been proposed to be either migration or apoptosis.

Results of previous studies have shown that only few apoptotic Langerhans cells can be detected after UVB irradiation [Kölgen et al. 2002] but migration of irradiated Langerhans cells into the draining lymph nodes can be followed by FITC-skin painting before exposure [Bennett et al 2005] and analysis of lymph nodes after UVR.

The immunomodulative effect could be DNA damage and DNA repair [Kölgen et al 2003] or the conversion of trans-urocanic acid into cis-urocanic acid by providing or acting as a

signaling molecule [Norval et al. 1990]. Another proposed candidate for activation of immunosuppression is the cytokine IL-10 [Yoshiki et al 2009].

In our experiments, the influence of the UVB-induced conversion of UCA into its cis-form on decrease of Langerhans cells was studied. As DNA damage was measured before, we could also include the proposed theory that DNA damage effects LC emigration. If DNA damage was a signal for LC to migrate out of the epidermis into the draining lymph nodes, the decrease of LC migration should be significantly stronger in histidase-mutant mice. If UV-induced cis-UCA is the critical factor in alteration of LC function, morphology and density in the epidermis, WT mice would show more change in number of Ia⁺-cells.

Our data suggest that DNA damage is not the only signal for Langerhans cells to emigrate from the epidermis into the dermis and the draining LN. Neither does the conversion of trans-UCA into cis-UCA provide significant evidence for being the critical and only initiating signal for LC alteration and decrease in LC density within the epidermis. The density of LC in unirradiated ears is comparable in WT, heterozygous and homozygous mice. Density of Langerhans cells after irradiation shows a range of variations between mice with the same genotype as well as between mice with the different genotypes i.e. WT-C57BL/6 and C57BL/6 Hal^{-/-}). Heterozygotes are comparable to WT mice in UCA content, UVB absorbance of SC extracts and distribution of LC after irradiation as the HAL mutation is recessive. They were included in the WT group.

Taken the data together, a trend that less Langerhans cells migrate out of the epidermis of his-mutant mice after UVB irradiation was observed. Blinded counting resulted in differences in LC density between WT and mutant mice, being not highly significant but showing a tendency towards more LC remaining in epidermal skin of UCA-deficient mice than in wild type mice. Using a single high-dose of UVB light, number of remaining LC in irradiated wild type ears was 28,4% less than in irradiated mutant ears.

In repeated low-dose UVB irradiation difference between wild type mice and histidinemic mice in LC decrease (with an unirradiated ear as inner parameter for each mouse) was 14% (age-matched mice) and 16% (littermates).

This leads to the conclusion that the conversion of UCA might play a role in initiating UV-induced Langerhans cell migration and UV-induced immunosuppression but it does not seem to be the critical signal for migration events. It is conceivable that the increased DNA damage in mutant mice counteracts missing signals from cis-UCA and provides enough influence on

LC migration behaviour. Still, the influence of converted cis-UCA may have more impact on LC-decrease as the distribution and density of LC in mutant mice tends to be higher after irradiation than in wild type or heterozygous mice. Furthermore, Langerhans cells would retain an accumulated signal of both DNA damage and cis-UCA.

Another factor in UV-induced immunosuppression might be histamine, which – like UCA – is derived from histidine. In this study, the basal level of histamine was determined whereas the change in histamine concentrations upon irradiation was not investigated. The detection of elevated concentrations of histamine in the urine of histidinemic mice indicates that histamine levels are generally upregulated, or at least not decreased in histidinemic mice. Histamine is known to influence immune cells in not fully determined mechanisms, but seems to alter also LC emigration [Gschwandtner et al, 2009]. Our data also showed elevated levels of histidine in the stratum corneum which probably leads to enhanced conversion of histidine into histamine in the skin mast cells resulting in altered histamine levels in the stratum corneum. Jawdat et al. (2004) suggested that histamine released from mast cells contributes to the migration of Langerhans cells from the epidermis. However, histamine requires other mast cell-derived factors under certain conditions [Jawdat et al, 2004] or does not play a critical role for mast cell-driven LC migration in response to bacterial peptidoglycan [Jawdat et al, 2006]. Impact of inflammation within the skin and tissue underneath might also account for changes in immune responses and alteration of Langerhans cell distribution, function and morphology. Alterations of LC morphology apparently do not vary between WT and mutant mice before or after irradiation. Both loose dendricity or become bigger with dendrites that appear irregular. Therefore neither DNA damage nor cis-UCA alone can be the influencing factor behind UV-induced modifications in LC structure.

Effects of inflammatory conditions, which can be seen in histology of cross sections of irradiated backs and also in the development of skin injuries after irradiation, may also be involved in changes of LC migration. Inflammation increases homeostatic turnover of dDC and LC [Kammath et al 2002] and higher amounts of Il-10 are secreted by LC after UVB irradiation [Yoshiki et al 2009].

4.4 Conclusion and future aims

In this study we have investigated and established the photoprotective role of UCA and the utility of the murine histidinemic model. Our results show that lack of urocanic acid in the

epidermis leads to increased DNA damage due to decreased protection against UVB irradiation.

This study also suggests that the conversion of trans-UCA into cis-UCA is critical for the UV-induced alteration of the density of Langerhans cells within the epidermis. However, UCA is not essential in initiating LC migration, indicating that UV-induced DNA damage is a second independent driver of immunosuppression. The latter is suppressed by endogenous UCA, indicating that UCA has a dual role in immunomodulation. Extensive evaluations of time and dose dependencies of these effects are necessary for a full evaluation of epidermal UCA.

Importantly, this study establishes histidinemic mice as a useful *in vivo* model for studies of epidermal UCA. In future studies, we plan to perform clinical studies involving human subjects with reduced concentrations of epidermal UCA such as histidinemia and atopic dermatitis. Upon confirmation of the value of the histidinemia mouse model, novel therapeutic approaches may be tested in these mice.

5. MATERIALS

5.1 Buffers

Lysis buffer – (tail) DNA preparation

50 mM Tris-Cl pH 8.0

0.1 M NaCl

20 mM EDTA

1% SDS

bidestillated water

Proteinase K (Quiagen; >600 mAU/ml, solution; Cat. No.: 19131)

Pronase E (Sigma; 4 units/mg; P881)

Lysis buffer – isolation of murine epidermal DNA

50 mM TrisHCl pH 8.5

1 mM EDTA

0.5 % SDS

100 mM NaCl

bidestillated water

Proteinase K (100µg/ml)

Protein-preparation

1% NP40 buffer

Protease-Inhibitor-Mix supplied in DMSO; Sigma, Cat. No.: P8340

5.2 Kits

iScript cDNA Synthesis Kit; BioRad, Cat. No.: 170-8891

RNeasy 96; Quiagen; Cat. No.: 74181

In Situ Cell Death Detection Kit; Roche, Cat. No. 1 684 795

LightCycler® 480 Genotyping Master Kit; Roche Applied Science, Cat. No.: 04707524001

LightCycler® 480 SYBR Green I Master Kit; Roche Applied Science, Cat. No.: 04887352001

Histamine-Elisa; IBL International GmbH, Cat. No.: RE59221

Precellys-Keramik-Kit, 1,4 mm 50x2,0 ml; Peqlab Biotechn. GmbH, Cat. No.: 91-PCS-CK14

5.3 Reagents and Solutions

Phenol/Chloroform/Isoamyl-alcohol 25:24:1; Sigma, Cat. No.: P2069

DPBS; Invitrogen/GIBCO, Cat. No.: 14190-094 (500 ml) & 14190-169 (10x500ml)

Normal Goat Serum; Szabo-Scandic, Cat. No.: S-1000

RNA later; Ambion, Cat. No.: 7020

Trizol; Invitrogen, Cat. No.: 15596018

Ammoniumthiocyanate; Merck, Cat. No.: 1012130500

Protamine sulfate salt from Salmon, Grade X; Sigma-Aldrich, Cat. No. P4020-5G

Blotting Dry Milk; Fa. Bio-Rad, Cat. No.: 170-6404

Tween 20; Bio-Rad, Cat. No.: 170-6531

ChemiGlow reagent; Biozyme Laboratories, South Wales, UK

D-Squame stripping discs, 14 mm; Cuderm, Dallas, TX

LSAB®2 Streptavidin-HRP; Dako, Cat. No.: K1016

Color Reagent A – stabilized peroxide solution; R&D Systems, Cat. No.: 895000

Color Reagent B – stabilized chromogen solution; R&D Systems, Cat. No.: 895001

Faramount Aqueous Mounting Medium Ready-to-use; Dako, Cat. No.: S3025

Aquamount Aqueous Mounting Medium; BDH, Cat. No.: 362262H

Neomount Mounting Medium; Merck, Cat. No.: 1.09016.7100

Fluoroprep Mounting Medium; bioMérieux, Cat. No.: 75521

Dako TRS buffer; Dako, Cat. No.: 1700

Ethanol 96 %, Merck, Cat. No.: 1.00971.100

Formaldehyde

Acetone, Merck, Cat. No.: 1.00014.1011

Eosin Y solution alcoholic; Sigma, Cat. No.: HT110180

Hämatoxylin (Papanicolaou) nach Harris; Merck, Cat. No.: 1.09269

Bovine Serum Albumine (BSA); Sigma-Aldrich, Cat. No.: A9647

Xylol; Fisher Scientific,

Paraffin

Chloroform; Merck, Cat. No.: 1.02447.0500

2-Propanol; Merck, Cat. No.: 1.09634.1011

Urocanic Acid (4-Imidazole Acrylic Acid); USB Corporation; Cat. No.: 231701 GM

PAP-PEN: Liquid Blocker; SCI Science Services

Needles 27Gx3/4"-Nr. 20 (0,4 mm x 19 mm); BD Microlance 3, Cat. No.: 302200

Kai sterile dermal biopsy punch 6 mm; Kai medical, Cat. No.: BP-60F

96-well ELISA plates; Nunclon flat-bottom, Nunc, Cat. No.: 167008

Anaesthesia

0,9% Natrium-Chlorid Infusionslösung; Mayrhofer Pharmazeutika, Cat. No.: 12578-1

Ketavet 100 mg/ml; Pfizer vet., Cat. No.: 7506004

Rompun 2% solution; Bayer HealthCare, Cat. No.: 35'464

5.4 Antibodies

Purified Rat Anti-Mouse I-A/I-E; BD Pharmingen, Cat. No.: 556999

Purified Rabbit Anti-Active Caspase-3; BD Pharmingen, Cat. No.: 559565

Anti-Thymine Dimer mAb, clone KTM53; Kamaiya Biomedical Company, Cat. No.: MC-062

Affinity Purified Rabbit Anti-human/mouse Caspase 3 Active; R&D Systems, Cat. No.: AF835

ECL Anti-Mouse IgG, Horseradish Peroxidase-Linked Species-Specific Whole Antibody (from sheep); GE Healthcare Amershaem, Cat. No.: NA931

Alexa Fluor 546 goat anti-rat IgG (H + L); Molecular Probes, Cat. No.: A-11081

Alexa Fluor 546 goat anti-rat IgG (H + L); Molecular Probes, Cat. No.: A -11010

FITC Rat Anti-Mouse I-A/I-E; BD Pharmingen, Cat. No.: 553623

Anti-Mouse-Loricrin Polyclonal Antibody; Covance, Cat. No.: PRB-145P

HAL (Western Blot): monoclonal antibody M04, clone 4F2 raised against the conserved C-terminus of histidase; Abnova, Taipei, Taiwan, Cat. No.: H00003202-B01P

Goat polyclonal Anti-Keratin; Abcam, Cat. No.: ab8572-1

Isotype-controls:

Monoclonal Mouse IgG1* Clone: MOPC 31C; AnCell Immunology Research Products, Cat. No.: 278-010

FITC Rat IgG2 a, κ Isotype Control; BD Pharmingen, Cat. No.: 553929

Rabbit anti-goat IgG polyclonal antibody; Dako, Cat. No.: PO 449

HRP-conjugated goat anti-mouse IgG antibody; Amersham Pharmacia Biotech, Cat. No.: NA9310

5.5 Primer

ALAS (aminolevulinic acid synthase)

forward: 5'- CCACTGGAAGAGCTGTGTGA-3'

reverse: 5'-TGGCAATGTATCCTCCAACA-3'

B2M (β -2-microglobulin)

forward: 5'-ATTCACCCCCACTGAGACTG-3'

reverse 5'-TGCTATTTCTTTCTGCGTGC-3'

HAL

genotyping:

forward: 5'-GGGCCTGGCACTCATCAAT-3'

reverse: 5'-CCTCCAGGGTCAAGGCAG-3'

[for mutation-specific probes (sensor: 5'-TGGCTCGCTCCAGGGCTTC-3'-fluorescein and anchor: LCRed640-5'-AGCCCAGGGAAGTGATCATCTGT-3'-phosphate)]

quantification:

forward: 5'-AGAAGCCCATGGACTGAAAC-3'

reverse: 5'-ATGGATGTCGGTATCGAAGG-3'

5.6 Mice

Mice carrying a mutation in the Hal (histidine ammonia lyase, alternative name histidase) gene were kindly provided by Clare Selden (UK). Cryo-preserved embryos of these mice were obtained from Medical Research Council (MRC), London, UK, and mice were rederived by Biomodels Austria, Vienna, Austria. The mouse line had been generated by crossing Peruvian mice, a strain that carries a natural mutation of the Hal gene, with C57 BL/6 mice. The resulting mice were then back-crossed with C57 BL/6 for more than 20 generations to obtain the mutation in a pure genetic background.

C57 BL/6 mice were provided by Professor Höger (Medical University of Vienna). Mutant mice did not show gross morphological abnormalities, and their behaviour appeared normal.

Homozygous Hal-mut / Hal-mut, heterozygous Hal-mut / wt mice and wildtype wt / wt mice were used for UV irradiation experiments. All experiments were approved by the ethics committee of the Medical University of Vienna (GZ66.009/0028-II/10b/2008 and GZ66.009/104-II/10b/2009).

5.7 Equipment

UVB Lamp

UVB irradiation was performed using F15/T8 15W Waldmann UVB lamps (280-340nm wavelength range). UVB dose was monitored with a UVB-meter (Waldmann).

ELISA plate-reader

Opsys MR Dynex Technologies; Serial number: 1 MRA1461

Microscope

Zeiss Axiovert 200 M laser scanning microscope (Carl Zeiss, Inc., Jena, Germany)

Spectrophotometer

NanoDrop ND-1000 spectrophotometer; PEQLAB Biotechnologie, Erlangen, Germany, Serial number: C678

Sarstedt centrifuge

Precellys 24; Peqlab, Serial number: 000.0779; 2008

Shaver

Silk Finish; Braun

5.8 Software

LightCycler® Probe Design Software 2.0 (Roche Applied Science, Basel, Switzerland)

Zeiss LSM 510 software (Carl Zeiss, Inc., Jena, Germany)

MetaMorph® 6.2r6; 1992-2004 Universal Imaging Corp.

6. METHODS

6.1 Animal handling and tissue preparation

All animal experiments were approved the Ethics Committee of the Medical University of Vienna. All mice were treated in accordance with institutional guidelines.

6.1.1 Tail DNA preparation for PCR analysis

About 5 mm of tail tip was put into 300 µl of lysis buffer. Proteinase K (2,25 µg per 300 µl lysis buffer) and E (7,5 µg per 300 µl lysis buffer) were added just prior to use. Incubation at 55°C followed over night. 300 µl Phenol/Chloroform/Isoamyl-alcohol was added, vortexed and centrifuged (15,000 rpm for 5 minutes). 10 µl of the supernatant were transferred to a new tube and diluted 1:50 with sterile water (490 µl).

6.1.2 Epidermis-dermis separation

Samples were taken 1 hour or 24 hours after radiation. Shock-frozen in liquid-nitrogen, unfrozen, put into ATZ (= 3.8 % ammonium-thiocyanate in PBS) to separate the epidermis from the dermis. Epidermis was put into lysis buffer (→ cf. Isolation of genomic DNA from murine epidermis or keratinocytes).

6.1.3 Isolation of genomic DNA from murine epidermis

Skin biopsies were incubated with dermis-side into ATZ, at 37°C for 30 minutes. Dermis and epidermis were separated using forceps and the epidermis was washed in PBS. Epidermal samples were put into 500 µl lysis buffer each and proteinase K (100 µg/ml) was added. Incubation at 56°C overnight (or for a few hours) in thermo-shaker (1200 rpm). 175 µl 5 M NaCl was added, shaken vigorously (on ice to prevent SDS-precipitation), centrifuged 10 minutes at full speed at 4°C. Supernatant was transferred to new tube (ca 600 µl) and 400 µl phenol/chloroform/isoamylalcohol was added and mixed gently to avoid DNA shearing. All was centrifuged 2 minutes at full speed at 4°C. Supernatant was transferred to a new tube and an equal volume of isopropanol was added and mixed until DNA-threads appeared (ca. 500 µl). DNA pellet was centrifuged 5 minutes full speed at 4°C; pellet was washed with 70% ethanol and after take off of as much ethanol as possible, air-dried and later on dissolved in 200 µl bidistilled water (= bidestillated water) (DNA dissolves within 2-3 h at 56°C or overnight at 4°C). Storage: 4°C for short-term or at -20°C for long-term storage.

6.1.4 Anesthesia

Mice were anesthetized by i.p. injection of 0.2 ml Ketavet/Rompun mix.

0.1 ml Rompun (2% solution)

0.1 ml Ketavet (100 mg/ml)

1,4 ml (NaCl 0,9%)

6.1.5 Tape-stripping of adult mice

Mice were shaved on their backs and anaesthetised with Rompun/Ketavit (cp. Anesthesia). Shaved back of mice was irradiated with UVB (cp. UVB-irradiation) before tape-stripping, the other group remained unirradiated. After chosen timepoint, mice were sacrificed by cervical dislocation. Of each mouse, 10 tape-strips were taken from irradiated back-skin. First three tape strips were discarded to avoid contaminations from hair. Abdomen was shaved post mortem and tape-strips from unirradiated skin were taken from abdominal skin as from irradiated back skin. Tape strips were extracted with KOH according to published protocol and UCA and histidine concentration was determined by HPLC as described previously [Kezic et al, 2009].

6.1.6 Tape-stripping of newborns

Newborns were aged between one or two days. Mice were sacrificed to avoid unnecessary pain and suffering and irradiated with UVB post mortem. After 1 hour, 10 tape-strips from irradiated back-skin of each mouse were taken. The first three tape strips were discarded to avoid contaminations. Tape-strips from unirradiated skin were taken from abdominal skin using the same protocol as for irradiated back skin. Tape strips were extracted with KOH according to a published protocol, and UCA and histidine concentrations were determined by HPLC as described previously [Kezic et al, 2009].

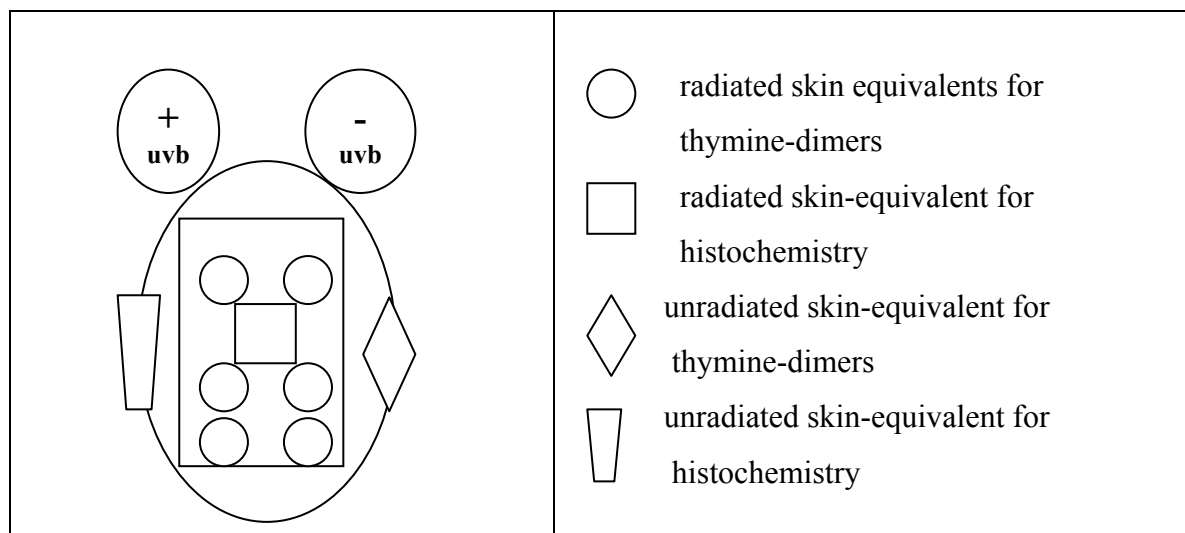
6.1.7 Topical UCA application

UCA was dissolved in DMSO (10mg/ml). 5 µl of this solution was mixed with ethanol absolute to a total volume of 20 µl (concentration: 50µg UCA in DMSO/Ethanol). Vehicle: DMSO:ethanol absolute (1:4). Newborns were aged between one or two days. Mice were killed and on back of each mouse 50 µg UCA in DMSO/ethanol or DMSO/ethanol vehicle was applied. After short incubation time of 10 minutes (in the dark), mice were irradiated on their backs using the low-dose irradiation protocol for CPD determination (e.g. 6.2.3). One hour after irradiation, mice were shock-frozen and stored at -80°C. For thymine dimer formation analysis, mice were defrozen and 2 skin examples of irradiated dorsal skin were taken and put into 3.8% ATZ to separate the epidermis from the dermis. Further processing → cf. Epidermis-dermis separation and Isolation of genomic DNA from murine epidermis).

6.2 Irradiation protocols

6.2.1 UVB irradiation for studying the effects of UVB on Langerhans cells

Eyes of mice were be shielded from irradiation in all irradiation protocols.



6.2.1.1 Single high-dose protocol

Wild type (HIS/HIS) and histidase mutant mice (*his/his*) at the age of 7-10 weeks were anesthetized and irradiated with 250 mJ/cm² UVB (irradiation time: 7 minutes 29 seconds at 50 cm distance from the lamp). Mice were sacrificed at day 1 after UVB exposure by cervical dislocation, and the both ears will be harvested and processed for analysis. Epidermal sheets were prepared and density and morphology of LC were assessed by immunohistochemical detection using an appropriate monoclonal antibody. For quantitative analysis, the density of LC in the irradiated ears was counted and calculated and differences in the LC density of wild-type and histidase-mutant mice was evaluated by Student's t-test.

6.2.1.2 Repeated low-dose protocol

Wild type (HIS/HIS) and histidase mutant mice (*his/his*) at the age of 7-10 weeks were anesthetized and exposed to 100 mJ/cm² UVB daily (irradiation time: 2 minutes 58 seconds at 50 cm distance from the UV lamp) for four consecutive days with a cumulative dose of 400 mJ/cm². One ear was protected from exposure and used as internal unirradiated control. Mice were sacrificed by cervical dislocation 24 hours after last UVB irradiation and both ears were harvested and processed for analysis. Epidermal sheets were prepared and density and morphology of LC was assessed by immunohistochemical detection using an appropriate monoclonal antibody. For quantitative analysis, the density of LC in the irradiated ear was divided by the density of LC in the non-irradiated ear of each mouse, yielding the UV-induced relative change of LC density. The mean deviation (variance) of LC density from the mean was calculated in both groups. Differences in the UV-induced relative change of LC density of wild-type and histidase-mutant mice were evaluated by Student's t-test.

6.2.2 UVB irradiation to study the long-term effects of UVB-light on the skin

Dorsal skin of wild type (HIS/HIS) and histidase mutant mice (*his/his*) at the age of 7-10 weeks was shaved 1 day or at least 1 hour before radiation and mice were anaesthetized prior irradiation. The UVB dose was chosen due to adjustments and results of prior experimental procedures. Chosen UVB dose was a single dose of 250 mJ/cm² (irradiation time: 7 minutes and 29 seconds at 50 cm distance from lamp). Macroscopically visible effects of UVB light on back skin was documented by photography 24, 48, 72, 96 and 120 hours after challenge. Microscopically visible effects of UVB light on back skin were documented by immunofluorescent and immunohistochemical stainings of skin samples 24, 48 and 72, 96 and 120 hours after challenge. For taking skin samples of ears and back skin, an adequate and

significant number of mice were sacrificed by cervical dislocation 24, 48, 72, 96 and 120 hours after challenge.

6.2.3 UVB irradiation for studying the photoprotective role of UCA – newborn mice

Wild type (HIS/HIS) and histidase mutant mice (*his/his*) at the age of 1-2 days were sacrificed prior irradiation. Dorsal skin was irradiated with an UVB dose adjusted by changing the duration of exposure to UVB and power of lamp (25 mJ/cm², 100 mJ/cm², 250 mJ/cm²).

Skin samples were taken 1 hour after irradiation. For thymine dimer formation analysis 3 skin examples of irradiated dorsal skin were taken and put into 3.8% ATZ to separate the epidermis from the dermis. Further processing → cf. Epidermis-dermis separation and Isolation of genomic DNA from murine epidermis).

6.2.4 UVB irradiation for studying the photoprotective role of UCA – adult mice

Dorsal skin of wild type (HIS/HIS) and histidase mutant mice (*his/his*) at the age of 7-10 weeks was shaved 1 day or at least 1 hour before radiation and mice were anaesthetized prior irradiation. The UVB dose was adjusted by changing the duration of exposure to UVB and power of lamp (25 mJ/cm², 100 mJ/cm², 250 mJ/cm²).

Mice were sacrificed 24 hours after radiation. For thymine dimer formation and apoptosis analysis skin examples of irradiated dorsal skin and non-irradiated flank skin were harvested 1 hour and 24 hours after irradiation using 6 mm punch biopsies, shock-frozen in liquid nitrogen and stored at -80°C till use. Skin examples of radiated dorsal skin and non-radiated flank skin for immunohistochemical analyses were fixed in formalin and paraffin-embedded.

6.2.5 Calculation mode for irradiation time (UVB irradiation of mouse skin)

$\frac{mJ/cm^2 \times 1000}{W/cm^2} = \text{irradiation time in seconds}$

W/cm^2

Chosen UVB dose was a single dose of 250 mJ/cm² (irradiation time: 7 minutes and 29 seconds at 50 cm distance from the Waldmann UV 180 lamp).

Power P: $P = W/t = E/t$ (when rate of energy conversion is constant.)

Irradiation time: $t = E / P = (E/A) / (P/A)$

$E/cm^2 = \text{UVB dose} = 250 \text{ mJ/cm}^2$

$P/cm^2 = x \text{ mW/cm}^2$ (measured with UV meter at lamp-to-skin distance)

$t = 250 [mJ/cm^2] / x \text{ mW/cm}^2$

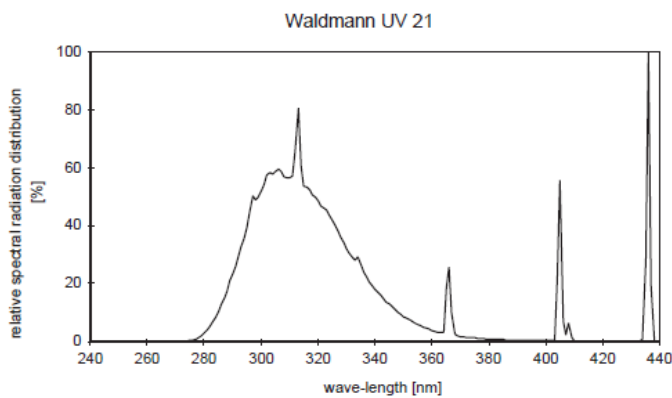
$x = 0.57 \text{ W}$ (measured with UV meter at lamp-to-skin distance)

Dose/area = cumulative energy over time per area

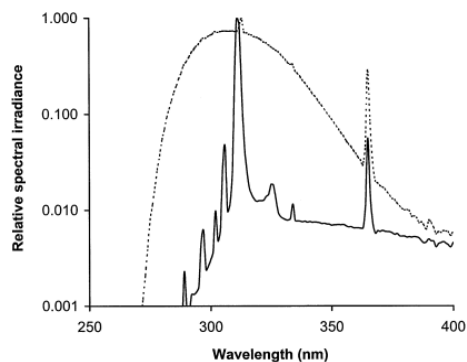
Irradiance = Power per area of electromagnetic radiation at a surface

6.2.6 UV-lamp-spectra-comparison

The following diagram shows the spectral radiation distribution of the UV lamp used for irradiation experiments.



For comparison, the emission spectrum of 2 lamps used in another study is shown below. Note that the values on the y-axis are shown on a logarithmic scale.



*The spectral power distribution for the two lamps.
Solid line, TL-01; dashed line, TL-12.*

[FROM: Similar Dose-Response and Persistence of Erythema with Broad-Band and Narrow-Band Ultraviolet B Lamps. Sharmila Das, James J Lloyd and Peter M Farr]

6.3 Molecular Biology

6.3.1 RNA-isolation using RNeasy 96 protocol for isolation of total RNA from animal cells

Tissue was put into RNA later (300 μl) and stored on ice/4°C immediately. Tissue-aliquot size: about one half of a split ear (dorsal or ventral half).

For further processing, tissue aliquot was taken out of RNA later and put on a soft tissue to wipe off RNA-later, cut into small pieces and was put it into a Precellys-tube. RLT-buffer from RNeasy-Quiagen-Kit was added. Tubes were placed in a Sarstedt centrifuge, shaken twice for 45 seconds at 5 500 rpm and immediately put on ice for 5 minutes. Samples were placed in a centrifuge and spinned for 10 minutes at 4°C, 13 000 rpm. An RNeasy 96 plate was placed on a vacuum-block and samples were applied into wells. Samples were then processed following Quiagen-standard-protocol for vacuum-technology (without step7 = DNA digestion). For elution 50 µl of RNase-free water/well was added and after incubation time of 2-3 minutes at room temperature, eluted. Elution step was repeated once. Samples were pipetted from 96-well to single 0.5 ml Eppendorf tubes and stored at -80°C.

6.3.2 RNA-isolation using Trizol

Tissue was cut into small pieces and put into trizol in Precellys tubes (750 µl) and put on ice immediately. Tissue-aliquot size: about one half of a split ear (dorsal half). Tubes were placed in a Sarstedt centrifuge, shaken twice for 45 seconds at 5 500 rpm and immediately put on ice for 5 minutes. Samples were placed in a centrifuge and spinned for 10 minutes at 4°C, 13 000 rpm. Supernatant was pipetted off and placed in a fresh Eppendorf tube (about 500 µl) and mixed with 150 µl chloroform by shaking for 15 seconds, then chilled on ice for 5 minutes. Samples were placed in a centrifuge and spinned for 20 minutes at 4°C, 13 000 rpm. Top, aqueous, phase was pipetted off into a fresh Eppendorf tube and mixed with an equal volume of 2-propanol (~250 µl) and frozen at -20°C for 30 minutes. Samples were placed in a centrifuge and spinned for 15 minutes at 4°C, 13 000 rpm. Supernatant was discarded. Pellet was washed with ice-cold ethanol absolut. Samples were placed in a centrifuge and spinned for 15 minutes at 4°C, 13 000 rpm. Supernatant was discarded. Pellet was air-dried, resolved in 50 µl sterile water and stored at -80°C.

6.3.3 cDNA-synthesis

RNA samples were defrozen and cDNA was generated by following users instructions of Bio-Rad-iScript cDNA Synthesis Kit.

6.3.4 Quantitative real time PCR (qPCR)

RNA was prepared from murine epidermis using the Trizol reagent (Invitrogen) according to the manufacturer's instructions and reverse-transcribed according to a standard protocol (Eckhart et al., 1999). qPCR was performed using the LightCycler® technology and the

LightCycler® 480 SYBR Green I Master Kit according to the manufacturer's protocol. Histidase cDNA was amplified with the primers for HAL, β -2-microglobulin and aminolevulinic acid synthase (ALAS). Same program (denaturation at 95°C for 10 minutes and 55 cycles consisting of incubations at 95°C for 10 seconds, 65 °C for 10 seconds, and 72 °C for 15 seconds) was used for all three genes. Relative expression of histidase was normalized to that of the house keeping gene β -2-microglobulin and ALAS and quantified using a mathematical model detailed elsewhere (Pfaffl 2001). Efficiency of the primer pairs were determined as described previously (Kadl et al. 2002).

6.3.5 Genotyping of mice

Mice were genotyped by integrated PCR amplification and detection of the a G965A point mutation in the Hal gene by fluorescence resonance energy transfer and probe melting curves according to a published protocol with modifications (Bernard et al. 1998). The LightCycler® Probe Design Software was used to design gene-specific primers and mutation-specific probes. Reactions were carried out with the LightCycler® technology and the LightCycler® 480 Genotyping Master Kit according to the manufacturer's protocol, whereby the concentration of the forward primer was 0.4 μ M and the concentrations of the reverse primer and the probes were 0.2 μ M. Amplification by 60 cycles of denaturation at 95°C for 10 seconds, annealing at 65°C for 10 seconds and extension at 72°C for 9 seconds was followed by melting point analysis which comprised heating to 95°C for 10 seconds, cooling down to 40°C, holding at 40°C for 15 sec hold at and heating up to 90°C. The validity of the genotyping assay was verified by DNA sequencing.

6.3.6 Protein isolation

Dorsal skin of wild type (HIS/HIS) and histidase mutant mice (*his/his*) at the age of 7-10 weeks was shaved 1 day or at least 1 hour before radiation and mice were anaesthetized prior irradiation. The UVB dose was adjusted by changing the duration of exposure to UVB and power of lamp (25 mJ/cm², 100 mJ/cm², 250 mJ/cm²; using a Waldmann UV 180 lamp).

Mice were sacrificed 24 hours after irradiation. For Western Blot analysis skin examples of irradiated dorsal skin and non-irradiated flank skin and irradiated ear-skin (dorsal side) were harvested after irradiation using 6 mm punch biopsies/whole ear. One part of the samples was immediately put into 1% NP40-buffer (300 μ l + 3 μ l Protease-Inhibitor-Cocktail/sample in Precellys tubes). The other part (ventral side of irradiated ear skin) was put onto 3.8% ATZ for half an hour at 37°C. Epidermis was separated from dermis and put into 1% NP40-buffer

(300µl + 3 µl Protease-Inhibitor-Cocktail/sample in Precellys tubes). All tubes were placed in a Sarstedt centrifuge, shaken twice for 45 seconds at 5 500 rpm and immediately put on ice for 5 minutes.

Samples were placed in a centrifuge and spun for 10 minutes at 4°C, 13 000 rpm. Protein solutions were pipetted into fresh Eppendorf tubes and stored at -20°C.

6.4 Biochemistry

6.4.1 Western blot analysis

Western blot analysis was performed essentially as described previously (Eckhart et al., 2008). Briefly, proteins from murine epidermis were prepared by incubation with ice-cold PBS containing 1% NP-40 and complete protease inhibitor. After removal of debris by centrifugation the supernatants were electrophoresed through a 8-18% gradient polyacrylamide gel (GE Healthcare) and blotted onto a nitrocellulose membrane. A monoclonal antibody M04, clone 4F2 raised against the conserved C-terminus of histidase (corresponding to human histidase amino acid residues 558-657) and Anti-Pan-Cytokeratin (control) (dilution: 1:2000) were used as first-step antibodies and HRP-conjugated goat anti-mouse IgG antibody (dilution 1:10000) and rabbit anti-goat IgG polyclonal antibody (dilution: 1:10000) for the Keratin-control were used as second step reagents. Reaction products were detected by chemiluminescence with the ChemiGlow reagent according to the manufacturer's instructions.

6.4.2 Determination of urocanic acid concentrations in the stratum corneum

The stratum corneum was prepared from the shaved back skin of mice by repeated tape stripping using D-Squame stripping discs. Tape strips were extracted with KOH according to a published protocol and UCA was determined by HPLC as described previously (Kezic et al., 2009).

6.4.3 Determination of UV absorption of stratum corneum extracts

Tape strips were prepared as described above. The stratum corneum adhering to the third to the sixth tape strip from the back skin of each mouse was extracted by incubation in 50 µl PBS buffer containing 1% Tween for 20 minutes. For each extract, UV absorbance in the wavelength range of 220 to 320 nm was measured using a NanoDrop ND-1000 spectrophotometer. For statistical analysis, the absorbance values at 280 nm were recorded and corrected for unspecific absorbance because of extraction of UV absorbing substances from the tape strip alone. Mean absorbance values of 4 tape strips from 5 mice per group were used to calculate the mean

absorbance and the standard error of the mean of each genotype. Statistical significance was evaluated using Student's t-test.

6.4.4 Vacuum-Dot-Blot (South-Western Blot for thymine dimers)

A nitrocellulose membrane was laid on a piece of Whatman paper and wet with bidistilled water. The vacuum dot-blot system was assembled and DNA samples (100 μ l per well) were applied (500 μ g – 250 μ g – 125 μ g – 62,5 μ g each in 100 μ l). Vacuum was applied and the membrane was washed once with bidest. Membrane was taken out and air-dried. Then, the membrane was put between 2 pieces of Whatman paper (like in an envelope), tape shut and baked at 80 °C for 15 minutes (oven). After baking, the membrane was blocked for 1 hours in blocking buffer (PBS+Tween20 (0.5 ml) + non-fat milk (25 g/500 ml)). The primary antibody was applied (α -thymine dimer) and incubated over night (dilution of 1st antibody was 1:1000; 1 μ l antibody were mixed with 999 μ l blocking buffer). Membrane was washed for 15 minutes with blocking buffer (3x) and incubated in α -mouse/HRP (1/10000) for 1 hour (5 μ l antibody + 49995 μ l blocking buffer). After an hour, the membrane was washed with PBS+Tween20 (0.5 ml/500 ml) for 15 minutes (4x) and once with PBS only.

Chemiluminescent reagent was applied and left on the membrane for 5 minutes. Detection followed (1x 5 minutes, 1x over night).

6.4.5 ELISA for thymine dimers (determination of DNA damage)

a. The coating of microtiter plates by protamine sulfate

A 0.003% protamine sulfate solution (in distilled water) was prepared and stirred for 1 hour. 50 μ l/well of the solution was distributed to 96 well microtiter plates and incubated over night at 37°C to coat protamine sulfate on plates by drying completely. Plates were washed three times with 100 μ l/well distilled water and stored in the dark (up to 6 month).

b. DNA-sample preparation

DNA concentration of samples was measured using Nanodrop. Requested concentration/well was prepared with 1x PBS (based on used UVB-dose and normalized standard-detection-curve). DNA samples were prepared in triplicons (total volume of DNA solution was 150 μ l) in 0,5 Eppendorf tubes and DNA was denatured by heating DNA solutions in a PCR machine at 100°C for 10 minutes. DNA solutions were rapidly chilled on ice for 15 minutes afterwards and then distributed 50 μ l/well of each denatured DNA solution to protamine sulfate precoated 96 well microtiter plates (in duplicates – 2 wells were used for each sample) and dried completely overnight at 37°C.

c. DNA damage detection

DNA-coated plates were washed 5 times with 150 µl/ well PBS-T (0.05% Tween-20 in 1xPBS). 200 µl/well blocking buffer, consisting of 0.25% skim milk in PBS-T (0.05% Tween-20 in 1xPBS) were distributed to each well to prevent non-specific antibody binding and incubated for 1 hour at 37°C.

Plates were washed 5 times with 150 µl/ well PBS-T. 100 µl/ well CPD antibody diluted 1:2000 to 0.25 µg/ml in 0.25% skim milk in PBS-T was added to DNA-coated wells and incubated for 1 hour at 27°C.

Plates were washed 5 times with 150 µl/ well PBS-T. Plate was incubated with a sheep anti mouse IgG antibody conjugated with peroxidase, diluted 1:1000 in 0.25% skim milk in PBS-T, 100 µl/ well, for 1 hour at 37°C. Plates were washed 5 times with 150 µl/ well PBS-T. 100 µl/ well of substrate solution (color reagent A and B mixed 1:2) was distributed to each well and incubated for 5 minutes at room temperature in the dark. Enzyme reaction was stopped by distribution of 50 µl/ well of 1M H₂SO₄ to each well.

After gentle mixing (by spectrophotometer), absorbance of each well was determined at 450 nm by a spectrophotometer.

6.4.6 Histamine-Elisa (IBL International GmbH)

Urine of mice was collected in Eppendorf-tubes and stored at -20°C.

Urine of mice was diluted 1:50 and 1:100 with 0,1 N HCl (as suggested in IBL Histamine-Elisa standard protocol). Diluted samples were treated as suggested in IBL-Histamine-Elisa-standard protocol.

6.5 Microscopy

After the mice were sacrificed, tissue samples were taken and according to the further protocols, tissues were fixed in formaldehyde (for HRP) or acetone (Immunofluorescence).

Formaldehyde-fixation was proceeded by another department in standard procedure.

6.5.1 Immunohistochemistry: paraffin (HRP) – staining (TUNEL, thymine-dimer and active caspase 3)

Skin specimens were fixed in phosphate-buffered 4.5% formaldehyde and embedded in paraffin. Paraffinblocks were cut in thin sections and put onto slides. Sections were heated until paraffin became liquid, then the sections were deparaffinized and washed in xylol, ethanol (100%-80%-50%-30%) and aqua dest.

Slides were put into Dako-buffer (= target retrieval solution = citrate-buffer, diluted 1:10 with H₂O) and heated in the microwave at 500 Watt (2x5 minutes), then left at room temperature to cool down (in the buffer).

After washing with PBS, sections were encircled with a PAP PEN.

Immunolabelling of active Caspase 3: Sections were incubated with 50 µl blocking buffer (10% normalserum (goat) in 2%BSA/PBS) for 30 minutes. Serum was poured off and primary antibody (affinity purified Rabbit Anti-Human/Mouse Caspase 3 active, 1:500 in 2% BSA/PBS) was applied (50 µl/section) and incubated for 1 hour. Sections were washed with PBS. Secondary antibody (Alexa Flour 546 Goat-Anti-Mouse antibody, 1:500 in 2%BSA/PBS) was incubated for 30 minutes, washed off twice with PBS. Streptavidin HRP DAKO was applied and incubated for 30 minutes, then washed off with PBS (2x5 minutes). Visualization with DAB (microscopical control) followed. After washing with water, counterstaining with HE, another washing with water, the sections were mounted with aqueous mounting medium.

Tunel-Kit (In Situ Cell Death Detection Kit with Fluorescein): sections were incubated with 10x labelling solution mixed 1:10 with enzyme (50 µl/section) for one hour at 37°C in the dark. After three washing steps with PBS (3-4 minutes), nuclei were stained with Hoechst staining (1:5000 dilution in PBS) for 5 minutes. Hoechst was washed off with water and sections were mounted with Fluoroprep.

Cyclobutane pyrimidine dimer (CPD; thymine dimer) labelling: Sections were incubated with 50 µl blocking buffer (10% normalserum (goat) in 2%BSA/PBS) for 30 minutes. Serum was poured off and a Mouse Anti-Thymine Dimer antibody (1:200) as primary antibody (in 2% BSA/PBS) was applied (50 µl/section) and incubated for 1 hour. Sections were washed with PBS. Secondary antibody was an Alexa Flour 546 Goat-Anti-Mouse antibody (1:500 in 2%BSA/PBS) and was incubated for 30 minutes, washed off twice with PBS. Streptavidin HRP DAKO was applied and incubated for 30 minutes, then washed off with PBS (2x5 minutes). Visualization with DAB (microscopical control) followed. After washing with water, counterstaining with HE, another washing with water, the sections were mounted with aqueous mounting medium.

6.5.2 Haematoxylin and Eosin (H&E) staining

Skin specimens were fixed in phosphate-buffered 4.5% formaldehyde and embedded in paraffin. Paraffinblocks were cut in thin sections and put onto slides. Sections were heated until paraffin became liquid, then the sections were deparaffinized and washed in xylol (2x10 min), 100% ethanol (2x2 min), 80% ethanol (2x2 min), 30% ethanol (2x2 min) and aqua dest.

(2x2 min). 1:2 with aqua dest. diluted hämatoxylin (papanicolaou) was pipetted onto sections and incubated for 10 minutes. Sections were washed for 10 minutes with aqua dest. 200 ml eosin was mixed with 345 µl acetic acid and sections were stained for 5 minutes. Sections were washed again in aqua dest. (2x2 min), 30% ethanol (2x2 min), 80% ethanol (2x2 min), 100% ethanol (2x2 min) and xylol (2x10 min) and embedded with Neomount.

6.5.3 Preparation/staining of ears for evaluation of LC-density:

Mice were sacrificed. Ears were cut off, separated, and put with dermis-portion into AZT (=3.8 % ammonium-thiocyanate). Incubation at 37°C for 30 minutes followed. Dermis and epidermis were separated and the epidermis was washed in 1x-PBS for 5 minutes, fixed in 4°C-cold acetone for 5 minutes, air-dried and washed again in 1x-PBS for 5 minutes. Blocking buffer (10% serum of the animal in which the second antibody was generated = goat in 2% BSA/PBS) was applied for 1 hour. Primary antibody was a purified Rat Anti-Mouse I-A/I-E antibody (concentration: 0.5 mg/ml) and was diluted 1:50 with 2% BSA/PBS. Anti-Rat IgG was used as negative control. Incubation was done at 4°C over night (antibody takes longer to bind within tissues). Epidermis was washed with PBS (2 x 5 minutes) and the second antibody was applied at room temperature for 1 hour. Second antibody was an Alexafluor546 Goat-Anti-Rat-antibody, diluted 1:500 with 2%BSA/PBS. Sheets were washed in PBS (2 x 5 minutes) and nuclei stained with Hoechst (1:5000 dilution in dH2O) for 5 minutes at room temperature. Ear sheets were washed once in PBS for 5 minutes afterwards and fixed on microscopy slides with Faramount Aqueous Mounting Medium. Samples were analyzed using a _40 objective.

For analysis, 20-40 representative areas were photographed per ear and Langerhans cells were counted manually with the help of Metamorph-counting program and statistically evaluated, using students T-test.

6.5.4 Preparation/double-staining of ears for active Caspase-3-positive cells

Mice were sacrificed. Ears were cut off, separated, and put with dermis-portion into AZT (=3.8 % ammonium-thiocyanate). Incubation at 37°C for 30 minutes followed. Dermis and epidermis were separated and the epidermis was washed in 1x-PBS for 5 minutes, fixed in 4°C-cold acetone for 5 minutes, air-dried and washed again in 1x-PBS for 5 minutes. Blocking buffer (10% serum of the animal in which the second antibody was generated = goat in 2% BSA/PBS) was applied for 1 hour. First antibody was a FITC-conjugated Rat Anti-Mouse I-A/I-E purified Rat Anti-Mouse I-A/I-E antibody (concentration: 0.5 mg/ml) and was diluted

1:200 with 2% BSA/PBS). FITC-conjugated Anti-Rat IgG was used as negative control. Incubation was done at 4°C over night. Epidermis was washed with PBS (2 x 5 minutes) and the second first antibody, a purified Rabbit Anti-Active Caspase-3 antibody was applied at room temperature for 2 hours (concentration: 0.5 mg/ml; dilution: 1:100 with 2% BSA/PBS). Anti-Rabbit IgG was used as negative control. Epidermis was washed with PBS (2 x 5 minutes) and the second antibody was applied at room temperature for 1 hour. Second antibody was an Alexafluor546 Goat-Anti-Rabbit-antibody, diluted 1:500 with 2%BSA/PBS. Sheets were washed in PBS (2 x 5 minutes) and nuclei stained with Hoechst (1:5000 dilution in dH₂O) for 5 minutes at room temperature. Ear sheets were washed once in PBS for 5 minutes afterwards and fixed on microscopy slides with Paramount Aqueous Mounting Medium. The samples were analyzed using 20x and 40x objectives.

6.6 Statistical analysis

The HIS/HIS group and the his/his group were compared in experiments 2, 4, and 6 (see tables 2, 4, 6). Variance of LC density and ear thickness within the groups was measured. Statistical analysis was performed using the Student's t-test.

7. REFERENCES

1. Aberer W, Schuler G, Stingl G, Hönigsmann H, Wolff K; 1981: Ultraviolet Light depletes surface markers of Langerhans cells. *J Invest Dermatol* 76: 202-210
2. Aberer W, Romani N, Elbe A, Stingl G; 1986: Effects of physicochemical agents on murine epidermal Langerhans cells and Thy-1-positive dendritic epidermal cells. *J Immunol* 136, 4
3. Agar N, Young AR; 2005: Melanogenesis: a photoprotective response to DNA damage? *Mutat Res* 571(1-2):121-32
4. Ahmad H, Mukhtar H; 2004: Toxicology of the skin: new and emerging concepts. *Toxicol Applied Pharm* 195, 265-266
5. Allan RS et al.; 2003: Epidermal viral immunity induced by CD8alpha+ dendritic cells but not by Langerhans cells. *Science* 301:1925-1928
6. Allan RS et al.; 2006 : Migratory dendritic cells transfer antigen to a lymph node-resident dendritic cell population for efficient CTL priming. *Immunity* 25:153-162
7. Andersen FA; 1995: Final Report on the Safety Assessment of Urocanic Acid. *Int J Toxicol* 14: 386-423
8. Anjuere F et al.; 1999: Definition of dendritic cell subpopulations present in the spleen, Peyer's patches, lymph nodes, and skin of the mouse. *Blood* 93: 590-598
9. Aubin F; 2003: Mechanisms involved in ultraviolet light-induced immunosuppression. *Eur J Dermatol* 13: 515-23
10. Bacci S, Romagnoli P, Streilein JW; 1998: Reduction in Number and Morphologic Alterations of Langerhans Cells After UVB Radiation In Vivo are Accompanied by an Influx of Monocytoid Cells into the Epidermis. *J Invest Dermatol* 111: 1134-1139
11. Bacci S, Alard P, Streilein JW; 2001: Evidence that ultraviolet B radiation transiently inhibits emigration of Langerhans cells from exposed epidermis, Thwarting contact hypersensitivity induction. *Eur J Immunol* 31: 3588-3594
12. Baden HP, Hori Y, Pathak MA, Levy HL; 1969: Epidermis in histidinemia. *Arch Dermatol* 100: 432-435
13. Baden HP, Pathak MA; 1967: The metabolism and function of urocanic acid in skin. *J Invest Dermatol* 48: 11-17
14. Banchereau J, Steinman RM; 1998: Dendritic cells and the control of immunity. *Nature* 392: 245-252.

15. Bennet CL, Noordegraaf M, Martina CA, Clausen BE; 2007: Langerhans cells are required for efficient presentation of topically applied haptens to T cells. *J Immunol* 179: 6830-6835
16. Bennet CL et al.; 2005: Inducible ablation of mouse Langerhans cells diminishes but fails to abrogate contact hypersensitivity. *J Cell Biol* 169: 596-576
17. Bergstresser PR, Toews GB, Streilein JW; 1980: Natural and perturbed distribution of Langerhans cells: responses to ultraviolet light, heterotopic skin grafting, and dinitrofluorobenzene sensitization. *J Invest Dermatol* 75: 73-77
18. Bologna, Jorizzo, Rapini et.al.; *Dermatology*, Volume 1 & 2, 2003; Mosby/Elsevier
19. Brash DE, Ziegler A, Jonason AS, Simon JA, Kunala S, Leffell DJ; 1996: Sunlight and sunburn in human skin cancer: p53, apoptosis, and tumor promotion. *J Invest Dermatol Symp Proc* 1: 136-42.
20. Brenneisen P, Wenk J, Klotz LO, Wlaschek M., Scharffetter-Kochanek K; 1998: Central role of ferrous/ferric iron in the ultraviolet B irradiation-mediated signaling pathway leading to increased interstitial collagenase (matrix-degrading metalloprotease (MMP)-1) and stromelysin-1 (MMP-3)mRNA levels in cultured human dermal fibroblasts. *J Biol Chem* 273: 5279-5287
21. Brookman J., Chacón JN, Sinclair RS; 2002: Some photophysical studies of cis- and trans-urocanic acid. *Photochem Photobiol Sci* 1(5):327-32
22. Bursch LS et al.; 2007: Identification of a novel population of Langerin⁺ dendritic cells. *J Exp Med* 204: 3147-3156
23. Chu DC, Haake AR, Holbrook K, Loomis CA; : The structure and development of the skin in: Freedberg IM, Eisen AZ, Wolff K, Austen KF; Goldsmith LA, Katz SI, Fitzpatrick's *Dermatology in General Medicine*, McGraw Hill, New York, 2003
24. Cruz PD JR, Nixon-Fulton J, Tigelaar RE, Bergstresser PR; 1989: Disparate effects of in vivo low-dose UVB irradiation on intravenous immunization with purified epidermal cell subpopulations for the induction of contact hypersensitivity. *J Invest Dermatol* 92:160
25. Cumberbatch M., Dearman R.J., Griffiths C.E., Kimber I.; 2003: Epidermal Langerhans cell migration and sensitisation to chemical allergens. *APMIS* 111: 797-804
26. Dandie GW, Clydesdale GJ, Jacobs I, Muller HK; 1998: Effects of UV on the migration and function of epidermal antigen presenting cells. *Mutat Res* 422:147-54

27. De Fabo EC, Noonan FP ; 1983 : Mechanism of immune suppression by ultraviolet irradiation in vivo. I. Evidence for the existence of a unique photoreceptor in skin and its role in photoimmunology. *J Exp Med* 158: 84-98
28. De Fabo EC, Kripke ML; 1979: Dose-response characteristics of immunologic unresponsiveness to UV-induced tumors produced by UV irradiation of mice. *Photochem Photobiol* 30: 385-390
29. De Fabo EC, Kripke ML; 1980: Wavelength dependence and dose-rate independence of UV radiation induced suppression of immunologic unresponsiveness of mice to a UV-induced fibrosarcoma. *Photochem Photobiol* 32: 183-188
30. De Fine OF, Wulf HC, Crosby J, Norval M; 1996: The sunscreens effect of urocanic acid. *Photodermatol Photoimmunol Photomed* 12: 95-99
31. Durbeej B, Eriksson LA; 2002: Reaction mechanism of thymine dimer formation in DNA induced by UV light. *J Photochem Photobiol* 152: 95-101
32. Duthie M.S., Kimber I., Dearman R.J., Norval M. 2000: Differential effects of UVA1 and UVB radiation on Langerhans cell migration in mice. *J Photochem Photobiol B* 57 (2-3): 123-31
33. Eckhart L, Schmidt M, Mildner M, Mlitz V, Abtin A, Ballaun C, Fischer H, Mrass P, Tschachler E; 2008: Histidase expression in human epidermal keratinocytes: regulation by differentiation status and all-trans retinoic acid. *J Dermatol Sci* 50, 209-215
34. El-Ghorr AA, Norval M., 1997: The effect of chronic treatment of mice with urocanic acid isomers. *Photochem Photobiol* 65, 866-872
35. El-Ghorr AA, Norval M; 1995: A monoclonal antibody to cis-urocanic acid prevents the ultraviolet-induced changes in Langerhans cells and delayed hypersensitivity responses in mice, although not preventing dendritic cell accumulation in lymph nodes draining the site of irradiation and contact hypersensitivity responses. *J Invest Dermatol* 105:264-268
36. El-Ghorr AA, Norval M; 1997: Biological effects of narrow-band (311 nm TL01) UVB irradiation: a review. *J Photochem Photobiol B* 38: 99–106
37. Honigsmann H; 1990: Phototherapy and photochemotherapy. *Semin Dermatol* 9: 84–90
38. Eller MS, Maeda T, Magnoni C, Atwal D, Gilchrest BA; 1997: Enhancement of DNA repair in human skin cells by thymidine dinucleotides: evidence for a p53-mediated mammalian SOS response. *PNAS*, 94: 12627–32.

39. Elmetts CA, Bergstresser PR, Tigelaar RE, Wood PJ, Streilein JW; 1983: Analysis of the mechanism of unresponsiveness produced by haptens painted on skin exposed to low dose ultraviolet radiation. *J Exp Med* 158: 781
40. Enari M, Sakahira H, Yokoyama H, Okawa K, Iwamatsu A, Nagata S; 1998: A caspase-activated Dnase that degrades DNA during apoptosis, and its inhibitor ICAD. *Nature* 391: 43-50
41. Fisher MS, Kripke ML; 1977: Systemic alteration induced in mice by ultraviolet irradiation and its relationship to ultraviolet carcinogenesis. *Proc Nat Acad Sci*, 74:1688
42. Fourtanier A, Moyal D, Seité S; 2008: Sunscreens containing the broad-spectrum UVA absorber, Mexoryl SX, prevent the cutaneous detrimental effects of UV exposure : a review of clinical study results . *Journal compilation © Blackwell Munksgaard Photodermatology, Photoimmunology & Photomedicine* 24, 164-174
43. Freedberg IM, Eisen AZ, Wolff K, Austen KF, Goldsmith LA, Katz SI; Fitzpatrick's Dermatology in General Medicine, 6th edition, Volume 1; New York, McGraw-Hill, 2003
44. Fritsch: Dermatologie Venerologie; 2.Auflage, Springer Verlag, Berlin, 2003
45. Fu PP, Howard CP, Culp S, Xia Q, Webb PJ, Blankenship L, Wamer WG, Bucher JR; 2002: Do topically applied skin creams containing retinyl palmitate affect the photocarcinogenicity of simulated solar light? *J Food Drug Anal* 10, 262-268.
46. Gibbs NK, Norval M, Traynor NJ, Crosby J, Lowe G, Johnson BE; 1993: Comparative potency of broad-band and narrow-band phototherapy sources to induce edema, sunburn cells and urocanic acid photoisomerization in hairless mouse skin. *Photochem Photobiol* 57:584-590, correction: *Photochem Photobiol* 58: 769
47. Gil EM, Kim TH; 2000: UV-induced immune suppression and sunscreen. *Photodermatol Photoimmunol Photomed* 16: 101–110.
48. Gilmour JW, Norval M; 1993: The effect of ultraviolet B irradiation, cis-urocanic acid and tumor necrosis factor-alpha on delayed hypersensitivity to herpes simplex virus. *Photodermatol Photoimmunol Photomed* 9:225-261
49. Ginhoux F, et al.; 2007: Blood-derived dermal langerin+ dendritic cells survey the skin in the steady state. *J Exp Med* 204:3133-3146
50. Gordon J, Barnes NM; 2007: Serotonin: A real blast for T cells; *Blood* 109, 3130-3131
51. Gschwandtner M, Rossbach K, Dijkstra D, Bäumer W, Kietzmann M, Stark H, Werfel T, Gutzmer R; 2009: Murine and human Langerhans cells express a functional

- histamine H(4) receptor: modulation of cell migration and function; *Allergy*, DOI:10.1111/j.1398-9995.2009.02279.x
52. Hanson KM, Simon JD; 1998: Epidermal trans-urocanic acid and the UV-A-induced photoaging of the skin. *Proc Natl Acad Sci U S A* 95: 10576-10578
53. Hedrich HJ, Bullock G: *The Laboratory Mouse*; 2004, Elsevier Limited
54. Hemelaar PG, Beijersbergen van Henegouwen; 1996: The protective effect of N-acetylcysteine on UVB-induced immunosuppression by inhibition of action of cis-urocanic acid. *Photochem Photobiol* 63: 322-327
55. Hemmi HM et al.; 2001: Skin antigens in the steady state are trafficked to regional lymph nodes by transforming growth factor-beta1-dependent cells. *Int Immunol* 13:695-704
56. Henri S et al.; 2001: The dendritic cell populations of mouse lymph nodes. *J Immunol* 167: 741-748
57. IJland SA J et al.; 1998: Urocanic acid does not photobind to DNA in mice irradiated with immunosuppressive doses of UVB. *Photochem Photobiol* 67(2): 222-226
58. Idzko M, Panther E, Stratz C, Muller T, Bayer H., Zissel G, Durk T, Sorichter S, Di Virgilio F, Geissler M, Fiebich B, Herouy Y, Elsner P, Norgauser J, Ferrari D; 2004: The serotonergic receptors of human dendritic cells: Identification and coupling to cytokine release. *J Immunol* 172, 6011-6019
59. Jaksic A, Finlay-Jones JJ, Watson CJ, Spencer LK, Santucci I, Hart PH; 1995: Cis-urocanic acid synergizes with histamine for increased PGE2 production by human keratinocyte: link to indomethacin-inhibitable UVB-induced immunosuppression. *Photochem Photobiol* 61: 303-309
60. Jawdat DM, Albert EJ, Rowden G, Haidl ID, Marshall JS; 2004: IgE-mediated mast cell activation induces Langerhans cell migration in vivo. *J Immunol* 173:5275-5282
61. Jawdat DM, Rowden G, Marshall JS; 2006: Mast cells have a pivotal role in TNF-independent lymph node hypertrophy and the mobilization of Langerhans cells in response to bacterial peptidoglycan. *J Immunol* 177:1755-62.
62. Jurkiewicz BA, Buettner GR; 1996: EPR detection of free radicals in UV-irradiated skin: mouse versus human. *Photochem Photobiol* 64: 918-922
63. Kamath AT et al.; 2002: Developmental kinetics and lifespan of dendritic cells in mouse lymphoid organs. *Blood* 100:1734-1741

64. Kammeyer A, Tuenissen MBM, Pavel S, De Rie MA, Bos JD; 1995: Photoisomerization spectrum of urocanic acid in human skin and in vitro: effects of simulated solar and artificial ultraviolet radiation. *Br J Dermatol* 132: 884-889
65. Kezic S, Kammeyer A, Calkoen F, Fluhr JW, Bos JD; 2009: Natural moisturizing factor components in the stratum corneum as biomarkers of filaggrin genotype: evaluation of minimally invasive methods. *Br J Dermatol* 161: 1098-1104.
66. Kissenpfennig A et al., 2005: Dynamics and function of Langerhans cells in vivo dermal dendritic cells colonize lymph node areas distinct from slower migrating Langerhans cells. *Immunity* 22: 643-654
67. Kock A, Schwarz T, Kirnbauer R, Urbansky A, Perry P, Ansel JC, Luger TA; 1990: Human keratinocytes are a source for tumor necrosis factor alpha: evidence for synthesis and release upon stimulation with endotoxin or ultraviolet light. *J Exp Med* 172: 1609-1614
68. Kölgen W, Both H, Van Weelden H, Guikers KL, Bruijnzeel-Koomen CA, Knol EF, Van Vloten WA, De Gruijl FR; 2002: Epidermal Langerhans cell depletion after artificial ultraviolet B irradiation of human skin in vivo: Apoptosis versus migration. *J Invest Dermatol* 118, 812-817
69. Kölgen W, van Steeg H, van der Horst GTJ, Hoeijmakers JHJ, van Vloten WA, de Gruijl FR, Garssen J; 2003: Association of transcription-coupled repair but not global genome repair with Ultraviolet-B-induced Langerhans cell depletion and local immunosuppression. *J Invest Dermatol* 121:751-756
70. Kripke ML, Cox PA, Bucana C, Vink AA, Alas L, Yarosh DB; 1996: Role of DNA damage in local suppression of contact hypersensitivity in mice by UV radiation. *Exp Dermatol* 5, 172-180
71. Kuby: Immunology; 6. Auflage, 2006, W.H.Freeman & Co Ltd
72. Kurimoto I, Streilein JW; 1992: Cis-urocanic acid suppression of contact hypersensitivity induction is mediated via tumor necrosis factor alpha. *J Immunol* 148: 3072-3078
73. Kuroguchi Y, Fukui Y, Nakagawa T, Yamamoto I; 1957: A note on cis-urocanic acid. *Jpn J Pharmacol* 6(2):147-52
74. Masaki H, Atsumi T, Sakurai H; 1995: Detection of hydrogen peroxide and hydroxyl radicals in murine skin fibroblasts under UVB irradiation. *Biochem Biophys Res Commun* 206: 474-479

75. Melnikova VO, Ananthaswamy HN; 2005: Cellular and molecular events leading to the development of skin cancer. *Mutat Res.* 571(1-2):91-106.
76. Mellor N, Themis M, Selden C, Jones M, Hodgson HJ; 2004: Characteristics of murine histidinaemia and its potential for genetic manipulation. *Liver Int* 24:354-360
77. Mommaas AM, Mulder AA, Vermeer M, Boom BW, Tseng C, Taylor JR, Streilein JW; 1993: Ultrastructural studies bearing on the mechanism of UVB-impaired induction of contact hypersensitivity to DNCB in man. *Clin Exp Immunol* 92:487-493
78. Moodycliffe AM, Kimber I, Norval M; 1992: The effect of ultraviolet B irradiation and urocanic acid isomers on dendritic cell migration. *Immunology* 77, 394-399
79. Nagao K et al.; 2009: Murine epidermal Langerhans cells and langerin-expressing dermal dendritic cells are unrelated and exhibit distinct function. *Pnas* 106/9:3312-3317
80. Nakagawa S, Koomen CW, Bos JD, Teunissen MB; 1999: Differential modulation of human epidermal Langerhans cell maturation by ultraviolet B radiation. *J Immunol* 163: 5192-200
81. Noonan FP, De Fabo EC, Kripke ML; 1981: Suppression of contact hypersensitivity by UV radiation and its relationship to UV-induced suppression of tumor immunity. *Photochem Photobiol* 34: 683-690
82. Noonan FP, De Fabo EC, Morrison H; 1988: Cis-urocanic acid, a product formed by ultraviolet B irradiation of the skin initiates an antigen presentation defect in splenic dendritic cells in vivo. *J Invest Dermatol* 90: 92-99
83. Noonan FP, De Fabo EC; 1992: Immunosuppression by ultraviolet B radiation: initiation by urocanic acid. *Immunol Today* 13, 250-254
84. Norval M; 2006: The mechanisms and consequences of ultraviolet-induced immunosuppression. *Prog Biophys Mol Biol* 92: 108–118.
85. Norval M, Gibbs NK, Gilmour J; 1995: The role of urocanic acid in UV-induced immunosuppression: recent advances (1992-1994). *Photochem Photobiol* 62: 209-17.
86. Norval M and El-Ghorr A. A; 2002: Studies to determine the immunomodulating effects of cis-urocanic acid. *Methods* 28:63-70
87. Norval M, Simpson TH, Bardshiri E, Crosby J; 1989: Quantification of urocanic acid isomers in human stratum corneum. *Photodermatol Photoimmunol Photomed* 6: 142-145
88. Norval M, Gilmour J, Simpson TJ; 1990: The effect of histamine receptor antagonists on immunosuppression induced by the cis-isomer of urocanic acid. *Photodermatol Photoimmunol Photomed* 7:243-248

89. Obata M, Tagami H, 1985: Alteration in murine epidermal Langerhans cell population by various UV irradiations: Quantitative and morphologic studies on the effects of various wavelengths of monochromatic radiation on Ia-bearing cells. *J Invest Dermatol* 84, 139-145
90. Park HY, Kosmadaki M, Yaar M, Gilchrest BA; 2009: Cellular mechanisms regulating human melanogenesis. *Cell Mol Life Sci* 2009 May;66(9):1493-506
91. Poulin LF, Henri S, de Bovis B, Devilard E, Kissenpfennig A, Malissen B; 2007: The dermis contains langerin+ dendritic cells that develop and function independently of epidermal Langerhans cells. *J Exp Med* 204: 3119-3131
92. Reilly SK, De Fabo EC ; 1991 : Dietary histidine increases mouse skin urocanic acid levels and enhances UVB-induced immune suppression of contact hypersensitivity. *Photochem Photobiol* 53(4): 431-8.
93. Romani N, Holzmann S, Tripp CH, Koch F, Stoitzner P; 2003: Langerhans cells – dendritic cells of the epidermis. *APMIS* 111: 725-740
94. Ruedl C, Koebel P, Bachmann M, Hess M, Karjalainen K; 2000: Anatomical origin of dendritic cells determines their life span in peripheral lymph nodes. *J Immunol* 165: 4910-4916
95. Sarasin A; 1999: The molecular pathways of ultraviolet-induced carcinogenesis. *Mutation Res* 428, 5-10
96. Schwarz A, Maeda A, Kernebeck K, Van Steeg H, Beissert S, Schwarz T; 2005: Prevention of UV radiation-induced immunosuppression by IL-12 is dependent on DNA repair. *J Exp Med* 201, 173-179
97. Schwarz A, Grabbe S, Grosse-Heitmeyer K, Roters B, Riemann H, Luger TA, Trinchieri G, Schwarz T; 1998: Ultraviolet light-induced immune tolerance is mediated via Fas/Fas-ligand system. *J Immunol* 160:4262-70
98. Schwarz T, 2005: Mechanisms of UV-induced immunosuppression. *Keio J Med* 54: 165–171.
99. Scott IR, Harding CR, Barrett JG; 1982: Histidine-rich protein of the keratohyalin granules. Source of the free amino acids, urocanic acid and pyrrolidone carboxylic acid in the stratum corneum. *Biochim Biophys Acta* 719: 110–117.
100. Schuler G, Steinman RM; 1985: Murine epidermal Langerhans cells mature into potent immunostimulatory dendritic cells in vitro. *J Exp Med* 161:526-546

101. Selden C, Calnan D, Morgan N, Wilcox H, Carr E, Hodgson HJ; 1995: Histidinemia in mice: a metabolic defect treated using a novel approach to hepatocellular transplantation. *Hepatology* 21:1405-12.
102. Slominski A, Pisarchik A, Zbytek B, Tobin DJ, Kauser S, Wortsman J; 2003: Functional activity of serotonergic and melatonergic systems expressed in the skin. *J Cell Physiol* 196: 144-153
103. Steinman RM, Nussenzweig MC; 2002: Avoiding horror autotoxicus: the importance of dendritic cells in peripheral T cell tolerance. *Proc Natl Acad Sci USA* 99: 351-358
104. Stingl G, Gazze-Stingl LA, Aberer W, Wolff K; 1981: Antigen presentation by murine epidermal Langerhans cells and its alteration by ultraviolet B light. *J Immunol* 127:1707
105. Tabachnik J; 1957: Urocanic acid, the major acid soluble UV absorbing compound in guinea pig epidermis. *Arch Biochem Biophys* 70: 295-297
106. Taylor RG, Lambert MA, Sexsmith E, Sadler SJ, Ray PN, Mahuran DJ, McInnes RR; 1990: Cloning and expression of rat histidase. Homology to two bacterial histidases and four phenylalanine ammonia lyases. *J Biol Chem* 265: 18192-18199
107. Taylor RG, Grieco D, Clarke GA, McInnes RR; Taylor BA; 1993: Identification of the mutation in murine histidinemia (his) and genetic mapping of the murine histidase locus (Hal) on chromosome 10. *Genomics* 16: 231-240
108. Taylor RG, Levy HL, McInnes RR; 1991: Histidase and histidinemia. Clinical and molecular considerations. *Mol Biol Med* 8(1):101-16
109. Timares L, Katiyr SK, Elmets CA; 2008: DNA Damage, Apoptosis and Langerhans Cells – Activators of UV-induced Immune Tolerance. *Photochem Photobiol* 84: 422-436
110. Toews GB, Bergstresser PR, Streilein JW; 1980: Epidermal Langerhans cell density determines whether contact hypersensitivity or unresponsiveness follows skin painting. *J Immunol* 124,1
111. Ullrich SE; 2002: Photoimmune suppression and photocarcinogenesis. *Front Biosci* 7:d684-703.
112. Vink AA, Strickland FM, Bucana C, Cox PA, Roza L, Yarosh B, Kripke ML; 1996: Localization of DNA damage and its role in altered antigen-presenting cell function in ultraviolet-irradiated mice. *J Exp Med* 183: 1491-1500
113. Vink AA, Moodycliffe AM, Shreedhar V, Ullrich SE, Roza L, Yarosh DB, Kripke ML; 1997: The inhibition of antigen-presenting activity of dendritic cells resulting from

- UV irradiation of murine skin is restored by in vitro photorepair of cyclobutane pyrimidine dimers. *Proc Natl Acad Sci USA* 94: 5255-60
114. Walterscheid JP, Nghiem DX, Kazimi N, Nutt LK, McConkey DJ, Norval M, Ullrich SE; 2006: Cis-urocanic acid, a sunlight-induced immunosuppressive factor, activates immune suppression via the 5-HT_{2A} receptor. *Proc Natl Acad Sci U S A* 103(46): 17420-5.
115. Wlaschek M, Tantcheva-Poór I, Naderi L, Ma W, Schneider L, Razi-Wolf Z, Schüller J, Scharffetter-Kochanek K; 2001: Solar UV irradiation and dermal photoaging. *J Photochem Photobiol* (63), 41-51
116. Wolff K, Goldsmith LA, Ktz SI, Gilchrest BA, Paller AS, Leffell DJ, Fitzpatrick's Dermatology in General Medicine, 7th edition, Volume 2; New York, McGraw Hill, 2008
117. Xia Q, Yin JJ, Wamer WG, Cherng SH, Boudreau MD, Howard PC, Yu H, Fu PP; 2006: Photoirradiation of retinyl palmitate in ethanol with ultraviolet light formation of photodecomposition products, reactive oxygen species, and lipid peroxides. *Int J Environ Res Public Health* 3(2), 185-190
118. Yasui H, Sakurai H; 2000: Chemiluminescent detection and imaging of reactive oxygen species in live mouse skin exposed to UVA. *Biochem Biophys Res Commun* 269: 121-126
119. Yoshikawa T, Streilein JW; 1990: Genetic basis of the effects of ultraviolet light B on cutaneous immunity. Evidence that polymorphism at the Tnf- α and Lps loci governs susceptibility. *Immunogenetics* 32:398-405
120. Yoshiki R, Kabashimi K, Sugita K, Nakamura M, Tokura Y; 2009: Local UVB-induced immunosuppression is mediated by IL-10-producing and OX40L-positive mature Langerhans cells. *ESDR* 2009, Oral 027
121. Zenisek A, Kral JA, Hais IM; 1955: Sun-screening effect of urocanic acid. *Biochim Biophys Acta* 18(4):589-91
122. <http://upload.wikimedia.org/wikipedia/commons/3/34/Skin.jpg>
123. <http://jaxmice.jax.org/strain/000664.html>

8. APPENDIX

8.1 List of Figures

Figure 1: Morphology of the skin; adapted from http://upload.wikimedia.org/wikipedia/commons/3/34/Skin.jpg	11
Figure 2: Conversion of histidine into Urocanic acid by deamination.....	15
Figure 3: Spontaneous mutation of HAL gene (R322Q).....	16
Figure 4: UV light induced thymine dimer formation; adapted from Durbeej B. et al. 2002.....	17
Figure 5: Scheme of thesis 1 (UV-induced DNA damage in histidase-mutant mice).....	25
Figure 6: Scheme of thesis 2 (impact of UVB irradiation on the number of Langerhans cells in the skin of histidase-mutant and in control mice).....	26
Figure 7: Quantification of HIS mRNA.....	27
Figure 8A-C: Histidase-protein expression in the epidermis (A) and in the liver (B) and Keratin-control.....	28
Figure 9A: Determination of concentration of urocanic acid in the epidermis (untreated).....	29
Figure 9b: Determination of concentration of urocanic acid in the epidermis (after UVB irradiation).....	30
Figure 10: UVB absorption curves of stratum corneum extracts.....	31
Figure 11: Comparison of UV-absorbance of stratum corneum extracts (quantitative).....	31
Figure 12: anti-CPD + Hoechst staining of prepared skin of heterozygous (WT/mut) mice and his-homozygous (mut/mut) mice 24 hours after UVB irradiation.....	32
Figure 13A: Quantification of DNA damage in heterozygous and homozygous newborns 1 hour after UVB irradiation with a dose of 250 mJ/cm ²	33
Figure 13B: Quantification of DNA damage in WT and homozygous adult mice 24 hour after UVB irradiation with a dose of 250 mJ/cm ²	33
Figure 14A: Quantification of DNA damage in heterozygous and homozygous newborns 1 hour after UVB irradiation with a dose of 25 mJ/cm ²	34
Figure 14B: Quantification of DNA damage in WT and homozygous adult mice 1 hour after UVB irradiation with a dose of 25 mJ/cm ²	34
Figure 15A: Active Caspase-3-positive cells (cells/field of view) 24 hours after UVB irradiation (250 mJ/cm ²).....	35
Figure 15B: Active Caspase-3-positive cells (cells/field of view) 24 hours after UVB irradiation (250 mJ/cm ²).....	35
Figure 16 (A-E): Changes in skin appearance of a homozygous his-mutant mouse after high-dose UVB irradiation (250 mJ/cm ²).....	36-37
Figure 17 (A-E): Changes in skin appearance of a WT mouse after high-dose UVB irradiation (250 mJ/cm ²).....	37
Figure 18: Evaluation of injury grade 96 hours after UVB irradiation with high-dose UVB (250 mJ/cm ²).....	38
Figure 19 (A-B): Number of active Caspase-3-positive cells and Tunel-positive cells in the epidermis of irradiated ears from WT and mutant mice 48 hours after irradiation (250 mJ/cm ²).....	39
Figure 20 (A-B): Number of active Caspase-3-positive cells and Tunel-positive cells in the epidermis of irradiated ears from WT and mutant mice 72 hrs after irradiation (250 mJ/cm ²).....	39
Figure 21 (A-B): Number of active Caspase-3-positive cells and Tunel-positive cells in the	

epidermis of irradiated ears from WT and mutant mice 96 hrs after irradiation (250 mJ/cm ²).....	39
Figure 22 (A-B): Number of active Caspase-3-positive cells and Tunel-positive cells in the epidermis of irradiated ears from WT and mutant mice 120 hrs after irradiation (250 mJ/cm ²).....	40
Figure 23 (A-B): MHC II/active Casp-3/Hoechst stained epidermal ear sheet, 48 hours post high-dose UVB irradiation (250 mJ/cm ²).....	40
Figure 24 (A-B): MHC II/active Casp-3/Hoechst stained epidermal ear sheet, 120 hours post high-dose UVB irradiation (250 mJ/cm ²).....	41
Figure 25 (A-B): MHC II/active Casp-3/Hoechst stained epidermal wild-type ear-sheets, 48 hours post irradiation (250 mJ/cm ²). magnification: x400.....	41
Figure 26 (A-B): MHC II/active Casp-3/Hoechst stained epidermal mutant ear-sheets, 48 hours post irradiation (250 mJ/cm ²). magnification: x400.....	42
Figure 27: MHC II/active Casp-3/Hoechst stained epidermal mutant ear-sheets, 48 hours post irradiation (250 mJ/cm ²). magnification: x200.....	42
Figure 28 (A-B): IF-staining for HAL expression 48 hours after irradiation (250 mJ/cm ²).....	43
Figure 29: H&E: back skin of a WT and a mutant mouse 24 hours post UVB irradiation (250 mJ/cm ²).....	44
Figure 30: H&E: back skin of a mutant mouse, 48 hours after high-dose UVB irradiation (250 mJ/cm ²).....	44
Figure 31: H&E: back skin of a WT mouse, 72 hours after high-dose UVB irradiation (250 mJ/cm ²).....	45
Figure 32: H&E: back skin of a mutant mouse, 96 hours after high-dose UVB irradiation (250 mJ/cm ²).....	45
Figure 33: H&E: back skin of a WT mouse, 120 hours after high-dose UVB irradiation (250 mJ/cm ²).....	46
Figure 34 (A-B): CPD staining of a cross section of an irradiated ear of a WT mouse (A) and of a histidinemic mouse (B) 48 h after UVB irradiation (250 mJ/cm ²).....	47
Figure 35 (A-B): CPD staining of a cross section of an irradiated ear of a histidinemic mouse (A) and of a WT mouse (B) 120 h after UVB irradiation (250 mJ/cm ²).....	47
Figure 36: Quantification of DNA damage after topical application of UCA.....	48
Figure 37: histamine concentration in urine of WT and his-mutant mice (untreated).....	49
Figure 38: histidine concentration in the stratum corneum of WT and his-mutant mice (untreated).....	50
Figure 39: Number of remaining Langerhans cells in irradiated epidermis of ears from WT and mutant mice.....	51
Figure 40: Boxplot showing the decrease-distribution of number of LCs in age-matched WT and in mutant mice after 4x100 mJ/cm ² UVB irradiation.....	52
Figure 41: Boxplot showing the decrease-distribution of number of LCs in a litter of WT, his-heterozygous and his-homozygous mice after 4x100 mJ/cm ² UVB irradiation.....	53
Figure 42 (A-C): Percent of remaining LC in irradiated epidermis of ears in WT and mutant mice after 4x100 mJ/cm ² UVB irradiation; littermates (A) and age-matched 1+2 (B-C).....	54
Figure 43: distribution and morphology of LC in unirradiated mouse ear-epidermis.....	55
Figure 44: UVB altered LC after 4x100 mJ/cm ² UVB irradiation.....	55
Figure 45: example for density and distribution of LC in irradiated his-mutant mouse ear epidermis.....	55
Figure 46: distribution and morphology of LC in irradiated WT and mutant mice 48 hours after 250 mJ/cm ² UVB irradiation.....	56

8.2 List of Tables

Table 1: Effects of UV-radiation in-vitro and in-vivo; adapted from Fitzpatrick et. Al, Dermatology in General Medicine, 4th edition, Volume 1; Table 132-1 and Table 132-2.....14

8.3 List of Abbreviations

aa	amino acid
APC	antigen-presenting cells
ATZ	amino-thiocyanate
BSA	bovine serum albumin
Casp-3	Caspase-3
CHS	contact hypersensitivity
CPD	cyclobutane pyrimidine dimer
DC	dendritic cells
dDC	dermal dendritic cells
DMSO	dimethylsulfoxide
DNA	de(s)oxyribonucleic acid
DTH	delayed-type hypersensitivity
EC	epidermal cell
ELISA	enzyme-linked immunosorbent assay
FITC	fluorescein isothiocyanate
Hal	L-histidine ammonia lyase
his	histidase
HPLC	high-performance liquid chromatography
Ig	immunglobulin
kDA	kilo-Dalton
KOH	Kalium-Hydroxid
LC	Langerhans cell
LN	lymph node
MHC	major histocompatibility complex
mJ	mili-Joule
mRNA	messenger ribonucleic acid
MUT	mutant
nm	nanometers
OD	optical density

PBS	phosphate buffered saline
ROS	reactive oxygen species
RT	room temperature
SC	stratum corneum
TD	thymine dimer
TUNEL	terminal deoxynucleotidyl transferase dUTP nick end labeling
UCA	urocanic acid
UVA	ultraviolet A
UVB	ultraviolet B
UVC	ultraviolet C
UVR	ultraviolet radiation
WT	wildtype

In addition, standard abbreviations were used for nucleotides, amino acids (one and three letter code) and chemical compounds.

8.4 Curriculum Vitae

Caroline Susanna Stremnitzer

birth date:

26. October 1983 in Vienna

education

since march 2009	diploma thesis “The Roles of Endogenous Urocanic Acid in the Response of Epidermal Cells to UVB”; Medical University of Vienna, Dep. of biology and pathobiology of the skin; supervisor: Dr. Erwin Tschachler
since 2004	studies of molecular biology at the University of Vienna
2002-2004	studies of law and political science
1998-2002	Gymnasium (high school) Sir-Karl-Popper-Schule at the Wiedner Gymnasium Wien
2002	Matura at the Sir-Karl-Popper-Schule
1994-1998	Gymnasium (junior high school) Piaristengymnasium Wien
1990-1994	Volksschule (elementary school) Notre Dame de Sion Wien

employment

2007:	technician (part-time)/ Hygieneinstitut/ Medical University of Vienna
2006:	holiday internship (2 months)/ Hygieneinstitut/ Medical University of Vienna
2005 – 2009	HLWD trainee (heart lung revival with defibrillator)/ St. Johanns Vienna
2005	holiday internship/ „Rotenhof“ pharmacy; 1100 Vienna
2001 – 2006	several employments as waitress and barman in Austria and Ireland
2003	reception & switchboard/ Dorda Brugger & Jordis Attorneys GmbH; 1010 Vienna
2000	holiday internship/ “Bank Austria”; 1080 Vienna